REPORT DOCUMENTATION PAGE

Form Approved
OMB No. 0704-0188

1. AGENCY USE ONLY (Leave Blank)	2. REPORT DATE	3. REPORT TYPE AND DATES COVERED
	9/30/2004	Phase II SBIR Final Report 20 Dec 00 through 30 Sep 04

4. TITLE AND SUBTITLE
Using Adaptive Simulated Annealing to Estimate Ocean Bottom Acoustic Properties from Acoustic Data

5. FUNDING NUMBERS
N00014-01-C-0087

6. AUTHOR(S)
Peter D. Neumann and Gregory Muncill

7. PERFORMING ORGANIZATION NAME(S) AND ADDRESS(ES)
Planning Systems Incorporated
12030 Sunrise Valley Drive
Suite 400, Reston Plaza 1
Reston, VA 20191-3453

8. PERFORMING ORGANIZATION REPORT NUMBER

9. SPONSORING/MONITORING AGENCY NAME(S) AND ADDRESS(ES)
Office of Naval Research
Attn: Larry Green, ONR 321US
Ballston Tower One
800 North Quincy Street
Arlington, VA 22217-5660

10. SPONSORING/MONITORING AGENCY REPORT NUMBER

11. SUPPLEMENTARY NOTES

12a. DISTRIBUTION/AVAILABILITY STATEMENT
Approved for public release; distribution unlimited.

12b. DISTRIBUTION CODE

13. ABSTRACT (Maximum 200 words)
Report developed under SBIR contract for topic N99-217. The effective use of active sonar systems in littoral environments relies on the accurate knowledge of the acoustic environment. This Phase II SBIR provides a solution to the problem of estimating the local, in-situ geoacoustic properties of the ocean bottom from measured acoustic data. The approach used in the Phase I and Phase II SBIR has been to use Navy standard models for transmission loss and reverberation prediction paired with the Adaptive Simulated Annealing (ASA) algorithm. The use of the ASA algorithm, first tested under the Phase I SBIR, produced significantly reduced run times compared to other variations of simulated annealing. The ASA based inversion software is now called GAIT GS (Geoacoustic Inversion Toolkit – Global Search) and PMW-150 has been funding its transition into an OAML product since FY 02. The current software includes ASTRAL 5.1, PE 5.1 and ASPM 5.1 with plans to add Nautilus 1.0 in FY 05. A report from the GAIT V&V committee is expected in late 2004 summarizing the results of their extensive testing of GAIT GS inversion results. Future plans include an extension to inversion of bistatic and multistatic reverberation data.

14. SUBJECT TERMS
SBIR Report
Simulated annealing, geoacoustic inversion, GAIT, LFBL, transmission loss, bottom scatter, reverberation, automated inversion, optimization

15. NUMBER OF PAGES

16. PRICE CODE

17. SECURITY CLASSIFICTION OF REPORT	18. SECURITY CLASSIFICTION OF THIS PAGE	19. SECURITY CLASSIFICTION OF ABSTRACT	20. LIMITATION OF ABSTRACT
Unclassified	Unclassified	Unclassified	

Standard form 298 (Rev.2-89)
Prescribed by ANSI Std. Z39-18
298-102

REF E

Planning Systems Incorporated

State College, PA

October 6, 2004

Dr. Larry Green
Office of Naval Research, Code 321 US
Ballston Tower One
800 North Quincy Street
Arlington, VA 22217-5660

Dear Mr. Green:

Enclosed you will find the summary report for the Phase II SBIR "Using Adaptive Simulated Annealing to Estimate Ocean Bottom Geoacoustic Properties from Acoustic Data" awarded under SBIR Topic N99-217. This summary report covers the entire Phase II period of performance from 22 December 2000 through 30 September 2004. Included with the hardcopy of the report is a CDR with the report in both Microsoft Word and Adobe Acrobat (PDF) format.

Sincerely,

Peter Neumann
Planning Systems Incorporated

cc: SBIR Program Coordinator, Attn: Doug Harry, ONR Code 362, Office of Naval Research, 800 North Quincy Street, Arlington, VA 22217-5660
DCM Virginia, 10500 Battleview Parkway, Suite 200, Manassas, VA 20109-2342
Defense Technical Information Center, 8725 John J. Kingman Road, Suite 0944, Fort Belvoir, VA 22060-6218
Director, Naval Research Lab, Attn: code 5227, 4555 Overlook Avenue, S.W., Washington, D.C. 20375-5326

741 GALEN DRIVE • STATE COLLEGE, PA • 16803-1121
PHONE: (814) 861-2612

Using Adaptive Simulated Annealing to Estimate Ocean Bottom Geoacoustic Properties from Measured Acoustic Data
SBIR Topic N99-217

Peter Neumann and Gregory Muncill
Planning Systems Inc.
12030 Sunrise Valley Drive
Suite 400, Reston Plaza 1
Reston, VA 20191-3453

Contract Number: N00014-01-C-0087

Phase II Technical Summary Report

UNCLASSIFIED

Issuing Agency:

Office of Naval Research
Attn: Larry Green, ONR 321US
Ballston Tower One
800 North Quincy Street
Arlington, VA 22217-5660

Table of Contents

EXECUTIVE SUMMARY 13

PHASE II FINDINGS AND PRODUCTS 13

INVERSION TECHNIQUE WORKSHOP (ITW) 15

ITW – Test Case 0 (Calibration Test Case) 17

ITW – Test Case 1 (Monotonic Downslope Test Case) 18

ITW – Test Case 2 (Shelf-break Test Case) 19

ITW – Test Case 3 (Flat Bottom Test Case with Range-Dependent Intrusion in Bottom) 19

ITW – Test Case 4 (Broadband Measured Data Test Case #1) 21

ITW – Test Case 5 (Broadband Measured Data Test Case #2) 22

ITW – Summary and Conclusions 23

GEOACOUSTIC INVERSION TOOLKIT (GAIT) GLOBAL SEARCH (GS) 24

Modifications to ASA Based TL Inversion Software to Create GAIT GS Version 1.0 24

Integration of Multiple Acoustic Models within the GAIT GS Version 1.0 Software 24

Using a System Based on Gradients and Ratios for N-layer Geoacoustic Parameter Bounds 24

Linking the Sediment Density Upper Bounds to the Sediment Compressional Sound Speed 33

Reduced Chi-Square, Mean-Square Difference and Correlation Cost Functions 34

GAIT GS Hardware and Software Requirements 35

GAIT V&V (Validation and Verification) Test Cases 36

GAIT GS – PE 5.1 37

GAIT V&V Test Cases 1A, 1B and 1C 37

GAIT V&V Test Case 2 43

GAIT V&V Test Case 3 46

GAIT V&V Test Case 4 47

GAIT V&V Test Case 6 49

GAIT V&V Test Case 10 51

GAIT GS – ASTRAL 5.1 53

GAIT V&V Test Case 1 54

GAIT V&V Test Case 2 54

GAIT V&V Test Case 3 54

GAIT V&V Test Case 4 55

GAIT V&V Test Case 6 55

GAIT V&V Test Case 10 56

GAIT GS – ASPM 5.1 *56*

GAIT V&V Test Case 7 58

GAIT V&V Test Case 8 59

GAIT GS – ASPM 5.1 Conclusions 61

GAIT GS – Nautilus 1.0 *62*

PHASE III TRANSITIONS OF PHASE II PRODUCTS **62**

ACKNOWLEDGEMENTS **63**

TABLES **65**

FIGURES **84**

REPORT PREPARATION **134**

List of Tables

Table 1: Summary of Inversion Results Using PE 5.0 (RAM) for ITW Synthetic Test Cases 65

Table 2: Summary of ASTRAL 5.0 and PE 5.0 Inversion Results for ITW Measured Test Cases 66

Table 3: Summary of ASTRAL 5.0 and PE 5.0 Inverted Geoacoustic Parameters for ITW Test Cases 4 and 5 67

Table 4: Summary of GAIT V&V Test Case 1A inversion results using GAIT GS Version 1.0 (PE 5.1). 68

Table 5: Summary of GAIT V&V Test Case 1B inversion results using GAIT GS Version 1.0 (PE 5.1). 69

Table 6: Summary of GAIT V&V Test Case 1C inversion results using GAIT GS Version 1.0 (PE 5.1). 70

Table 7: Summary of GAIT V&V Test Case 2 inversion results using GAIT GS Version 1.0 (PE 5.1) for one-layer (N=1). 71

Table 8: Summary of GAIT V&V Test Case 3 inversion results using GAIT GS Version 1.0 (PE 5.1) for one-layer (N=1) and TL from 0 to 5,000 meters. 72

Table 9: Summary of GAIT V&V Test Case 4A (no added noise) inversion results using GAIT GS Version 1.0 (PE 5.1) for one-layer (N=1). 73

Table 10: Summary of GAIT V&V Test Case 4B (15 dB SNR) inversion results using GAIT GS Version 1.0 (PE 5.1) for one-layer (N=1). 74

Table 11: Summary of GAIT V&V Test Case 4C (5 dB SNR) inversion results using GAIT GS Version 1.0 (PE 5.1) for one-layer (N=1). 75

Table 12: Summary of GAIT V&V Test Case 4D (0 dB SNR) inversion results using GAIT GS Version 1.0 (PE 5.1) for one-layer (N=1). 76

Table 13: Summary of GAIT V&V Test Case 6 inversion results using GAIT GS Version 1.0 (PE 5.1) for one-layer (N=1) and 53 to 503 Hz TL data. 77

Table 14: Summary of GAIT V&V Test Case 6 inversion results (10-parameter LFBL geoacoustic parameter format) using GAIT GS Version 1.0 (ASTRAL 5.1). 78

Table 15: Summary of GAIT V&V Test Case 10A inversion results using GAIT GS Version 1.0 (PE 5.1) for one-layer (N=1) using 20, 40, 80, 160, 315 and 630 Hz TL data. 79

Table 16: Summary of GAIT V&V Test Case 10B inversion results using GAIT GS Version 1.0 (PE 5.1) for one-layer (N=1) using 20, 40, 80, 160, 315 and 630 Hz TL data. 80

Table 17: Summary of GAIT V&V Test Case 10C inversion results using GAIT GS Version 1.0 (PE 5.1) for one-layer (N=1) using 20, 40, 80, 160, 315 and 630 Hz TL data. 81

Table 18: Summary of GAIT V&V Test Case 10A, 10B and 10C inversion results (10-parameter LFBL geoacoustic parameter format) using GAIT GS Version 1.0 (ASTRAL 5.1) using 20, 40, 80, 160, 315 and 630 Hz TL data. 82

Table 19: Summary of GAIT V&V Test Cases 7, 8A and 8B inversion results (10-parameter LFBL geoacoustic parameter format with a bottom backscatter coefficient) using GAIT GS Version 1.0 (ASPM 5.1). 83

Table of Figures

Figure 1: ITW Test Case 0 (25 Hz data) - Comparison between synthetic data (black line), PE 5.0 output using true environment and PE 5.0 output using ASA inversion environment. Top plot shows 25 meter receiver depth and bottom plot shows 85 meter receiver depth. 84

Figure 2: ITW Test Case 0 (200 Hz data) - Comparison between synthetic data (black line), PE 5.0 output using true environment and PE 5.0 output using ASA inversion environment. Top plot shows 25 meter receiver depth and bottom plot shows 85 meter receiver depth. 85

Figure 3: Comparison between true geoacoustics (solid black line) and best-fit (25, 50, 100 and 200 Hz) inverted parameters (dashed black line) for test case 0 (calibration case). 86

Figure 4: ITW Test Case 0 (80 Hz data) - Comparison between synthetic data (red line) and PE 5.0 output using ASA inversion environment (black line). 87

Figure 5: ITW Test Case 0 (220 Hz data) - Comparison between synthetic data (red line) and PE 5.0 output using ASA inversion environment (black line). 87

Figure 6: Comparison between true geoacoustics (solid black line) and best-fit (25, 50, 100 and 200 Hz) inverted parameters (dashed black line) for test case 1 (monotonic downslope). 88

Figure 7: ITW Test Case 1 (80 Hz data) - Comparison between synthetic data (red line) and PE 5.0 output using ASA inversion environment (black line). 89

Figure 8: ITW Test Case 1 (220 Hz data) - Comparison between synthetic data (red line) and PE 5.0 output using ASA inversion environment (black line). 89

Figure 9: Comparison between true geoacoustics (solid black line) and best-fit (50, 100 and 200 Hz) inverted parameters (dashed black line) for test case 2 (shelfbreak). 90

Figure 10: ITW Test Case 2 (80 Hz data) - Comparison between synthetic data (red line) and PE 5.0 output using ASA inversion environment (black line). 91

Figure 11: ITW Test Case 2 (220 Hz data) - Comparison between synthetic data (red line) and PE 5.0 output using ASA inversion environment (black line). 91

Figure 12: Comparison between true geoacoustics (solid black line) and best-fit inverted parameters (dashed line) for test case 3 background environment (0 - 1,100 meters and 2,900 – 5,000 meters). 92

Figure 13: Comparison between true geoacoustics (solid black line) and best-fit inverted parameters (dashed line) for test case 3 intrusion environment (1,100 - 2,900 meters). 92

Figure 14: ITW Test Case 3 (400 Hz data) - Comparison between synthetic data (black line), PE 5.0 output using true environment (purple line), PE 5.0 output using inverted fit for 1-layer range-independent (red line), PE 5.0 output using inverted fit for 2-layer range-independent (blue line) and PE 5.0 output using inverted fit for 1-layer range-dependent (green line). Top plot shows 25 meter receiver depth and bottom plot shows 85 meter receiver depth. 93

Figure 15: ITW Test Case 3 (80 Hz data) - Comparison between synthetic data (red line) and PE 5.0 output using ASA inversion environment (black line). 94

Figure 16: ITW Test Case 3 (220 Hz data) - Comparison between synthetic data (red line) and PE 5.0 output using ASA inversion environment (black line). 94

Figure 17: ITW Test Case 4 – Comparison of measured octave band TL data (black diamonds) with inversion using ASTRAL 5.0 with 3,000 iterations (red line) and 10,000 iterations (blue line). 95

Figure 18: ITW Test Case 5 – Comparison of measured octave band TL data (black diamonds) with inversion using ASTRAL 5.0 with 3,000 iterations (red line) and 10,000 iterations (blue line). 96

Figure 19: ITW Test Case 5 – Comparison of measured octave band TL data (black diamonds) with inversion using PE 5.0 with 10,000 iterations (red line) and the range-average output of PE 5.0 (blue line). 97

Figure 20: Figure 7 from Edwin L. Hamilton, "Sound velocity-density relations in sea floor sediments and rock," Journal of Acoustical Society of America, 63 (2), pp. 366-377 (1978). 98

Figure 21: GAIT V&V Test Case 1A (50 Hz data) - Comparison between synthetic data (black line) and PE 5.1 output using geoacoustic parameters from GAIT GS Version 1.0. Top plot shows 25 meter receiver depth and bottom plot shows 85 meter receiver depth. 99

Figure 22: GAIT V&V Test Case 1A (200 Hz data) - Comparison between synthetic data (black line) and PE 5.1 output using geoacoustic parameters from GAIT GS Version 1.0. Top plot shows 25 meter receiver depth and bottom plot shows 85 meter receiver depth. 100

Figure 23: GAIT V&V Test Case 1A (5 meter range step for PE 5.1 with reduced chi-square cost function using TL data) – Plot of cost function values versus unknown parameters with left column – layer thickness, second column– sound speed, third column – density and fourth column – attenuation. 101

Figure 24: GAIT V&V Test Case 1A (speeddial = 2 for PE 5.1 with reduced chi-square cost function using TL data) – Plot of cost function values versus unknown parameters with left column – layer thickness, second column– sound speed, third column – density and fourth column – attenuation. 102

Figure 25: GAIT V&V Test Case 1A (speeddial = 3 for PE 5.1 with reduced chi-square cost function using TL data) – Plot of cost function values versus unknown parameters with left column – layer thickness, second column– sound speed, third column – density and fourth column – attenuation. 103

Figure 26: GAIT V&V Test Case 1A (speeddial = 3 for PE 5.1 with correlation cost function using TL data) – Plot of cost function values versus unknown parameters with left column – layer thickness, second column– sound speed, third column – density and fourth column – attenuation. 104

Figure 27: GAIT V&V Test Case 1B (5 meter range step for PE 5.1 with reduced chi-square cost function using TL data) – Plot of cost function values versus unknown parameters with left column – layer thickness, second column– sound speed, third column – density and fourth column – attenuation. 105

Figure 28: GAIT V&V Test Case 1B (speeddial = 4 for PE 5.1 with reduced chi-square cost function using TL data) – Plot of cost function values versus unknown parameters with left column – layer thickness, second column– sound speed, third column – density and fourth column – attenuation. 106

Figure 29: GAIT V&V Test Case 1C (5 meter range step for PE 5.1 with reduced chi-square cost function using TL data) – Plot of cost function values versus unknown parameters with left column – layer thickness, second column– sound speed, third column – density and fourth column – attenuation. 107

Figure 30: GAIT V&V Test Case 1C (speeddial = 4 for PE 5.1 with reduced chi-square cost function using TL data) – Plot of cost function values versus unknown parameters with left

column – layer thickness, second column– sound speed, third column – density and fourth column – attenuation. 108

Figure 31: GAIT V&V Test Case 2 (speeddial = 3 for PE 5.1 with reduced chi-square cost function using TL data) – Plot of cost function values versus unknown parameters with left column – layer thickness, second column– sound speed, third column – density and fourth column – attenuation. 109

Figure 32: GAIT V&V Test Case 2 full-field transmission loss plots (source depth 20 m) for 16 Hz (left column), 31 Hz (middle column) and 63 Hz (right column). The top row is the ground-truth TL. The bottom row is the GAIT GS TL. (Graphics courtesy of Martin Siderius – SAIC) 110

Figure 33: GAIT V&V Test Case 2 full-field transmission loss plots (source depth 20 m) for 126 Hz (left column), 251 Hz (middle column) and 502 Hz (right column). The top row is the ground-truth TL. The bottom row is the GAIT GS TL. (Graphics courtesy of Martin Siderius – SAIC) 110

Figure 34: GAIT V&V Test Case 2 – Targets are generated at each range/depth cell on a 60 m vertical array using the ground-truth seabed properties. These are correlated with the same range-depth cell calculated using the geoacoustic properties from the GAIT GS inversion. Perfect agreement is red (0 dB) and blue indicates poorer agreement. The top left is 16 Hz, middle top is 31 Hz, top right is 63 Hz, bottom left is 126 Hz, middle bottom is 251 Hz and bottom right is 502 Hz. (Graphics courtesy of Martin Siderius – SAIC) 111

Figure 35: GAIT V&V Test Case 2 – Depth averaged matched field error showing the GAIT GS solution as the red line. The blue line denotes another inversion algorithm (RGC) also evaluated by the GAIT V&V committee. The top left is 16 Hz, middle top is 31 Hz, top right is 63 Hz, bottom left is 126 Hz, middle bottom is 251 Hz and bottom right is 502 Hz. (Graphics courtesy of Martin Siderius – SAIC) 112

Figure 36: GAIT V&V Test Case 3 – Ground truth geoacoustic properties plotted against the inversion results from GAIT GS (red line). The blue line denotes the inversion results from the RGC algorithm also evaluated by the GAIT V&V committee. (Graphics courtesy of Martin Siderius – SAIC) 112

Figure 37: GAIT V&V Test Case 3 – Targets are generated at each range/depth cell on a 60 m vertical array using the ground-truth seabed properties. These are correlated with the

same range-depth cell calculated using the geoacoustic properties from the GAIT GS inversion. Perfect agreement is red (0 dB) and blue indicates poorer agreement. The top left is 16 Hz, middle top is 31 Hz, top right is 63 Hz, bottom left is 126 Hz, middle bottom is 251 Hz and bottom right is 502 Hz. (Graphics courtesy of Martin Siderius – SAIC) 113

Figure 38: GAIT V&V Test Case 3 – Depth averaged matched field error showing the GAIT GS solution as the red line. The blue line denotes the RGC inversion algorithm also evaluated by the GAIT V&V committee. The top left is 16 Hz, middle top is 31 Hz, top right is 63 Hz, bottom left is 126 Hz, middle bottom is 251 Hz and bottom right is 502 Hz. (Graphics courtesy of Martin Siderius – SAIC) 114

Figure 39: GAIT V&V Test Case 4 – Actual SNR values for 1 km segments at 25 Hz for the 25 meter receiver depth. Test case 4c (5 dB SNR) is shown in the top plot in red and test case 4d (0 dB SNR) is shown in the bottom plot in blue. The acoustic before the noise was added is shown as a black line in each plot. (Graphics courtesy of Tracianne Neilsen – ARL/UT) 115

Figure 40: GAIT V&V Test Case 4 – Actual SNR values for 1 km segments at 250 Hz for the 25 meter receiver depth. Test case 4c (5 dB SNR) is shown in the top plot in red and test case 4d (0 dB SNR) is shown in the bottom plot in blue. The acoustic before the noise was added is shown as a black line in each plot. (Graphics courtesy of Tracianne Neilsen – ARL/UT) 116

Figure 41: GAIT V&V Test Case 4A (no added noise) – Targets are generated at each range/depth cell on a 60 m vertical array using the ground-truth seabed properties. These are correlated with the same range-depth cell calculated using the geoacoustic properties from the GAIT GS inversion. Perfect agreement is red (0 dB) and blue indicates poorer agreement. The top left is 16 Hz, middle top is 31 Hz, top right is 63 Hz, bottom left is 126 Hz, middle bottom is 251 Hz and bottom right is 502 Hz. (Graphics courtesy of Martin Siderius – SAIC) 117

Figure 42: GAIT V&V Test Case 4A (no added noise) – Depth averaged matched field error showing the GAIT GS solution as the red line. The blue line denotes the RGC inversion algorithm also evaluated by the GAIT V&V committee. The top left is 16 Hz, middle top is 31 Hz, top right is 63 Hz, bottom left is 126 Hz, middle bottom is 251 Hz and bottom right is 502 Hz. (Graphics courtesy of Martin Siderius – SAIC) 118

Figure 43: GAIT V&V Test Case 4B (15 dB SNR) – Depth averaged matched field error showing the GAIT GS solution as the red line. The blue line denotes the RGC inversion algorithm also evaluated by the GAIT V&V committee. The top left is 16 Hz, middle top is 31 Hz, top right is 63 Hz, bottom left is 126 Hz, middle bottom is 251 Hz and bottom right is 502 Hz. (Graphics courtesy of Martin Siderius – SAIC) 119

Figure 44: GAIT V&V Test Case 4C (5 dB SNR) – Depth averaged matched field error showing the GAIT GS solution as the red line. The blue line denotes the RGC inversion algorithm also evaluated by the GAIT V&V committee. The top left is 16 Hz, middle top is 31 Hz, top right is 63 Hz, bottom left is 126 Hz, middle bottom is 251 Hz and bottom right is 502 Hz. (Graphics courtesy of Martin Siderius – SAIC) 120

Figure 45: GAIT V&V Test Case 4D (0 dB SNR) – Targets are generated at each range/depth cell on a 60 m vertical array using the ground-truth seabed properties. These are correlated with the same range-depth cell calculated using the geoacoustic properties from the GAIT GS inversion. Perfect agreement is red (0 dB) and blue indicates poorer agreement. The top left is 16 Hz, middle top is 31 Hz, top right is 63 Hz, bottom left is 126 Hz, middle bottom is 251 Hz and bottom right is 502 Hz. (Graphics courtesy of Martin Siderius – SAIC) 121

Figure 46: GAIT V&V Test Case 4D (0 dB SNR) – Depth averaged matched field error showing the GAIT GS solution as the red line. The blue line denotes the RGC inversion algorithm also evaluated by the GAIT V&V committee. The top left is 16 Hz, middle top is 31 Hz, top right is 63 Hz, bottom left is 126 Hz, middle bottom is 251 Hz and bottom right is 502 Hz. (Graphics courtesy of Martin Siderius – SAIC) 122

Figure 47: GAIT V&V Test Case 6 – Targets are generated at each range/depth cell on a 60 m vertical array using the ground-truth seabed properties. These are correlated with the same range-depth cell calculated using the geoacoustic properties from the GAIT GS inversion. Perfect agreement is red (0 dB) and blue indicates poorer agreement. The top left is 16 Hz, middle top is 31 Hz, top right is 63 Hz, bottom left is 126 Hz, middle bottom is 251 Hz and bottom right is 502 Hz. (Graphics courtesy of Martin Siderius – SAIC) 123

Figure 48: GAIT V&V Test Case 6 – Depth averaged matched field error showing the GAIT GS solution as the red line. The blue line denotes the RGC inversion algorithm also evaluated by the GAIT V&V committee. The top left is 16 Hz, middle top is 31 Hz, top

right is 63 Hz, bottom left is 126 Hz, middle bottom is 251 Hz and bottom right is 502 Hz. (Graphics courtesy of Martin Siderius – SAIC) 124

Figure 49: GAIT V&V Test Case 10A – Geoacoustic properties (sound speed, density and attenuation from left to right) for ground-truth (black line) and GAIT GS inversion using PE 5.1 (red line). (Graphics courtesy of Martin Siderius – SAIC) 124

Figure 50: GAIT V&V Test Case 10A – One third octave band averages at center frequencies (from top left to bottom) 16, 31, 63, 126, 251 and 502 Hz. The black curves were generated using the ground-truth geoacoustic properties and the red curves were generated from the GAIT GS inverted geoacoustic parameters. (Graphics courtesy of Martin Siderius – SAIC) 125

Figure 51: GAIT V&V Test Case 10A – Targets are generated at each range/depth cell on a 60 m vertical array using the ground-truth seabed properties. These are correlated with the same range-depth cell calculated using the geoacoustic properties from the GAIT GS inversion. Perfect agreement is red (0 dB) and blue indicates poorer agreement. The top left is 16 Hz, middle top is 31 Hz, top right is 63 Hz, bottom left is 126 Hz, middle bottom is 251 Hz and bottom right is 502 Hz. (Graphics courtesy of Martin Siderius – SAIC) 126

Figure 52: GAIT V&V Test Case 10B – Geoacoustic properties (sound speed, density and attenuation from left to right) for ground-truth (black line) and GAIT GS inversion using PE 5.1 (red line). (Graphics courtesy of Martin Siderius – SAIC) 126

Figure 53: GAIT V&V Test Case 10B – One third octave band averages at center frequencies (from top left to bottom) 16, 31, 63, 126, 251 and 502 Hz. The black curves were generated using the ground-truth geoacoustic properties and the red curves were generated from the GAIT GS inverted geoacoustic parameters. (Graphics courtesy of Martin Siderius – SAIC) 127

Figure 54: GAIT V&V Test Case 10B – Targets are generated at each range/depth cell on a 60 m vertical array using the ground-truth seabed properties. These are correlated with the same range-depth cell calculated using the geoacoustic properties from the GAIT GS inversion. Perfect agreement is red (0 dB) and blue indicates poorer agreement. The top left is 16 Hz, middle top is 31 Hz, top right is 63 Hz, bottom left is 126 Hz, middle bottom is 251 Hz and bottom right is 502 Hz. (Graphics courtesy of Martin Siderius – SAIC) 128

Figure 55: GAIT V&V Test Case 10C – Geoacoustic properties (sound speed, density and attenuation from left to right) for ground-truth (black line) and GAIT GS inversion using PE 5.1 (red line). (Graphics courtesy of Martin Siderius – SAIC) 128

Figure 56: GAIT V&V Test Case 10C – One third octave band averages at center frequencies (from top left to bottom) 16, 31, 63, 126, 251 and 502 Hz. The black curves were generated using the ground-truth geoacoustic properties and the red curves were generated from the GAIT GS inverted geoacoustic parameters. (Graphics courtesy of Martin Siderius – SAIC) 129

Figure 57: GAIT V&V Test Case 10C – Targets are generated at each range/depth cell on a 60 m vertical array using the ground-truth seabed properties. These are correlated with the same range-depth cell calculated using the geoacoustic properties from the GAIT GS inversion. Perfect agreement is red (0 dB) and blue indicates poorer agreement. The top left is 16 Hz, middle top is 31 Hz, top right is 63 Hz, bottom left is 126 Hz, middle bottom is 251 Hz and bottom right is 502 Hz. (Graphics courtesy of Martin Siderius – SAIC) 130

Figure 58: GAIT V&V Test Case 7 –Band averaged reverberation data (black circles) at center frequencies (from top left to bottom) of 50, 100, 200, 400 and 800 Hz. The black curves were generated using the GAIT GS (using ASPM 5.1) inverted geoacoustic parameters. 131

Figure 59: GAIT V&V Test Case 8A –Band averaged reverberation data (black circles) at center frequencies (from top left to bottom) of 100, 200, 400 and 800 Hz. The black curves were generated using the GAIT GS (using ASPM 5.1) inverted geoacoustic parameters. 132

Figure 60: GAIT V&V Test Case 8B –Band averaged reverberation data (black circles) at center frequencies (from top left to bottom) of 100, 200, 400 and 800 Hz. The black curves were generated using the GAIT GS (using ASPM 5.1) inverted geoacoustic parameters. 133

Executive Summary

The effective use of active sonar systems in littoral environments relies on the accurate knowledge of the acoustic environment. This Phase II SBIR provides a solution to the problem of estimating the local, in-situ geoacoustic properties of the ocean bottom from measured acoustic data. The approach used in the Phase I and Phase II SBIR has been to use Navy standard models for transmission loss and reverberation prediction paired with the Adaptive Simulated Annealing (ASA) algorithm. The use of the ASA algorithm, first tested under the Phase I SBIR, produced significantly reduced run times compared to other variations of simulated annealing. The ASA based inversion software is now called GAIT GS (Geoacoustic Inversion Toolkit – Global Search) and PMW-150 has been funding its transition into an OAML product since FY 02. The current software includes ASTRAL 5.1, PE 5.1 and ASPM 5.1 with plans to add Nautilus 1.0 in FY 05. A report from the GAIT V&V committee is expected in late 2004 summarizing the results of their extensive testing of GAIT GS inversion results. Future plans include an extension to inversion of bistatic and multistatic reverberation data under a future release of GAIT.

Phase II Findings and Products

Under the Phase I SBIR tasking, the ASA algorithm was paired with both the ASTRAL propagation loss model and the SCARAB bottom scatter model. During the Phase II, the ASA algorithm was paired with the Navy standard propagation loss model PE Version 5.0. This addition to the suite of models was necessary to compete in the Inversion Technique Workshop (ITW) held in May 2001. An overview of the results from the ITW is provided in the following section of this summary report. The ITW proved to be an important forum for showing the capabilities of the ASA based inversion products developed under this SBIR. Among the recommendations that came from the ITW results, the PSI developed inversion software recommended for inclusion in a PMW-155 (now PMW-150) product to be called GAIT (Geoacoustic Inversion Techniques).

Following the ITW in mid-2001, a number of improvements to the ASA based inversion software (now called GAIT GS where GS stood for Global Search) were made. The geoacoustic parameter bounds used for the Phase I SBIR testing and for the ITW test cases with PE 5.0 used minimum and maximum values for the sound speed, density and attenuation at the top and bottom of each layer. This approach resulted in some unphysical results because it lacked the control over the gradient within each sediment layer and over the ratio between the bottom of

one layer and the top of the next layer. The solution to this problem which changed to parameter bounds based upon a gradient and ratio description for the geoacoustic properties of the sediment is described beginning on page 24 of this summary report.

An additional problem highlighted in the ITW results was the problem of inverted geoacoustic parameter sets that were not consistent. The most common example of this was a very high density value paired with a lower sound speed for the sediment. This problem was common in many of the ASTRAL based inversion results and required a solution. Using the work of Hamilton, an upper bound on the sediment density was computed based upon the sediment sound speed and that upper bound was changed for each step the ASA algorithm took. This solution solved the problem of erroneously high sediment density values and also served to reduce the side of the solution space that the ASA algorithm had to search. The computation overhead for this solution was negligible requiring just a set of conditional statements and a simple linear equation to compute the new sediment density upper bound. More details are providing beginning on page 33 including the equations describing the relationship between sediment sound speed and sediment density.

An outcome of the GAIT working group meetings was an interest in adding several additional cost functions to the GAIT GS software. David Knobles and Bob Koch of ARL/UT were tasked to develop and deliver these new cost functions to PSI for integration into the GAIT GS software. The cost functions added are described in detail beginning on page 34. The GAIT V&V inversion results described in this report did not find conclusive evidence for the superiority of any one particular cost function as all performed similarly on the GAIT V&V test cases.

With the decision to include the ASA based inversion within GAIT, recommendations were made for the acoustic models to be included. ASTRAL 5.1 and PE 5.1 were both necessary to handle inversion of broadband and narrow-band transmission loss data. The decision was made to add ASPM 5.1 for the inversion of monostatic reverberation data. Last, Nautilus 1.0 was recommended for GAIT GS to handle the inversion of broadband time series data. A summary of the component models and their recommended application for acoustic data inversion is summarized in the following list.

- ASTRAL 5.1 – Inversion of broadband transmission loss data (capable of handling multiple frequency data) producing an estimate of the geoacoustic bottom properties in a 10-parameter LFBL format.

- PE 5.1 (RAM) – Inversion of narrowband transmission loss data (capable of handling multiple frequency data) producing an estimate of the geoacoustic bottom properties in an N-layer LFBL format.
- ASPM 5.1 – Inversion of broadband reverberation data (capable of handling multiple frequency data) producing an estimate of the geoacoustic bottom properties in a 10-parameter LFBL format with the bottom scatter kernel currently described by a Lambert's Law μ coefficient.
- Nautilus 1.0 – Inversion of broadband time series data producing an estimate of the geoacoustic bottom properties in an N-layer LFBL format.

At the time this summary report was completed, the integration of ASTRAL 5.1, PE 5.1 and ASPM 5.1 were completed. The integration of Nautilus 1.0 is scheduled to be completed in the October – December 2004 time frame under funding from PMW-150. The use of Nautilus 1.0 for time series inversion replaced the effort planned for this SBIR to invert broadband time series using the ASTRAL model.

The GAIT V&V committee has currently planned a summary report of the GAIT V&V test cases with their recommendations which will cover the GAIT GS software developed under this SBIR. As of September 2004, the current plan is to include just the GAIT GS software as the initial GAIT Version 1.0 submitted to OAML. Documentation is partially completed for the GAIT GS software and that documentation will be completed with PMW-150 support during FY 05. The transition of the ASA based inversion software first developed in late 1999 and early 2000 under the Phase I SBIR from ONR into an OAML approved GAIT Version 1.0 is currently underway. Additional transitions to particular Fleet platforms are currently being explored. In August 2004, PSI submitted a Phase I SIBR proposal to NAVAIR under SBIR Topic N04-247 to extend the capabilities developed under this ONR SBIR to bistatic and multistatic geometries for Fleet air ASW assets. PSI is teaming with APL/UW on this Phase I SBIR proposal bringing together PSI's experience with geoacoustic inversion software and APL/UW's work on GABIM (Geophysical Bottom Interaction Model).

Inversion Technique Workshop (ITW)

The ITW was held in May 2001 in Gulfport, MS and co-sponsored by SPAWAR PMW-155 (now PMW-150) and ONR Code 32. Stanley Chin-Bing (NRL-SSC) and N. Ross Chapman (U. of Victoria) were co-chairs of the workshop. The workshop was organized in a manner similar to

the previous PE workshops and the Vancouver workshop on geoacoustic inversion.[1] A series of test cases, both synthetic and measured data, were provided to the workshop participants in early 2001 with the participants presenting their results at the workshop in May before the workshop organizers revealed the actual geoacoustic properties for the test cases. The purpose of the workshop was to determine the current status of geoacoustic inversion techniques in the represented communities and provide both SPAWAR PMW-155 and ONR Code 32 a baseline for current and future programs.

The synthetic test cases for the ITW were generated using the RAM Version 1.5 propagation loss model. The predictions generated by RAM were checked against those from the COUPLE propagation loss model to insure that the results were consistent between these two high-fidelity models. The workshop participants were provided with complex acoustic pressure at a large number of frequencies (25 Hz to 199 Hz in 1 Hz steps and 200 Hz to 500 Hz in 5 Hz steps), at a number of vertical array locations (500 meters to 5000 meters in 500 meters steps with complex pressure provided from 20 meters to 80 meters depth in 1 meter increments) and at a two horizontal array locations (25 meters and 85 meters depth in 5 meter range steps from 5 meters to 5000 meters in range from the source location).[2] The synthetic data sets represented a majority of the ITW test cases and presented a type of acoustic data, narrow-band TL data, that ASTRAL is poorly equipped to predict. To better illustrate the capabilities of the ASA based TL inversion software, the ASA based TL inversion code was implemented using Navy standard PE 5.0. The inversion software utilized the RAM portion of PE 5.0 and not the Split-Step PE (SSPE) portion of PE 5.0.

The characterization of the ocean bottom for the synthetic ITW test cases was an N-layer geoacoustic profile which differed from the 10-parameter LFBL geoacoustic representation of the ocean bottom used for inversions with ASTRAL during the Phase I tasking. This characteristic of the synthetic ITW test cases also made the used of ASTRAL undesirable. The ASA based TL inversion software using PE 5.0 (RAM) was written for several specific cases including the inversion of a single layer (N = 1), two layers (N = 2) and for a range-dependent

---

[1] A. Tolstoy, N. R. Chapman and G. Brooke, "Workshop '97: Benchmarking for Geoacoustic Inversion in Shallow Water," *Journal of Computational Acoustics*, **6** (1), pp. 1-28 (1998).

[2] Description of complex pressure data sets was taken from "Inversion Technique Workshop" document distributed by the ITW organizers on the FTP site with the acoustic data files.

bottom that modeled a range-dependent intrusion present in the sediment of test case 3. A complete summary of the ITW test cases and the results using the ASA based TL inversion software is provided in the Phase II SBIR summary report.

An overview of the ITW with papers by many of the workshop participants is being published in two special issues of the IEEE Journal of Oceanic Engineering (J of OE) during 2003.[3] A paper highlighting the results using the ASA based inversion software is scheduled to appear in the second of the two special issues. Much of the text and graphics used in the following sections describing the results for the ITW test cases comes from the paper submitted for the special issues of the IEEE J of OE.

ITW – Test Case 0 (Calibration Test Case)

The details of test case 0 (calibration case) are available in the paper by the GAIT organizers in part I of the special issue on geoacoustic inversion.[3] The purpose of this test case was to provide a test case with a known geoacoustic ocean bottom description to the workshop participants.

The input file used for RAM 1.5 was converted into an input file for PE 5.0 and the output from PE 5.0 compared with the synthetic data provided. The comparison between PE 5.0 and RAM 1.5 at 25 Hz for both the 25 and 85 meter receiver depth is shown in Figure 1. The plots show what was summarized in Table 1. The reduced chi-square value for the true environment was 5.6142; significantly higher than the reduced chi-square of 2.0354 the ASA based inversion obtained using the 25, 50, 100, 200, 400 and 500 Hz TL data. The same comparison is made for test case 0 at 200 Hz and shown in Figure 2. Unlike the results for 25 Hz, the predictions from PE 5.0 using both the true environment and the ASA inversion environment each match the synthetic data quite well.

The three plots in Figure 3 provide a graphical comparison between the true environment and the inverted geoacoustic properties from ASA algorithm for a two-layer bottom using the 25, 50, 100 and 200 Hz synthetic data. A comparison of the two sets of parameters shows that the values of some parameters (sediment layer thickness, sound speed at the top and bottom of the sediment layer, sound speed in the basement and density at the top of the sediment layer) are very similar.

---

[3] N. R. Chapman, S. Chin-Bing, D. King and R. E. Evans, "Benchmarking geoacoustic inversion methods for range dependent waveguides," *IEEE Journal of Oceanic Engineering*, **28**, 2003.

However, the remaining geoacoustic parameters (density at the bottom of the sediment layer, density in the basement and all the attenuation values) were significantly dissimilar.

An interesting test that was conducted during the workshop was to take the geoacoustic parameters produced by the inversion algorithm and use them to calculate the acoustic field at a different frequency, source depth and receiver depth. For test case 0, the new source depth was 70 meters and new receiver depth was 30 meters. The frequencies chosen were 80 and 220 Hz and the synthetic data was again computed using RAM 1.5. The results of this comparison for the geoacoustic parameters in Figure 3 are shown in Figure 4 for 80 Hz and in Figure 5 for 220 Hz. The agreement between the synthetic data, generated using RAM 1.5, and the inverted geoacoustic parameters using PE 5.0 is reasonably good for both frequencies with better agreement at 220 Hz.

ITW – Test Case 1 (Monotonic Downslope Test Case)

Test case 1, a monotonic downslope case, began a series of three synthetic test cases where the geoacoustic properties of the ocean bottom were unknown. The details of this test case are available in the paper by the ITW organizers in this issue of the IEEE J of OE. Test case 1 presented the first opportunity to invert for a geoacoustic bottom with more than one sediment layer. The inversion results from test case 1 had a better fit using two sediment layers than using one sediment layer as measured by the reduced chi-square value. No inversions were done using three or more sediment layers.

Table 1 shows that the inverted fit using PE 5.0 for either set of frequencies was better than the fit using PE 5.0 with the true environment for test case 1. These results show that the inverted fit worsens with the addition of the 400 and 500 Hz data while the fit using the true environment improves with the addition of the 400 and 500 Hz data. This effect is consistent for all the synthetic test cases in the ITW. The three plots in Figure 6 provide a graphical comparison between the true environment and the inverted geoacoustic properties from the ASA algorithm for a two-layer bottom using the 25, 50, 100 and 200 Hz synthetic data.

A comparison between the synthetic TL data and the TL predicted using the inverted geoacoustic parameters for test case 1 was also done at 80 and 220 Hz for a source depth of 70 meters and a receiver depth of 30 meters. The comparison at 80 Hz (shown in Figure 7) and at 220 Hz (shown in Figure 8) show that the inverted geoacoustic parameters are able to produce TL that closely matches the synthetic TL data though not to the same degree as observed in test case 0 (shown in

Figure 4 for 80 Hz and in Figure 5 for 220 Hz). Similar to the results for test case 0, the agreement between the synthetic TL data and the TL predicted using the inverted geoacoustic parameters is better at 220 Hz than at 80 Hz.

ITW – Test Case 2 (Shelf-break Test Case)

Test case 2, a shelf-break case, featured an upslope section of bathymetry for the first 2,100 meters and then a constant bathymetry section for the remaining 2,900 meters. The geoacoustic properties of the bottom were unknown with the exception that the geoacoustic properties were constant over the 5 km range.

The lowest reduced chi-square value for test case 2, presented in Table 1, was the result of the inversion using the 50, 100 and 200 Hz TL data with a one-layer representation of the sediment overlying a basement layer. The three plots in Figure 9 show the compressional sound speed, density and attenuation for the sediment as a function of depth for both the true environment and for the best inverted fit to the synthetic data. For this inversion of the test case 2 synthetic data, the thickness of the first sediment layer is comparable to that of the true environment. The sound speed in both the sediment layer and the basement, the density at the top of the sediment layer and the attenuation in the sediment layer are quite comparable to the true environment. However, the density at the bottom of the sediment layer and the density and attenuation of the basement are all significantly different from the true environment.

The inverted geoacoustic parameters for test case 2 were used to predict the TL at 80 and 220 Hz for a source depth of 70 meters and a receiver depth of 30 meters. The comparison between the synthetic TL data using the true environment and the TL predicted using the inverted geoacoustic parameters are shown in Figure 10 for 80 Hz and in Figure 11 for 220 Hz. The agreement between the synthetic and predicted TL is better at 220 Hz than at 80 Hz as was observed in both of the previous synthetic test cases.

ITW – Test Case 3 (Flat Bottom Test Case with Range-Dependent Intrusion in Bottom)

Unlike test cases 0 through 2 which had range-dependent bathymetry but range-independent geoacoustic properties, test case 3 featured range-independent bathymetry with range-dependent geoacoustic properties. The following notation, "There is a range dependence in the geoacoustics that models an intrusion in the sediment," was provided with the description of test case 3.

For test case 3, inversions with the following bottom descriptions were performed.

1. Range-independent bottom with one-layer.
2. Range-independent bottom with two-layers.
3. Range-dependent (one change in bottom properties with range) bottom with one-layer in each geoacoustic region over a basement.
4. Range-dependent (two changes in bottom properties with range) bottom with one-layer in each geoacoustic region over a basement/intrusion.

These bottom descriptions progress from a simple range-independent bottom description with a single-layer to a bottom description that most closely approximates the actual bottom used to generate the synthetic data for test case 3. Prior to the workshop, we were able to make a limited number of runs for bottom types 1 through 3 but added bottom type 4 after the workshop to investigate whether there was sufficient sensitivity to determine both the start and end range of the intrusion as well as other properties of the sediment not defined in the prior bottom descriptions.

The inversion results shown in Table 1 for test case 3 are for bottom type 4 that most closely approximates the true environment used to generate the synthetic data and results in the best fit to the synthetic TL data as measured by the reduced chi-square values from the inversions. The inversion using the 25, 50, 100, 200, 400 and 500 Hz TL data predicted the range extent of the intrusion to be between 1,096.1 and 2,837.3 meters which compared quite favorably with the true values of 1,100 and 2,900 meters. The inverted geoacoustic parameters for the background environment (from 0 to 1,100 meters and from 2,900 to 5,000 meters) are shown with the true geoacoustic parameters used to generate the synthetic TL data are shown in Figure 12. The comparison between the inverted and true geoacoustic parameters for the intrusion (from 1,100 to 2,900 meters) are shown in Figure 13.

An example of the subtle difference between the different bottom types assumed by the inversion software for test case 3 is shown in Figure 14 for the 400 Hz data. The inverted fits to the synthetic data are nearly indistinguishable at the shorter ranges (less than 2 km) and are still a reasonable representation of the synthetic data out to the maximum range of 5 km. The reduced chi-square values for the various bottom types varied from a high value of 7.664 for the 1-layer range-independent bottom type (type 1 from the list above) to a low value of 5.712 for the 1-layer range-dependent bottom type (type 4 from the list above). The ability of the inversion

algorithm to match the synthetic data did improve with the increasing complexity of the bottom description but not as dramatically as one might expect. The very simple one-layer, range-independent bottom description provided a reasonable facsimile to the synthetic data at most ranges and frequencies.

The inverted geoacoustic parameters were again used to generated predicted TL at a different frequency (80 and 220 Hz), source depth (70 meters) and receiver depth (30 meters). These predicted TL were compared with the synthetic TL data and are shown in Figure 15 for 80 Hz and in Figure 16 for 220 Hz. For test case 3 the comparison between the synthetic and predicted TL showed some significant differences at longer ranges (greater than 3 km) for the 220 Hz comparison.

ITW – Test Case 4 (Broadband Measured Data Test Case #1)

The measured data test cases were inverted using the ASA algorithm paired with PE 5.0 (RAM) and ASTRAL 5.0. There is a considerable difference in runtimes for inversions using these two propagation loss models. An inversion that makes 3,000 calls to the ASTRAL 5.0 model can take between 3 and 6 minutes on an Athlon 1.3 GHz PC while an inversion that makes 3,000 calls to PE 5.0 takes from 12 to 24 hours on the same hardware. The runtimes using PE 5.0 were somewhat variable due to the fact that the basement thickness was treated as an unknown and the thickness of the basement has a considerable effect on the computational effort for PE 5.0. The inversions with ASTRAL 5.0 used the TL data at 50, 100, 200, 400 and 800 Hz while the inversion with PE 5.0 used the TL data at 25, 50, 100, 200 and 400 Hz. The TL data at 800 Hz was not used to in the inversions using PE 5.0 due to the significant increase in runtimes that would be incurred for running PE 5.0 at 800 Hz. For both test cases 4 and 5 the geoacoustic properties of the bottom were taken to be range-independent over the ranges for which TL data were provided.

Test case 4 included a single transmission loss data set with TL data in octave bands from 25 to 800 Hz and third-octave bands at 3.5 and 6.5 KHz. In addition to range-dependent bathymetry along the TL track, there were seven BT (Bathythermograph) profiles provided along the TL track. Both the range-dependent bathymetry and range-dependent BT information were included in the environmental information provided to the inversion algorithm and propagation loss models.

The inversion results using ASTRAL 5.0 are shown in Figure 17 and include the octave band TL data from 25 Hz to 800 Hz and the bathymetry and BT profiles along the TL track. The inversion was not run on the 25 Hz due to the lower frequency limit of 50 Hz on the ASTRAL 5.0 propagation loss model. There are two inversion fits to the TL data showing the fit after running 3,000 steps through the inversion algorithm (red line) and 10,000 steps through the inversion algorithm (blue line). The interest in the comparison between the two inversion fits is to show that there is a negligible improvement in the goodness of fit (reduced chi-square value) for the increase in computational effort. The reduced chi-square value drops from a value of 10.73692 for 3,000 steps to a value of 10.18124 for 10,000 steps. A summary of the inverted geoacoustic parameters for test case 4 is shown in Table 3 for both the ASTRAL 5.0 and PE 5.0 inversions.

ITW – Test Case 5 (Broadband Measured Data Test Case #2)

Test case 5 included four sets of TL data in octave bands from 25 to 800 Hz. An example of the ASTRAL 5.0 based inversions of TL post 1 from test case 5 is shown in Figure 18. The results are presented in the same manner as those for test case 4 with ASTRAL 5.0 based inversion runs for 3,000 and 10,000 steps shown for comparison. A summary of the measured data TL inversion results is shown in Table 2. This table summarizes the inversion results using both ASTRAL 5.0 and PE 5.0. While a direct comparison of the results cannot be made due to the inversions being done over different sets of frequencies, ASTRAL 5.0 used 50 to 800 Hz TL data and PE 5.0 used 25 to 400 Hz TL data, the results show that the ASTRAL 5.0 inversion is able to produce a fit to the measured TL data that can be called at least comparable to that obtained from PE 5.0. A summary of the inverted geoacoustic parameters for test case 5 is shown in Table 3 for both the ASTRAL 5.0 and PE 5.0 inversions.

For clarity, it should be noted that the PE 5.0 based inversions of the measured data cases used the single-frequency, unaveraged results for the inversion. As the data has been averaged across an octave band, this puts the inversion using PE 5.0 at a disadvantage to ASTRAL 5.0 which has a default range-averaging in its output that can be equated to the octave band averaging and the uncertainty inherent in the ranges for the measured TL data.

A sample of the PE 5.0 based inversion of the measured data cases is shown in Figure 19. The results shown include the PE 5.0 inversion results for 10,000 steps. The red line in Figure 19 is the unaveraged output from PE 5.0 using the best-fit geoacoustic parameters (one-layer over a semi-infinite basement). The blue line in Figure 19 is the range-averaged output from PE 5.0 using the same set of geoacoustic parameters. The range-averaged output is certainly a closer

approximation to the octave band TL data. These results are indicative of those for both test cases 4 and 5 where the inversion using PE 5.0 produced results that were a poorer fit, as measured by the reduced chi-square value, to the measured TL data than the results using ASTRAL 5.0 with the inversion software.

ITW – Summary and Conclusions

The synthetic test cases from the ITW provided a unique challenge for the TL inversion software. Unlike measured data, these synthetic test cases do not include the noise and uncertainty present in measured TL data. However, the subtle effect of different versions of propagation loss models resulted in the unexpected result that the inversion software was able to find a better fit to the synthetic data than from the true environment. The results did show that the ASA based TL inversion software using PE 5.0 was both robust in searching the solution space for a best-fit to the synthetic TL data and reasonably efficient, in terms of the number of inversion steps, when compared with the ASTRAL 5.0 based inversion software.

The question of which propagation loss model to use is certainly more complex than simply what type of acoustic data is available. The application of the inferred ocean bottom geoacoustics must also be considered. For example, inverting broadband TL for use in an application that uses ASTRAL 5.0 with an inversion algorithm using PE 5.0 will produce results that are less optimal than inverting the acoustic data using ASTRAL 5.0. This contradicts the assumption that a higher fidelity propagation loss model will always produce better results when used for as part of an inversion.

Automated inversions of acoustic data for an inferred estimate of the geoacoustic properties of the ocean bottom are a valuable tool but should not be considered a magic bullet. The inversion algorithm are not designed to understand the propagation loss models that they are manipulating and do not have any understanding of mechanisms responsible for the deposition of sediments on the ocean bottom. The inversion algorithms are instructed to minimize a cost function that expresses in a mathematical expression the difference between an observed data set, in our case observed TL data, and a model prediction. By carefully selecting both how the geoacoustic parameters are described and by intelligently selecting the bounds on these parameters, the inversion algorithm can be guided to search only the portion of the solution space that represents "plausible" ocean bottoms.

Geoacoustic Inversion Toolkit (GAIT) Global Search (GS)

Following the ITW in May 2001, PSI was informed in late 2001 that it had been selected as a developer of the SPAWAR PMW-155 acoustic data inversion product to be called GAIT.[4] The GAIT logo from by PMW-155 (now PMW-150) is shown to the right.

Modifications to ASA Based TL Inversion Software to Create GAIT GS Version 1.0

The ASA based TL inversion used for the 2001 Gulfport Workshop has been significantly modified to achieve the requirements set forth for GAIT GS Version 1.0. The manner by which the bounds on the geoacoustic parameters for an N-layer bottom were specified was significantly changed to both provide more control over the searched solution space and to provide a method by which unphysical bottom characterizations could be avoided. Other more subtle changes were added to the software including linking the parameter bounds for the sediment bulk density to the sediment compressional sound speed and adding two additional cost functions developed by ARL-UT. Details of each of these changes will be provided in the subsequent sections.

Integration of Multiple Acoustic Models within the GAIT GS Version 1.0 Software

The software products developed under the Phase I SBIR were individually tailored for specific acoustic model (ASTRAL, PE) with the result that the source code for each of these different products was maintained separately. The goal of GAIT GS was to bring the suite of acoustic models (ASTRAL, PE, Nautilus, ASPM) under the single main program so that certain common elements were used and consistent for all the acoustic models.

Using a System Based on Gradients and Ratios for N-layer Geoacoustic Parameter Bounds

With the change to an N-layer bottom with an arbitrary number of layers, it became necessary to change the method by which the parameters were constrained for the inversion. Previous techniques for one or two layers used parameter bounds for each geoacoustic parameter that were the actual physical value of each parameter (e.g., sound speed value were bounded by an upper and lower bound that were physical sound speeds). The technique, while easy to understand, has some significant problems. First, it can result in unphysical values for the resulting inverted

[4] GAIT was originally an acronym for Geoacoustic Inversion Techniques but was later changed to an acronym for Geoacoustic Inversion Toolkit to more accurately reflect its makeup.

geoacoustic parameter such as a negative sound speed gradient or negative density gradient within a sediment layer.

A simple change for a single layer bottom is to change to a ratio and gradient based representation of the bottom properties (sound speed, density and attenuation). This representation is still easy to understand and implement but becomes problematic when it is extended to two or more layers for the following reason. With the geoacoustic properties for each layer now bounded by a ratio and gradient, it is difficult to place an upper bound on each geoacoustic property (sound speed, density and/or attenuation). The reason for this is that there are an infinite number of combinations of layer thicknesses, ratios and gradient and some of these combinations will produce values for the geoacoustic properties that exceed normal bounds for the properties.

A new approach is detailed in this technical note that relies upon a priori information such as maximum sound speed allowed in the sediment and basement, maximum sound speed gradient allowed in the sediment layers, minimum and maximum ratio of sound speed between layers (corresponding values exist for density and attenuation). For each geoacoustic property, a section will provide the necessary equations to parameterize the geoacoustic properties with bounds from 0 to 1, $[0,1]$, within the ASA algorithm and translate those bounds into the proper bounds controlled by the user (or algorithm developer).

Sediment Sound Speed Profile:

This is an example just for the sound speed in the sediment layers and basement. There are a number of a priori values that must be defined for this to work. Assume for now that the a priori values for maximum sound speed gradient and minimum and maximum sound speed ratio between layers are the same for all sediment layers (could be made unique for each layer in this formulation). Also, assume that layer #1 in the first layer below the LFBL layer and that there are two layers in this sediment stack.

A priori values:

- $c_{\max}$ (maximum sound speed in sediment and basement)
- $c'_{\max}$ (maximum sound speed gradient in sediment layer)
- $c_{ratio,min}$ (minimum ratio between sound speed at top of sediment layer and sound speed at bottom of previous sediment layer)

- $c_{ratio,max}$ (maximum ratio between sound speed at top of sediment layer and sound speed at bottom of previous sediment layer)

Terminology:

- c_{LFBL} (sound speed at the bottom of the top LFBL layer)
- c_{top}^{i} (sound speed at the top of layer i)
- c_{bottom}^{i} (sound speed at the bottom of layer i)
- h_i (thickness of sediment layer i)
- $c_{basement}$ (sound speed in the basement)
- $[0,1]$ (uniform random variable from 0 to 1)

Expression for sound speed at the top of layer #1:

$$c_{top}^{1} = c_{LFBL} \bullet \left([0,1] \bullet \min\left(\left(c_{ratio,max} - c_{ratio,min} \right), \left(\frac{c_{max}}{c_{LFBL}} - c_{ratio,min} \right) \right) + c_{ratio,min} \right)$$

In the case where $[0,1]$ is equal to 0, then c_{top}^{1} is equal to $c_{LFBL} \bullet c_{ratio,min}$. In the case where $[0,1]$ is equal to 1, then c_{top}^{1} is equal to $c_{LFBL} \bullet c_{ratio,max}$ if $\left(c_{ratio,max} - c_{ratio,min}\right) \le \left(c_{max}/c_{LFBL} - c_{ratio,min}\right)$ and equal to c_{max} if $\left(c_{ratio,max} - c_{ratio,min}\right) > \left(c_{max}/c_{LFBL} - c_{ratio,min}\right)$. Note that c_{top}^{1} can never be greater than c_{max} in this expression.

Expression for sound speed at the bottom of layer #1:

$$c_{bottom}^{1} = c_{top}^{1} + [0,1] \bullet \min\left(\left(c'_{max} \bullet h_1 \right), \left(c_{max} - c_{top}^{1} \right) \right)$$

In the case where $[0,1]$ is equal to 0, then c_{bottom}^{1} is equal to c_{top}^{1}. In the case where $[0,1]$ is equal to 1, then c_{bottom}^{1} is equal to $c_{top}^{1} + c'_{max} \bullet h_1$ if $\left(c'_{max} \bullet h_1\right) \le \left(c_{max} - c_{top}^{1}\right)$ and equal to c_{max} if $\left(c'_{max} \bullet h_1\right) > \left(c_{max} - c_{top}^{1}\right)$. Note that c_{bottom}^{1} can never be greater than c_{max} in this expression and that gradient in this layer can not exceed the a priori limit of c'_{max}.

Expression for sound speed at the top of layer #2:

$$c_{top}^{2} = c_{bottom}^{1} \bullet \left([0,1] \bullet \min\left(\left(c_{ratio,max} - c_{ratio,min} \right), \left(\frac{c_{max}}{c_{bottom}^{1}} - c_{ratio,min} \right) \right) + c_{ratio,min} \right)$$

In the case where [0,1] is equal to 0, then c^2_{top} is equal to $c^1_{bottom} \bullet c_{ratio,min}$. In the case where [0,1] is equal to 1, then c^2_{top} is equal to $c^1_{bottom} \bullet c_{ratio,max}$ if $(c_{ratio,max} - c_{ratio,min}) \leq (c_{max}/c^1_{bottom} - c_{ratio,min})$ and equal to c_{max} if $(c_{ratio,max} - c_{ratio,min}) > (c_{max}/c^1_{bottom} - c_{ratio,min})$. Note that c^2_{top} can never be greater than c_{max} in this expression.

Expression for sound speed at the bottom of layer #2:

$$c^2_{bottom} = c^2_{top} + [0,1] \bullet \min((c'_{max} \bullet h_2), (c_{max} - c^2_{top}))$$

In the case where [0,1] is equal to 0, then c^2_{bottom} is equal to c^2_{top}. In the case where [0,1] is equal to 1, then c^2_{bottom} is equal to $c^2_{top} + c'_{max} \bullet h_2$ if $(c'_{max} \bullet h_2) \leq (c_{max} - c^2_{top})$ and equal to c_{max} if $(c'_{max} \bullet h_2) > (c_{max} - c^2_{top})$. Note that c^2_{bottom} can never be greater than c_{max} in this expression and that gradient in this layer can not exceed the a priori limit of c'_{max}.

Expression for sound speed in the basement:

$$c_{basement} = c^2_{bottom} + [0,1] \bullet (c_{max} - c^2_{bottom})$$

In the case where [0,1] is equal to 0, then $c_{basement}$ is equal to c^2_{bottom}. In the case where [0,1] is equal to 1, then $c_{basement}$ is equal to c_{max}. Note that $c_{basement}$ can never be greater than c_{max} in this expression and assumes that the sound speed in the basement is greater than or equal to the sound speed at the bottom of the deepest sediment layer.

Sediment Density Profile:

This is an example just for the density in the sediment layers and basement. There are a number of a priori values that must be defined for this to work. Assume for now that the a priori values for maximum density gradient and minimum and maximum density ratio between layers are the same for all sediment layers (could be made unique for each layer in this formulation). Also, assume that layer #1 in the first layer below the LFBL layer and that there are two layers in this sediment stack.

A priori values:

- ρ_{max} (maximum density in sediment and basement)
- ρ'_{max} (maximum density gradient in sediment layer)

- $\rho_{ratio,min}$ (minimum ratio between density at top of sediment layer and density at bottom of previous sediment layer)
- $\rho_{ratio,max}$ (maximum ratio between density at top of sediment layer and density at bottom of previous sediment layer)

Terminology:

- ρ_{LFBL} (density at the bottom of the top LFBL layer)
- ρ_{top}^{i} (density at the top of layer i)
- ρ_{bottom}^{i} (density at the bottom of layer i)
- h_i (thickness of sediment layer i)
- $\rho_{basement}$ (density in the basement)
- $[0,1]$ (uniform random variable from 0 to 1)

Expression for density at the top of layer #1:

$$\rho_{top}^{1} = \rho_{LFBL} \bullet \left([0,1] \bullet \min\left(\left(\rho_{ratio,max} - \rho_{ratio,min} \right), \left(\frac{\rho_{max}}{\rho_{LFBL}} - \rho_{ratio,min} \right) \right) + \rho_{ratio,min} \right)$$

In the case where $[0,1]$ is equal to 0, then ρ_{top}^{1} is equal to $\rho_{LFBL} \bullet \rho_{ratio,min}$. In the case where $[0,1]$ is equal to 1, then ρ_{top}^{1} is equal to $\rho_{LFBL} \bullet \rho_{ratio,max}$ if $\left(\rho_{ratio,max} - \rho_{ratio,min}\right) \leq \left(\rho_{max} / \rho_{LFBL} - \rho_{ratio,min}\right)$ and equal to ρ_{max} if $\left(\rho_{ratio,max} - \rho_{ratio,min}\right) > \left(\rho_{max} / \rho_{LFBL} - \rho_{ratio,min}\right)$. Note that ρ_{top}^{1} can never be greater than ρ_{max} in this expression.

Expression for density at the bottom of layer #1:

$$\rho_{bottom}^{1} = \rho_{top}^{1} + [0,1] \bullet \min\left(\left(\rho'_{max} \bullet h_1 \right), \left(\rho_{max} - \rho_{top}^{1} \right) \right)$$

In the case where $[0,1]$ is equal to 0, then ρ_{bottom}^{1} is equal to ρ_{top}^{1}. In the case where $[0,1]$ is equal to 1, then ρ_{bottom}^{1} is equal to $\rho_{top}^{1} + \rho'_{max} \bullet h_1$ if $\left(\rho'_{max} \bullet h_1\right) \leq \left(\rho_{max} - \rho_{top}^{1}\right)$ and equal to ρ_{max} if $\left(\rho'_{max} \bullet h_1\right) > \left(\rho_{max} - \rho_{top}^{1}\right)$. Note that ρ_{bottom}^{1} can never be greater than ρ_{max} in this expression and that gradient in this layer can not exceed the a priori limit of ρ'_{max}.

Expression for density at the top of layer #2:

$$\rho_{top}^{2} = \rho_{bottom}^{1} \bullet \left([0,1] \bullet \min\left(\left(\rho_{ratio,max} - \rho_{ratio,min} \right), \left(\frac{\rho_{max}}{\rho_{bottom}^{1}} - \rho_{ratio,min} \right) \right) + \rho_{ratio,min} \right)$$

In the case where $[0,1]$ is equal to 0, then ρ_{top}^{2} is equal to $\rho_{bottom}^{1} \bullet \rho_{ratio,min}$. In the case where $[0,1]$ is equal to 1, then ρ_{top}^{2} is equal to $\rho_{bottom}^{1} \bullet \rho_{ratio,max}$ if $\left(\rho_{ratio,max} - \rho_{ratio,min}\right) \leq \left(\rho_{max} / \rho_{bottom}^{1} - \rho_{ratio,min}\right)$ and equal to ρ_{max} if $\left(\rho_{ratio,max} - \rho_{ratio,min}\right) > \left(\rho_{max} / \rho_{bottom}^{1} - \rho_{ratio,min}\right)$. Note that ρ_{top}^{2} can never be greater than ρ_{max} in this expression.

Expression for density at the bottom of layer #2:

$$\rho_{bottom}^{2} = \rho_{top}^{2} + [0,1] \bullet \min\left(\left(\rho'_{max} \bullet h_2 \right), \left(\rho_{max} - \rho_{top}^{2} \right) \right)$$

In the case where $[0,1]$ is equal to 0, then ρ_{bottom}^{2} is equal to ρ_{top}^{2}. In the case where $[0,1]$ is equal to 1, then ρ_{bottom}^{2} is equal to $\rho_{top}^{2} + \rho'_{max} \bullet h_2$ if $\left(\rho'_{max} \bullet h_2\right) \leq \left(\rho_{max} - \rho_{top}^{2}\right)$ and equal to ρ_{max} if $\left(\rho'_{max} \bullet h_2\right) > \left(\rho_{max} - \rho_{top}^{2}\right)$. Note that ρ_{bottom}^{2} can never be greater than ρ_{max} in this expression and that gradient in this layer can not exceed the a priori limit of ρ'_{max}.

Expression for density in the basement:

$$\rho_{basement} = \rho_{bottom}^{2} + [0,1] \bullet \left(\rho_{max} - \rho_{bottom}^{2} \right)$$

In the case where $[0,1]$ is equal to 0, then $\rho_{basement}$ is equal to ρ_{bottom}^{2}. In the case where $[0,1]$ is equal to 1, then $\rho_{basement}$ is equal to ρ_{max}. Note that $\rho_{basement}$ can never be greater than ρ_{max} in this expression and assumes that the density in the basement is greater than or equal to the density at the bottom of the deepest sediment layer.

Sediment Attenuation Profile:

This is an example just for the attenuation in the sediment layers and basement. There are a number of a priori values that must be defined for this to work. Assume for now that the a priori values for maximum attenuation gradient and minimum and maximum attenuation ratio between layers are the same for all sediment layers (could be made unique for each layer in this formulation). Also, assume that layer #1 in the first layer below the LFBL layer and that there are two layers in this sediment stack.

A priori values:

- $\alpha_{\max}$ (maximum attenuation in sediment and basement)
- $\alpha_{\min}$ (minimum attenuation in sediment and basement) – Optional constraint
- $\alpha'_{\max}$ (maximum attenuation gradient in sediment layer)
- $\alpha'_{\min}$ (minimum attenuation gradient in sediment layer) – Optional constraint
- $\alpha_{ratio,min}$ (minimum ratio between attenuation at top of sediment layer and attenuation at bottom of previous sediment layer)
- $\alpha_{ratio,max}$ (maximum ratio between attenuation at top of sediment layer and attenuation at bottom of previous sediment layer)

Terminology:

- α_{LFBL} (attenuation at the bottom of the top LFBL layer)
- α^i_{top} (attenuation at the top of layer i)
- α^i_{bottom} (attenuation at the bottom of layer i)
- h_i (thickness of sediment layer i)
- $\alpha_{basement}$ (attenuation in the basement)
- $[0,1]$ (uniform random variable from 0 to 1)

Expression for attenuation at the top of layer #1:

$$\alpha^1_{top} = \alpha_{LFBL} \bullet \left([0,1] \bullet \min\left((\alpha_{ratio,max} - \alpha_{ratio,min}), \left(\frac{\alpha_{max}}{\alpha_{LFBL}} - \alpha_{ratio,min} \right) \right) + \alpha_{ratio,min} \right)$$

In the case where $[0,1]$ is equal to 0, then α^1_{top} is equal to $\alpha_{LFBL} \bullet \alpha_{ratio,min}$. In the case where $[0,1]$ is equal to 1, then α^1_{top} is equal to $\alpha_{LFBL} \bullet \alpha_{ratio,max}$ if $(\alpha_{ratio,max} - \alpha_{ratio,min}) \leq (\alpha_{max}/\alpha_{LFBL} - \alpha_{ratio,min})$ and equal to α_{max} if $(\alpha_{ratio,max} - \alpha_{ratio,min}) > (\alpha_{max}/\alpha_{LFBL} - \alpha_{ratio,min})$. Note that α^1_{top} can never be greater than α_{max} in this expression.

With Optional Constraints:

$$\alpha^1_{top} = \alpha_{LFBL} \bullet \left(\begin{array}{l} [0,1] \bullet \min\left(\left(\alpha_{ratio,max} - \max\left(\left(\frac{\alpha_{min}}{\alpha_{LFBL}} \right), \alpha_{ratio,min} \right) \right), \left(\frac{\alpha_{max}}{\alpha_{LFBL}} - \max\left(\left(\frac{\alpha_{min}}{\alpha_{LFBL}} \right), \alpha_{ratio,min} \right) \right) \right) \\ + \max\left(\left(\frac{\alpha_{min}}{\alpha_{LFBL}} \right), \alpha_{ratio,min} \right) \end{array} \right)$$

In the case where $[0,1]$ is equal to 0, then α^1_{top} is equal to $\alpha_{LFBL} \bullet \alpha_{ratio,min}$ if $(\alpha_{ratio,min}) \geq (\alpha_{min} / \alpha_{LFBL})$ and equal to α_{min} if $(\alpha_{ratio,min}) < (\alpha_{min} / \alpha_{LFBL})$. In the case where $[0,1]$ is equal to 1, then α^1_{top} is equal to $\alpha_{LFBL} \bullet \alpha_{ratio,max}$ if $(\alpha_{ratio,max} - \max((\alpha_{min} / \alpha_{LFBL}), \alpha_{ratio,min})) \leq (\alpha_{max} / \alpha_{LFBL} - \max((\alpha_{min} / \alpha_{LFBL}), \alpha_{ratio,min}))$ and equal to α_{max} if $(\alpha_{ratio,max} - \max((\alpha_{min} / \alpha_{LFBL}), \alpha_{ratio,min})) > (\alpha_{max} / \alpha_{LFBL} - \max((\alpha_{min} / \alpha_{LFBL}), \alpha_{ratio,min}))$. Note that α^1_{top} can never be greater than α_{max} or less than α_{min} in this expression.

Expression for attenuation at the bottom of layer #1:

$$\alpha^1_{bottom} = \alpha^1_{top} + [0,1] \bullet \min\left((\alpha'_{max} \bullet h_1), (\alpha_{max} - \alpha^1_{top}) \right)$$

In the case where $[0,1]$ is equal to 0, then α^1_{bottom} is equal to α^1_{top}. In the case where $[0,1]$ is equal to 1, then α^1_{bottom} is equal to $\alpha^1_{top} + \alpha'_{max} \bullet h_1$ if $(\alpha'_{max} \bullet h_1) \leq (\alpha_{max} - \alpha^1_{top})$ and equal to α_{max} if $(\alpha'_{max} \bullet h_1) > (\alpha_{max} - \alpha^1_{top})$. Note that α^1_{bottom} can never be greater than α_{max} in this expression and that gradient in this layer can not exceed the a priori limit of α'_{max}.

With Optional Constraints:

$$\alpha^1_{bottom} = \alpha^1_{top} + \left(\begin{array}{l} [0,1] \bullet \left(\min\left((\alpha'_{max} \bullet h_1), (\alpha_{max} - \alpha^1_{top}) \right) - \max\left((\alpha'_{min} \bullet h_1), (\alpha_{min} - \alpha^1_{top}) \right) \right) \\ + \max\left((\alpha'_{min} \bullet h_1), (\alpha_{min} - \alpha^1_{top}) \right) \end{array} \right)$$

In the case where $[0,1]$ is equal to 0, then α^1_{bottom} is equal to $\alpha^1_{top} + \alpha'_{min} \bullet h_1$ if $(\alpha'_{min} \bullet h_1) \geq (\alpha_{inx} - \alpha^1_{top})$ and equal to α_{min} if $(\alpha'_{min} \bullet h_1) < (\alpha_{inx} - \alpha^1_{top})$. In the case where $[0,1]$ is equal to 1, then α^1_{bottom} is equal to $\alpha^1_{top} + \alpha'_{max} \bullet h_1$ if $(\alpha'_{max} \bullet h_1) \leq (\alpha_{max} - \alpha^1_{top})$ and equal to α_{max} if $(\alpha'_{max} \bullet h_1) > (\alpha_{max} - \alpha^1_{top})$. Note that α^1_{bottom} can never be greater than α_{max} or less than α_{min} in this expression and that gradient in this layer can not exceed the a priori limit of α'_{max} or α'_{min}.

Expression for attenuation at the top of layer #2:

$$\alpha_{top}^{2} = \alpha_{bottom}^{1} \bullet \left([0,1] \bullet \min\left(\left(\alpha_{ratio,max} - \alpha_{ratio,min} \right), \left(\frac{\alpha_{max}}{\alpha_{bottom}^{1}} - \alpha_{ratio,min} \right) \right) + \alpha_{ratio,min} \right)$$

In the case where $[0,1]$ is equal to 0, then α_{top}^{2} is equal to $\alpha_{bottom}^{1} \bullet \alpha_{ratio,min}$. In the case where $[0,1]$ is equal to 1, then α_{top}^{2} is equal to $\alpha_{bottom}^{1} \bullet \alpha_{ratio,max}$ if $\left(\alpha_{ratio,max} - \alpha_{ratio,min}\right) \le \left(\alpha_{max} / \alpha_{bottom}^{1} - \alpha_{ratio,min}\right)$ and equal to α_{max} if $\left(\alpha_{ratio,max} - \alpha_{ratio,min}\right) > \left(\alpha_{max} / \alpha_{bottom}^{1} - \alpha_{ratio,min}\right)$. Note that α_{top}^{2} can never be greater than α_{max} in this expression.

With Optional Constraints:

$$\alpha_{top}^{2} = \alpha_{bottom}^{1} \bullet \left(\begin{array}{l} [0,1] \bullet \min\left(\left(\alpha_{ratio,max} - \max\left(\left(\frac{\alpha_{min}}{\alpha_{bottom}^{1}} \right), \alpha_{ratio,min} \right) \right), \left(\frac{\alpha_{max}}{\alpha_{bottom}^{1}} - \max\left(\left(\frac{\alpha_{min}}{\alpha_{bottom}^{1}} \right), \alpha_{ratio,min} \right) \right) \right) \\ + \max\left(\left(\frac{\alpha_{min}}{\alpha_{bottom}^{1}} \right), \alpha_{ratio,min} \right) \end{array} \right)$$

In the case where $[0,1]$ is equal to 0, then α_{top}^{2} is equal to $\alpha_{bottom}^{1} \bullet \alpha_{ratio,min}$ if $\left(\alpha_{ratio,min}\right) \ge \left(\alpha_{min} / \alpha_{bottom}^{1}\right)$ and equal to α_{min} if $\left(\alpha_{ratio,min}\right) < \left(\alpha_{min} / \alpha_{bottom}^{1}\right)$. In the case where $[0,1]$ is equal to 1, then α_{top}^{2} is equal to $\alpha_{bottom}^{1} \bullet \alpha_{ratio,max}$ if $\left(\alpha_{ratio,max} - \max\left(\left(\alpha_{min} / \alpha_{bottom}^{1}\right), \alpha_{ratio,min}\right)\right) \le \left(\alpha_{max} / \alpha_{bottom}^{1} - \max\left(\left(\alpha_{min} / \alpha_{bottom}^{1}\right), \alpha_{ratio,min}\right)\right)$ and equal to α_{max} if $\left(\alpha_{ratio,max} - \max\left(\left(\alpha_{min} / \alpha_{bottom}^{1}\right), \alpha_{ratio,min}\right)\right) > \left(\alpha_{max} / \alpha_{bottom}^{1} - \max\left(\left(\alpha_{min} / \alpha_{bottom}^{1}\right), \alpha_{ratio,min}\right)\right)$. Note that α_{top}^{2} can never be greater than α_{max} or less than α_{min} in this expression.

Expression for attenuation at the bottom of layer #2:

$$\alpha_{bottom}^{2} = \alpha_{top}^{2} + [0,1] \bullet \min\left(\left(\alpha'_{max} \bullet h_2 \right), \left(\alpha_{max} - \alpha_{top}^{2} \right) \right)$$

In the case where $[0,1]$ is equal to 0, then α_{bottom}^{2} is equal to α_{top}^{2}. In the case where $[0,1]$ is equal to 1, then α_{bottom}^{2} is equal to $\alpha_{top}^{2} + \alpha'_{max} \bullet h_2$ if $\left(\alpha'_{max} \bullet h_2\right) \le \left(\alpha_{max} - \alpha_{top}^{2}\right)$ and equal to α_{max} if $\left(\alpha'_{max} \bullet h_2\right) > \left(\alpha_{max} - \alpha_{top}^{2}\right)$. Note that α_{bottom}^{2} can never be greater than α_{max} in this expression and that gradient in this layer can not exceed the a priori limit of α'_{max}.

With Optional Constraints:

$$\alpha^2_{bottom} = \alpha^2_{top} + \begin{pmatrix} [0,1] \bullet \left(\min\left((\alpha'_{max} \bullet h_2), (\alpha_{max} - \alpha^2_{top})\right) - \max\left((\alpha'_{min} \bullet h_2), (\alpha_{min} - \alpha^2_{top})\right)\right) \\ + \max\left((\alpha'_{min} \bullet h_2), (\alpha_{min} - \alpha^2_{top})\right) \end{pmatrix}$$

In the case where $[0,1]$ is equal to 0, then α^2_{bottom} is equal to $\alpha^2_{top} + \alpha'_{min} \bullet h_2$ if $(\alpha'_{min} \bullet h_2) \geq (\alpha_{inx} - \alpha^2_{top})$ and equal to α_{min} if $(\alpha'_{min} \bullet h_2) < (\alpha_{inx} - \alpha^2_{top})$. In the case where $[0,1]$ is equal to 1, then α^2_{bottom} is equal to $\alpha^2_{top} + \alpha'_{max} \bullet h_2$ if $(\alpha'_{max} \bullet h_2) \leq (\alpha_{max} - \alpha^2_{top})$ and equal to α_{max} if $(\alpha'_{max} \bullet h_2) > (\alpha_{max} - \alpha^2_{top})$. Note that α^2_{bottom} can never be greater than α_{max} or less than α_{min} in this expression and that gradient in this layer can not exceed the a priori limit of α'_{max} or α'_{min}.

Expression for attenuation in the basement:

$$\alpha_{basement} = \alpha^2_{bottom} + [0,1] \bullet (\alpha_{max} - \alpha^2_{bottom})$$

In the case where $[0,1]$ is equal to 0, then $\alpha_{basement}$ is equal to α^2_{bottom}. In the case where $[0,1]$ is equal to 1, then $\alpha_{basement}$ is equal to α_{max}. Note that $\alpha_{basement}$ can never be greater than α_{max} in this expression and assumes that the attenuation in the basement is greater than or equal to the attenuation at the bottom of the deepest sediment layer.

Summary:

All the expressions are easily evaluated for the cases where $[0,1]$ is equal to 0 or 1 and show the correct behavior. It would also be possible to add a lower limit, e.g. α_{min} for cases where it was acceptable to have a negative gradient. With this formulation, all the sediment parameters would be given bounds of $[0,1]$ with the exception of the top LFBL layer and the thickness of each layer, h_i.

I think this method will work in the same way as the synthetic test case that had an inclusion at an unknown range. The ASA algorithm searches over a $[0,1]$ space while the propagation loss model maps the $[0,1]$ values into sound speeds, densities and attenuations. All that is needed is to provide the a priori values these geoacoustic parameters as noted on the first page.

Linking the Sediment Density Upper Bounds to the Sediment Compressional Sound Speed

A common problem that occurs with most inversion techniques is the determination of a best fit to the acoustic data being ascribed to a non-physical set of geoacoustic parameters. Perhaps the most common example of this problem that occurs in non-linear inversion algorithms is the

inversion algorithm estimating too high a density for a well determined compressional sound speed. The relationship linking compressional sound speed to bulk density was taken from the work of Edwin Hamilton.[5] Figure 7 in Hamilton's article presents a summary of the results and is provided to the reader of this report in Figure 20. The upper bound on the sediment density is related to the sediment sound speed by the following relationships.

$$1400 < c_{\text{sediment}} \leq 2000 \text{, then } \rho_{\max} = 1.8 + 0.4 \bullet (c_{\text{sediment}} - 1400)/600$$

$$2000 < c_{\text{sediment}} \leq 3000 \text{, then } \rho_{\max} = 2.2 + 0.4 \bullet (c_{\text{sediment}} - 2000)/1000$$

$$3000 < c_{\text{sediment}} \leq 6500 \text{, then } \rho_{\max} = 2.6 + 0.5 \bullet (c_{\text{sediment}} - 3000)/3500$$

These simple relationships, implemented within the GAIT GS Version 1.0, both prevent the

Reduced Chi-Square, Mean-Square Difference and Correlation Cost Functions

In the development of the ASA based TL inversion software, the reduced chi-square cost function was the only cost function implemented within the software. During the planning for GAIT, the use of other cost functions was considered and it was decided that two additional cost functions would be implemented within the GAIT GS Version 1.0 software. Details on all three cost functions are presented for completeness is the following sections.

For each of these cost function, the summations over the number of observed data points, D_i, represented in the above equations can be changed to a summation over the number of modeled data points, M_i. This will occur in the GAIT GS Version 1.0 when the number of modeled data points is less than the number of observed data points at a particular frequency.

All three cost function can be utilized on any of the types of acoustic data. Acoustic data for inversions using PE and ASTRAL are commonly presented in terms of transmission loss and the cost function can be evaluated using either transmission loss or P^2.

Reduced Chi-Square Cost Function

The Reduced Chi Square cost function is given in the following equation.

[5] Edwin L. Hamilton, "Sound velocity-density relations in sea floor sediments and rock," *Journal of Acoustical Society of America*, **63** (2), pp. 366-377 (1978).

$$C = \chi^2 = \frac{1}{\nu} \sum_{i=ranges,\, freqencies} \frac{(D_i - M_i)^2}{D_i}$$

The variables D_i and M_i are the observed data and modeled acoustic data. The variable ν is the degrees of freedom for the system, equal to the number of data points minus the number of independent variables for fitting. For systems with relatively few degrees of freedom such as a number of fitting variables and limited observations the reduced Chi Square will reflect the increased uncertainty.

Mean-Square Difference Cost Function

The following two cost functions were developed and provided for implementation into GAIT GS Version 1.0 by Robert A. Koch of ARL/UT (Koch, 2002). The mean-square difference cost function is given in the following equation.

$$C = \frac{1}{2} \frac{\sum_{i=ranges,\, frequewncies} (D_i - M_i)^2}{\sqrt{\sum_{i=ranges,\, frequencies} D_i^2 \sum_{i=ranges,\, frequencies} M_i^2}}$$

This cost function calculates a mean square difference between the observed data and the modeled acoustic data.

Correlation Cost Function

The correlation cost function is given in the following equation.

$$C = 1 - \frac{\sum_{i=ranges,\, frequencies} D_i M_i}{\sqrt{\sum_{i=ranges,\, frequencies} D_i^2 \sum_{i=ranges,\, frequencies} M_i^2}}$$

This cost function calculates the correlation value between the observed data and the modeled acoustic data.

GAIT GS Hardware and Software Requirements

The current hardware used for the benchmarking of the GAIT GS software is a Dell Dimension 8300 desktop PC running a Pentium 4 processor at 3.0 GHz with an 800 MHz FSB (front-side bus) speed for the memory. The Dell PC was initially equipped with 256 MB of memory which

is more than sufficient for the current version of the GAIT GS software. The current executable program size is less than 1 MB with output files generated by GAIT GS frequently being in the tens of MB in size. All run times listed for the GAIT V&V test cases will be given for this hardware configuration.

The GAIT GS has been developed using both Fortran[6] and C source code.[7] The Microsoft Developer Studio environment has been used for software development coupled with the Compaq Visual Fortran 6.x[8] and Microsoft Visual C/C++ 6.x compilers. GAIT GS Version 1.0 uses a command line interface (CLI) with all input file format in standard ASCII file format. A complete description of the input files for the software is being drafted as part of the submission of GAIT to the OAML-SRB. All testing and validation to date has been done under the Windows XP Home or Windows XP Professional operating systems.

GAIT V&V (Validation and Verification) Test Cases

In preparation for submittal to the OAML-SRB for acceptance as a Navy standard algorithm, a series of test cases were put forward by the GAIT V&V committee.[9] The test cases varied in complexity and were derived from the 1997 Vancouver Workshop and the 2001 Gulfport Workshop with several test cases building upon those test cases with much longer ranges or added noise. The GAIT V&V test cases are grouped together according to the model used for the inversion (PE 5.1, ASTRAL 5.1, ASPM 5.1 and Nautilus 1.0). The effect of the different cost functions and on the different data types (TL versus pressure squared) was also investigated

---

[6] The Navy standard propagation loss models (PE 5.1, ASTRAL 5.1 and Nautilus 1.0) are written entirely in Fortran. Portions of the ASPM 5.1 code are written in Fortran.

[7] The ASA algorithm is written entirely in C code and some portions of the ASPM 5.1 code are written in C code.

[8] In late 2002 Compaq decided to discontinue future development of its Compaq Visual Fortran (CVF) product and recommend a transition to Intel Fortran Version. In future development work on GAIT GS, a transition to Intel Fortran may be made.

[9] The GAIT V&V committee is chaired by John Perkins (NRL-DC) with David Knobles (ARL-UT), Martin Siderius (SAIC), Jim Fulford (NRL-SSC) and David King (NRL-SSC) also serving on the committee.

using the GAIT V&V test cases. A summary report from the GAIT V&V committee is planned for publication in 2004 as a NRL Technical Memorandum (likely on CD).[10]

GAIT GS – PE 5.1

The first version of the GAIT GS software developed used the Navy standard PE 5.1 propagation loss model. This is an updated version of the PE 5.0 model used for the ITW test cases in 2001 and includes a number of features that are significant and useful for its application to inversion of TL data. This version of the GAIT GS software was completed in early May 2003 and has been tested extensively on the GAIT V&V test cases and the ITW test cases from 2001. A summary of the results for each of the GAIT V&V test cases inverted using PE 5.1 is provided in the following sections.

GAIT V&V Test Cases 1A, 1B and 1C

The first GAIT V&V test case is derived from the 1997 Vancouver Workshop and features a range-independent bottom in terms of both bathymetry and bottom properties. This test case had three different sub-cases each having different bottom properties. This test case, while not challenging in terms of the actual inversion, did show that the convergence of the ASA based TL inversion software can be slower for cases where the sound speed ratio at the water sediment interface is less than one. Results for these three test cases, referred to as 1A, 1B and 1C, will be summarized in the following sections.

The water column properties were identical for test cases 1A, 1B and 1C. The sound speed is downward refracting, range independent, and has a constant c^{-2} gradient. The sound speed at the surface is 1480 m/s and is 1460 m/s at the bottom of the water column (depth 100 meters). All of the bottom profiles consist of single fluid layer sediment with constant c^{-2} gradient and constant density, overlying a uniform fluid half-space. The attenuation (dB/m/kHz) is the same at the top and bottom of the sediment layer. All bottom sound speed values are between 1400 m/s and 2000 m/s. All bottom density values are between 1.3 g/cc and 2.5 g/cc. All bottom attenuation values are between 0.001 dB/m/kHz and 1.0 dB/m/kHz. All sediment thickness values are between 0.1

---

[10] Planned for publication as a NRL Technical Memorandum, the tentative title for the GAIT V&V report is "Recommendations for the Geoacoustic Inversion Toolkit (GAIT)" authored by the members of the GAIT V&V committee.

m and 100 m.[11] The acoustic fields were generated by versions of Orca and Nautilus and were verified in selected bands and range intervals with versions of RAM and Nautilus.

GAIT V&V Test Case 1A

The most time consuming computations for each synthetic test case involves running PE 5.1 at the same range step and depth mesh as the original data. For test case 1A the run with a range step of 5 meters and a depth mesh of 0.1 meters was run to 5,000 generated cases for six frequencies (25, 50, 100, 200, 400 and 500 Hz) with the cost function computed as a sum of the cost functions for all six frequencies.

Graphs showing the comparison between the synthetic acoustic data and the acoustic model prediction using the inverted geoacoustic parameters are shown in Figure 21 for 50 Hz and Figure 22 for 200 Hz for an inversion using a range step of 5 meters and a depth mesh of 0.1 meters. It should be noted for clarity that the geoacoustic parameters used for these two graphs are the same set of parameters as the inversion was done concurrently for all six frequencies noted in the previous paragraph. The graphs for 50 Hz and 200 Hz show the shallower receiver (25 meter depth) and the deeper receiver (85 meter depth) on the top and bottom of the graph respectively. This type of display can certainly provide a good visual comparison between the synthetic TL data and the TL predictions using the inverted geoacoustic parameters. However, this type of display does not provide the reader with any significant insight into the uncertainty in each of the inverted geoacoustic parameters.

Another type of display commonly used to show geoacoustic inversion results plots the cost function versus each individual geoacoustic parameter. For the GAIT V&V test case 1A, there are ten unknown parameters[12] that the inversion estimates. These parameters are plotted in Figure 23 for an inversion using a range step of 5 meters and a depth mesh of 0.1 meters. The data in this figure correspond to the graphs shown in Figure 21 and Figure 22. The top left graph in Figure 23 shows the cost function as a function of the number of generated cases and illustrates how quickly the ASA algorithm can converge for certain cases.

---

[11] The description of the environment for GAIT V&V test case 1a, 1b and 1c was taken from a document titled "GAIT Validation Cases" written by Robert A. Koch and David P. Knobles of ARL/UT.

[12] The density and attenuation in the sediment layer are constant, according to the test case description, so the density gradient and attenuation gradient are set to 0.0 in the inversion.

The graph immediately below the top left graph shows the sediment layer thickness plotted versus the cost function. The minimum, while certainly not as distinct as for certain other parameters, is easy to observe. The next column of graphs to the right illustrate the sediment sound speed (at the top of the sediment layer, at the bottom of the sediment layer and in the basement half-space) plotted versus the cost function. The plot of sediment sound speed at the top of the sediment layer versus the cost function has what is clearly the most distinct minimum among the set of unknown parameters. The sound speeds for the bottom of the sediment layer and for the basement half-space show progressively less distinct minimums. The trend of the most distinct minimum occurring for parameters near or at the water-sediment interface is one that occurs in the vast majority of inversion cases.

The graphs in the next column to the right show sediment density versus the cost function. The same trend is present as was observed for the sound speed. The density at the top of the sediment layer shows the most distinct minimum with the minimum becoming less distinct for locations deeper into the sediment. The final column of graphs shows attenuation versus the cost function. These graphs show the same behavior observed in the graphs of sound speed and density.

The inversion results presented in Figure 21, Figure 22 and Figure 23 were generated using a manual setting for PE 5.1 which resulted in a run time of 8:45:17 (H:M:S) on the hardware previously described. The effect of using the speeddial setting with PE 5.1[13] was of particular interest for the evaluation of the GAIT V&V test cases as it can considerably reduce the run times required for the inversions. However, the reduction in run times comes with a reduced level of fidelity and the effect of that drop in fidelity on the inversion needed to be quantified.

The GAIT V&V test case 1A was run with a speeddial setting of 1, 2, 3 and 4 using the reduced chi-square cost function and using TL as the acoustic data type. Other comparisons were made between the various cost functions and data types and those will be presented later in this summary report. The reduction in run times with the increase in the speeddial setting was considerable with the inversion running in 0:8:22 (H:M:S) with a speeddial setting of 4. A

[13] The speeddial setting in PE 5.1 controls both the range step (dR) and the depth mesh (dZ) through a single parameter called speeddial. More details on speeddial can be found in Appendix A of the Software Test Description for PE 5.1, OAML-STD-22. A speeddial setting of 1 corresponds to range step of 1.25λ and a depth mesh of λ/20 while a speeddial setting of 5 corresponds to a range step of 17 λ and a depth mesh of λ/4.5.

summary of the inversion results for the various speeddial settings is provided in Table 4 which also includes the best fit geoacoustic parameters for each speeddial setting. For this test case, there is a monotonic relationship between the cost function and the run time with longer run times producing results with smaller cost functions. However, only when the inversion is run with a speeddial setting of 4 does the resulting geoacoustic parameter significantly diverge from those results for small speeddial settings.

For all the GAIT V&V test cases inverted using PE 5.1, a comparison between the three cost functions and the two data types was made for a subset of the speeddial settings. For test case 1A, this comparison was done for both speeddial settings 2 and 3. For a speeddial setting of 2, all the cost function and data type combinations produced similar estimates for the sound speed ratio at the water-sediment interface and for the sediment layer thickness. However, a speeddial setting of 3 produced significantly different results between the three cost functions and the two data types. An example of the difference observed is shown in Figure 25 (speeddial setting 3 with the reduced chi-square cost function using TL data) and in Figure 26 (speeddial setting 3 with the correlation cost function using TL data). The correlation cost function using TL data estimates a very thin sediment layer (roughly 1 meter thick) and a sound speed at the top of the sediment layer that is slower than predicted in general. The densities predicted using the correlation cost function were also lower than predicted in the other inversion runs which is most likely a result of the very thin sediment layer predicted. The reduced chi-square cost function using TL data and a speeddial setting of 3 is also showing some noticeable differences, compared to the results shown in Figure 23 and Figure 24, with a sediment thickness of roughly 26 meters versus a value of 32 meter predicted with the more computationally expensive inversion runs. The sound speed at the top of the sediment layer is 1597.0 m/s which compares favorably with the values of roughly 1620 m/s for speeddial settings of 1 and 2. The ASA algorithm employs an intelligent random search so the results from this single test case should not be perceived as a universal result. It should be noted that the significant difference in results for the various cost functions and data types observed in test case 1A was not apparent in test case 1B or 1C with different geoacoustic bottom properties.

GAIT V&V Test Case 1B

The initial inversion results from test case 1B were not successful with cost function values much higher than in previous test cases being the result. An inquiry to David Knobles of ARL/UT who authored the test case confirmed that the acoustic data was indeed correct and

appeared to put the problem squarely with the GAIT GS software. Using the same initial parameters to control the ASA algorithm, the software was not showing any convergence of the type observed for test case 1A. Following this setback, test cases 1C, 2 and 4a were processed with the GAIT GS software before returning to test case 1B. Believing that the problem with the ASA algorithm rested in its inability to find the global minimum solution to the problem, two changes were made to the input parameters. First, the temperature ratio was changed from 0.001 to 0.01 which has the effect of allowing the ASA algorithm to "cool" the system at a slower rate. Second, the number of generated cases was increased from 5,000 to 25,000 to determine if the global minimum could be found with a much longer inversion run.

The result of these changes was a solution to the test case 1B problem that was, as measured by the cost functions, as good as that for test case 1A. However, the increase in the number of generated cases resulted in a corresponding increase in the overall run time. The cause of the problems noted for this test case appears to be a direct result of the type of geoacoustic bottom present. The sound speed at the top of the sediment layer is less than at the bottom of the water column resulting in what is commonly referred to as a "slow" bottom. A conversation with David Knobles in early July of 2003, once the inversion runs had been completed for this test case, confirmed that this test case had a "slow" bottom. It also confirmed that this diminished performance for inversions using algorithms based upon the simulated annealing with "slow" geoacoustic bottoms had been observed in his work at ARL/UT using other propagation loss models and different inversion algorithms.

This result is important in that it shows that the performance of the GAIT GS software on acoustic data will not be consistent at all sites due to certain geoacoustic properties. In general, sites that are believed to be characterized by "slow" geoacoustic bottoms should be inverted using a larger number of generated cases. An additional approach that may also yield improved performance of the GAIT GS software is to use geoacoustic parameter bounds that are tailored to several broad ocean bottom types. For example, areas which are characterized by "slow" geoacoustic bottoms would be better served by having the upper bound for the sound speed ratio at the water-sediment interface constrained to a value lower than that used when there is no a priori information about the characteristics of the ocean bottom. It should be noted that this approach is not necessary to the success of the GAIT GS software but may result in a reduction in the run time compared to using the global bounds for the sound speed ratio at the water-sediment interface.

The inversion results for test case 1B, once the changes noted above were made, were quite consistent for the various speeddial settings and for the various cost function and data type combinations. Inverting test case 1B with a speeddial setting of 4, which resulted in a run time some 40 times shorter compared to the inversion using a fixed range step and depth mesh, produced an estimated sound speed ratio and sediment layer thickness were nearly identical with the other inversion runs. For the 17 inversion runs done for test case 1B, the estimate of the sound speed ratio at the water sediment interface was always between 0.9795 and 0.9961, a difference of less than 25 m/s, with the sediment thickness always between 14.91 and 15.39 meter, a difference of less than 0.5 meters. Indeed, among all the GAIT V&V test cases, the results from test case 1B show the least variability as measured by the differences in the significant parameters of sound speed ratio at the water-sediment interface and sediment thickness. A comparison between the inversion results for the reduced-chi square cost function is shown in Figure 27 for a fixed range step of 5 meters and a fixed depth mesh of 0.1 meters and in Figure 28 for a speeddial setting of 4. The inversion using a speeddial setting of 4 took roughly 2.2% of the time for the inversion using a fixed 5 meter range step.

These results should not be interpreted that the same information can be derived from an inversion using a fixed range step of 5 meters and a fixed depth mesh of 0.1 meters as from an inversion using a speeddial setting of 4. While the estimated geoacoustic parameters may be nearly identical, a closer examination of the graphs of each parameter versus the cost function shows that the longer run time inversion do provide a higher degree of confidence for these synthetic test cases. The value added of these longer inversion runs on synthetic test cases with added noise will be investigated in test cases 4b, 4c and 4d and on a measured data test case in test cases 6 and 10.

The effect of a "slow" geoacoustic bottom was also observed in GAIT V&V test case 3 which was inverted after test case 1B and benefited greatly from the lessons learned in processing test case 1B.

GAIT V&V Test Case 1C

GAIT V&V test case 1C was the third in the series of the flat-bottom test cases. Unlike test case 1B which had a "slow" bottom and caused some problems in the inversion processing, test case 1C was a "fast" bottom case which presented no problems to the GAIT GS inversion software. As with test cases 1A and 1B, the GAIT GS software was run with a range of speeddial settings and with a variety of cost functions. Among the 17 inversion runs done on test case 1C the

estimated sound speed ratio fell between 1.0279 and 1.0356 (a difference of 11.24 m/s). The estimated sediment thickness fell between 38.6 and 45.5 meters with all but two estimates falling between 40.20 and 40.85 meters.

The computer run times for test case 1C were nearly identical to those for test case 1A with the longest run time being nearly 9 hours for the inversion using a fixed range step (5.0 meters) and depth mesh (0.1 meters). The shortest run time was achieved using a speeddial setting of 4 which resulted in a run time of roughly 8.5 minutes. All run time comparisons are based upon the same hardware and software configurations as described in the section of this report titled "GAIT GS Hardware and Software Requirements" on page 35.

Figure 29 (fixed 5.0 meter range step) and Figure 30 (speeddial setting of 4) show the trade-off between the uncertainties in the estimated geoacoustic parameters for the significant reduction in computational time. The ability to estimate sediment thickness and sediment sound speed is largely unaffected by the use of a longer range step within PE 5.1 (RAM). However, in nearly every case the ability to estimate the sediment density and attenuation is degraded as the range step selected is increased. The importance of this trade-off will largely depend upon the sensitivity of the resulting active system performance predictions to the increased uncertainty in the estimated geoacoustic parameters and in particular the sediment density and attenuation.

GAIT V&V Test Case 2

The second GAIT V&V test case is a repeat of ITW test case 1 that featured a downslope bottom with range-independent bottom properties. While the acoustic data for this test case are unchanged from the ITW workshop in May 2001, the results presented in this section were generated using the GAIT GS 1.0 software with PE 5.1 integrated while the results shown previously from the ITW were generated using the ASA TL Inversion software with PE 5.0. The GAIT GS software using PE 5.1 was exercised on test case 2 for both a one-layer and two-layer geoacoustic bottom. For test case 2 the actual geoacoustic properties of the bottom were a two-layer bottom overlying a basement half-space. How close an approximation to both the geoacoustic properties and the acoustic data can be achieved using a single layer representation of the ocean bottom was documented by the GAIT V&V committee as part of their summary report.

Inversion results were generated for test case 2 for both one-layer and two-layer geoacoustic bottom profiles as well as for a variety of range steps varying from a fixed range step of 5.0

meters up to a speeddial setting of 3. The two inversions with the lowest cost function were the inversions using a fixed range step which follows the trend observed in all the synthetic inversion test cases. When a speeddial setting of 3 was used for the inversion, the results were quite similar but with a significant reduction in run time.[14]

The results shown in Figure 31 show the same trend observed in test cases 1A, 1B and 1C. The sediment layer thickness and sediment sound speed are well estimated with little uncertainty but the attenuation and density are not estimated as well or as uniquely. This is a direct result of how sensitive the acoustic data provided to the inversion algorithm is to each of the geoacoustic parameters.

As part of the GAIT V&V committee review, a number of different metrics were generated and plotted. The metrics plotted by the GAIT V&V committee and planned for inclusion in their summary report on GAIT are as follows:

1. Plots of sediment sound speed profile, sediment density profile and sediment attenuation profile comparing the ground-truth values with the geoacoustic values produced by the GAIT software.
2. Plots showing full-field transmission loss for ground-truth and inverted geoacoustic parameters for a range of frequencies (octave band values from 16 Hz to 502 Hz) for ranges up to 50 km (10 times longer than the acoustic data provided to the GAIT software for test case 2).
3. Plots of one-third octave averaged transmission loss for ground-truth and inverted geoacoustic parameters averaged over receiver depths (10 meter to 90 meters in 10 meter steps) with an error in detection range computed for a hypothetical figure of merit (FOM).
4. Plots of error in detection range for figures of merit between 60 and 70 dB for one-third octave averaged frequency bands.
5. Plots of reflection loss for a range of frequencies (octave band values from 16 to 502 Hz) for ground-truth and inverted geoacoustic parameters.

[14] The run time for a one-layer inversion using a fixed range step (5.0 meters) was 27 hours 56 minutes versus a run time of 52 minutes for a speeddial setting of 3.

6. Plots of matched field correlation for a range of frequencies (octave band values from 16 to 502 Hz) for range depth locations (0 to 100 meters depth and 0 to 10 km range for test case 2).

Each of these metrics provides a characterization of the robustness of the inverted geoacoustic parameters that when taken together provides a better measure of the inversion results than a simple comparison using transmission loss. The GAIT V&V report will include a complete set of plots for these metrics for each of the test cases. This Phase II SBIR summary report will present a subset of these metrics to highlight the performance of the GAIT GS software.

A comparison of the full-field transmission loss at 16, 31, and 63 Hz is shown in Figure 32 with the comparison at 126, 251 and 502 Hz presented in Figure 33. The most significant difference between the ground-truth TL and GAIT GS TL is apparent at the lowest frequency, 16 Hz, in particular in the long range, near surface transmission loss predictions. This result is not unexpected for several reasons. First, the lowest frequency data used for the inversion was 25 Hz so the 16 Hz comparison is at a frequency lower than the lowest frequency used for the GAIT GS inversion. Second, the results shown in Figure 31 indicate that the inversion produces results with the least uncertainty for the near-surface sediment geoacoustic properties. The 16 Hz transmission loss predictions are more sensitive to the basement properties than the higher frequency predictions and will consequently be most effected by errors in the inverted geoacoustic properties for the sediment basement.

This effect can also be seen in the plots of matched field correlation (see Figure 34) produced by the GAIT V&V committee for test case 2. The agreement between the ground-truth predictions and the GAIT GS geoacoustic parameters, now represented by a correlation coefficient, improves with increasing frequency. This type of display highlights the differences much more clearly than the full-field transmission loss plots shown in Figure 32 and Figure 33 which rely upon a visual comparison between two full-field plots. The results shown in Figure 35 show the depth average matched-field correlation as a function of range for the GAIT GS geoacoustic parameters for test case 2. The results in Figure 35 clearly show how the correlation varies both as a function of range as a function of frequency once the depth dependence has been removed. For frequencies of 63 Hz to 502 Hz, the depth averaged matched-field error is always less than 1 dB for test case 2.

GAIT V&V Test Case 3

GAIT V&V test case 3 is a modified version of ITW test case 1 with a 20 km section of flat bottom added to the downslope section. The resulting test case has acoustic data over 25 km with a downslope section, starting at 90 meters and ending at 150 meters depth, from 0 to 5 km and a flat bottom from 5 to 25 km with a depth of 150 meters. Test case 3 is a "slow" bottom with a sound speed ratio estimated to be roughly 0.98 from the GAIT GS inversion. As noted in the discussion of test case 1B, there are some issues regarding the inversion of acoustic data from areas characterized by a sound speed less than 1.0. In addition, the longer ranges and "slow" bottom for test case 3 resulted in longer run times compared to the prior test cases.

As with the prior GAIT V&V test cases, the sound speed ratio was very well estimated from the GAIT GS software. For the range of speeddial settings employed for PE 5.1 and the variety of cost functions evaluated, the sound speed ratio estimated fell between 0.9751 and 0.9829 with the exception of two inversions that were easily identified as problematic due to the high final cost function. The estimation of the sediment layer thickness was consistently within ±1 meter of 50 meters with the exception of three inversions that produced estimates of sediment thickness from 80 to 93 meters. These three inversions were clearly effected by the actual geoacoustic profile that was composed of two sediment layers over a basement as shown in Figure 36.

The matched field correlation plots (see Figure 37) show the effect of the difference between the two-layer ground truth sediment profile and the one-layer sediment profile produced by the GAIT GS software most clearly at the three lowest frequencies (16, 31 and 63 Hz). The three higher frequencies (126, 251 and 502 Hz) show a much higher degree of correlation which is to be expected as these frequencies are far less effected by the deeper sediment layers than are the lower frequencies. The depth averaged matched field error plots (see Figure 38) again clearly shows this frequency dependence. The higher frequencies (126, 251 and 502 Hz) all show errors of less than 1 dB for all ranges which the lower frequencies (16, 31 and 63 Hz) show errors of up to 4 dB at some ranges.

The longer range (25 km versus 5 km) and the "slow" bottom both contributed to the longest run times measured for any of the GAIT V&V test cases. The longest run made used a fixed range step of 5.0 meters and a depth mesh of 0.1 meters took over 160 hours to run to completion with

each inversion step[15] taking an average of 23.15 seconds. Inversion runs using a speeddial setting of 3 ran in 12 to 13 hours with each range step taking an average of just under 2 seconds. The significance of the inversion runs using longer range steps (through the use of the speeddial setting in PE 5.1) will be discussed in the next section where a random noise component is added to the synthetic acoustic data where it will be shown that the advantage of using a very fine range step for PE 5.1 is largely removed when there is a signal-to-noise ratio of 5 dB or less at the maximum range for the acoustic data.

GAIT V&V Test Case 4

GAIT V&V test case 4 is a modified version of the ITW test case 2 that features added noise of various signal to noise ratios (SNR). This test case was composed of four sub-cases with test case 4a having no added noise, test case 4b having 15 dB SNR, test case 4c having 5 dB SNR and test case 4d having 0 dB SNR. The signal-to-noise ratio was measured over the last 1 km of the acoustic data (between 4 and 5 km). Plots showing the noisy acoustic data for test cases 4c and 4d are shown in Figure 39 for 25 Hz and in Figure 40 for 250 Hz. The signal-to-noise ratio averaged over 1 kilometer segments in range is annotated on each plot. The goal of test case 4 was to evaluate how well the GAIT GS inversion software performed when the synthetic acoustic data had a random noise component added. This type of acoustic data more closely mimics measured acoustic data without the uncertainty introduced by variability in the geoacoustic bottom properties, water column properties and in source and receiver locations. The discussion of test case 4 will be divided into four sections, one for each sub-case. For each sub-case, the GAIT GS inversion was run using five different settings for PE 5.1 (fixed range step of 5.0 meters and depth mesh of 0.1 meters, speeddial setting 1, speeddial setting 2, speeddial setting 3 and speeddial setting 4).

GAIT V&V Test Case 4A (No added noise)

The results for test case 4a are similar to those presented for the ITW test case (see page 19) but are slightly different due to the use of the PE 5.1, instead of PE 5.0, propagation loss model. The inversion run times varied from nearly 22 hours for the fixed range step case to just 17 minutes

[15] Each inversion step is composed of the PE 5.1 calculations for all the frequencies used for the inversion (25, 50, 100, 200, 400 and 500 Hz for the synthetic GAIT V&V test cases).

for the speeddial setting 4 run. The geoacoustic parameters estimated for all inversion runs for test case 4A produced consistent results (sound speed ratio of approximately 1.04 and a sediment thickness of 18 meters) with the exception of the results using speeddial setting 1 which produced a sound speed ratio of 1.04 but a sediment thickness of 95.5 meters. A closer examination reveals that sound speed gradient estimated by the speeddial setting 1 inversion run was 2.95, consistent with the other inversion runs. However, the cost function from the inversion run was considerably higher than the other inversion runs with the exception of the speeddial setting 4 inversion run. This result indicates the inversion using a speeddial setting 1 became trapped in a local minimum due to too rapid reduction in the ASA temperature value. This result can be easily corrected but is included to show that because the ASA algorithm is being cooled faster than the rate at which the determination of the global minimum is guaranteed, it is possible for the algorithm to be trapped within a local minimum and produce a less than satisfactory result.

The matched-field correlation plots (see Figure 41) for the inversion using a fixed range step show the high degree of correlation using the GAIT GS inverted geoacoustic parameters. Even at the lowest frequencies, where several of the other GAIT V&V test cases showed some degree of mismatch, the results for test case 4A show very good agreement. The depth averaged matched-field error plot (see Figure 42) shows the very low errors at all six frequencies.

GAIT V&V Test Case 4B (15 dB SNR)

The test case 4B results that had a 15 dB SNR at the longest range were quite similar to those for test case 4A with no added noise. The cost function values were only slightly higher for test case 4B compared to test case 4A and the estimated geoacoustic parameters were also quite comparable. The depth averaged matched-field error plot (see Figure 43) shows the very low errors across all the frequencies.

GAIT V&V Test Case 4C (5 dB SNR)

Test case 4C presents an interesting example of a statistically based search algorithm such as the ASA algorithm can produce unexpectedly poor results. The inversion results for test case 4C for speeddial 1 through 4 produce very consistent results in terms of the estimated sound speed ratio and sediment thickness and one would expect the inversion result from the fixed range step of 5.0 meters to produce results that are as good as or better than those results due to the increased accuracy from the reduced range step. However, the fixed range step inversion produced both the

highest cost function and the least accurate estimate of the sediment layer thickness. Similar to the results presented for test case 4A, the estimate of the sound speed gradient within the sediment layer was comparable to the other inversion results but the estimated layer thickness was far too large. This error in sediment layer thickness is manifested in the matched-field error plot (see Figure 44) that shows significant errors at 16, 31, 63 and 126 Hz with much lower errors for 251 and 502 Hz. This result is consistent with an error in the sediment layer thickness which is far less important for the higher frequency predictions but will produce significant errors at lower frequencies.

GAIT V&V Test Case 4D (0 dB SNR)

The results from test case 4D which had a 0 dB SNR over the last 1 km of the acoustic data show the capability of the GAIT GS software to work on acoustic data with significant amounts of noise contamination. To provide a comparison with the test case 4A results, the matched-field correlation plots are shown in Figure 45. The extremely high correlation that was present in the test case 4A in Figure 41 has been degraded in the test case 4D results, especially in the 31 Hz results. However, across the entire frequency range examined the depth averaged matched-field error (see Figure 46) is almost always below 2 dB.

It is important to also look at the computational costs for inverting these noisy test cases. The increase in run time from test case 4A with no noise to test case 4D with a 0 dB SNR was at most 10-20% due to the ASA algorithm having to search a larger number of possible geoacoustic solutions with thicker sediment layers. While test case 4 is not a conclusive study of the effects of noise on the GAIT GS software, it certainly provides some encouraging results for use on data sets with low SNR.

GAIT V&V Test Case 6

GAIT V&V test case 6 is composed of measured TL data from narrow-band sources in a shallow water site in the Gulf of Mexico. The site is approximately 110 meter deep with a downward refracting sound speed profile. The TL data extend to a maximum range of 9 km at 53, 103, 153,

503 and 953 Hz.[16] As with the synthetic TL data sets, the GAIT GS software was setup to run automatically and was not provided with any information unique to this data set to improve the inversion results. This approach is in keeping with the intent of the GAIT GS software which is designed to run without an "expert in the loop."

As test case 6 uses measured data, the process for comparing the geoacoustic parameters estimated by the GAIT GS software with the "ground-truth" data was slightly different. A determination was made by the GAIT V&V committee as to a set of "ground-truth" geoacoustic parameters which they believed best represented the bottom properties at the experiment site. It bears repeating that the current GAIT GS software does not have the capability to invert for range-dependent geoacoustic properties but can handle range-dependence in the bathymetry and water-column properties which are provided at the beginning of the inversion run. With the "ground-truth" set of geoacoustic parameters in place, the comparisons are done using the same metrics applied to the synthetic data sets.

Unlike the synthetic test cases which displayed very high correlation values, the plots showing the matched-field correlation (see Figure 47) show considerably poorer results. This is not an unexpected result for two reasons. First, the GAIT GS inversion software currently makes the approximation that the geoacoustic properties of the ocean bottom do not vary over the entire track that the provided acoustic data covers. In a shallow water environment, such as the area in which the data for test case 6 was taken, this is likely to be a rough approximation. Second, the acoustic data that the GAIT GS software uses includes the effects of range-dependent bottom properties that are not reflected in the "ground-truth" predictions against which it is being compared. The depth averaged matched-field errors (see Figure 48) provide an overview of the errors as a function of both frequency and range.

While the results from test case 6 do highlight some of the limitations in the GAIT GS software, and more generally in any acoustic inversion algorithm, there are some positive aspects to be noted. The inversion results from test case 6 were fairly consistent across a wide range of

[16] D. P. Knobles, R. A. Koch, L. A. Thompson, K. C. Focke and P. E. Eisman, "Broadband sound propagation in shallow water and geoacoustic inversion," *Journal of Acoustical Society of America*, **113** (1), pp. 205-222 (2003).

speeddial settings[17] and across the various cost functions. The inversions took as long as 37 hours for speeddial 1 to as short as 75 minutes for speeddial 5.

GAIT V&V Test Case 10

Test case 10 was composed of three measured data test cases (test case 10A, 10B and 10C) each having transmission loss data in one-third octave band averages. The center frequencies covered were 20, 25, 31.5, 40, 50, 63, 80, 100, 125, 160, 200, 250, 315, 400, 500, 630, 800 and 1000 Hz. The GAIT GS software used the 20, 40, 80, 160, 315 and 630 Hz data for its inversion for each of the test cases. For each test case the range-dependent bathymetry, water column sound velocity profiles and wind speed was provided. The GAIT GS software was run for each test case using speeddial settings of 3, 4 and 5 to look at the effect the range step in PE 5.1 had on the inversion results.

GAIT V&V Test Case 10A

Test case 10A provided transmission loss to a maximum range of 36 km with a source depth of 18 meters and receiver depths of 9.1, 21.0 and 48.0 meters. The GAIT GS software used the transmission loss data at all three receiver depths. There were eight sound velocity profiles provided covering the 36 km track. The bathymetry began at a depth of 74.7 meters getting as deep as 101.8 meters at 21.1 km and then becoming shallower toward the end of the track.

A comparison of the predicted third-octave band transmission loss at 16, 31, 63, 126, 251 and 502 Hz for the "ground-truth" and the GAIT GS inverted geoacoustic parameters for a source depth of 20 meters and a receiver depth of 70 meters is shown in Figure 50. These plots show fairly good agreement with the mean square error between the two curves indicated for each frequency. This reasonably successful agreement for third-octave band averages is not carried over to a comparison of narrow-band results such as shown in Figure 51. The matched-field correlation using a narrow-band calculation shows the significant problem of using frequency averaged acoustic data to generate geoacoustic parameters which are then used for narrow-band predictions. In contrast to the synthetic test cases where the matched-field correlation plots usually showed poorer agreement at the lower frequencies, the matched-field correlation plots for test case 10A show progressively worse agreement with increasing frequency. While this

[17] Speeddial settings of 1, 2, 3, 4 and 5 were used for test case 6.

result is not unexpected, it may surprise some readers at how poor the results are when taken from third-octave band averages and applied to a narrow-band prediction.

GAIT V&V Test Case 10B

Test case 10B also provided third-octave band transmission loss data to a maximum range of 36 km with a source depth of 18 meter and receiver depths of 9.1, 12.92 and 41.05 meters. Following the approach used for test case 10A, the GAIT GS software used the transmission loss data at all three receiver depths for the inversion. There were six sound velocity profiles provided but all but one were located too far away to be of use. The bathymetry was nearly constant varying only between 74.0 and 79.9 meters over the 36 km track.

Figure 53 shows a comparison of the predicted third-octave band transmission loss at 16, 31, 63, 126, 251 and 502 Hz for the "ground-truth" and the GAIT GS inverted geoacoustic parameters for a source depth of 20 meters and a receiver depth of 70 meters. The mean square errors shown in Figure 53 are higher than those in Figure 50 for test case 10A but the general character and trend in the third-octave band data is still reasonably well represented. The matched-field correlation for test case 10B is shown in Figure 54 and, like test case 10A, shows the poor results when geoacoustic parameters, inverted from third-octave band transmission loss data are used for narrow-band predictions. Unlike the synthetic test cases where narrow-band transmission loss data was used for the inversion and test case 6 which provided measured, narrow-band TL data, test case 10A and 10B highlight this significant limitation in this approach to in-situ environmental characterization.

GAIT V&V Test Case 10C

Test case 10C, unlike test cases 10A and 10B, had only one receiver depth, 18 meters, with a source depth of 18 meters. The transmission loss data was third-octave band averaged data with a maximum range of 36 km. The bathymetry was nearly constant varying between 108 and 115 meters over the 36 km track. There was one sound velocity profile provided for test case 10C that was used for the entire track.

The third-octave band averaged transmission loss comparison for test case 10C is shown in Figure 56 and as first look does not appear significantly different than those shown for test cases 10A and 10B. However, a closer look at Figure 56 reveals that the third-octave band TL data has significantly more structure than the other two test cases. The comparison for 251 and 502 Hz

clearly show that the prediction using the GAIT GS inverted geoacoustic parameters is able to match much of the coherent structure in the TL curves generated using the "ground-truth" geoacoustics. However, the mean square error between the two TL curves is not significantly better than that observed for test cases 10A and 10B.

The matched-field correlation for test case 10C is shown in Figure 57. It is noticeably different from the results from test cases 10A and 10B showing some degree of correlation out to the longest range (10 km) at all six frequencies. This is in sharp contrast the results for test case 10A (see Figure 51) and test case 10B (see Figure 54) which showed little or no correlation (on the color scale of the plots) at the three highest frequencies (126, 251 and 502 Hz). At present it is not known if the GAIT V&V committee will hypothesize a reason for this noticeable difference the matched-field correlation between test case 10C and test cases 10A and 10B. However, the authors of this report believe that structure observed in the third-octave band transmission loss at the higher frequencies of test case 10C carried the information that allowed the GAIT GS inversion software to produce an estimate of the geoacoustic properties that was considerably more accurate when applied to the higher frequency predictions.

GAIT GS – ASTRAL 5.1

The second iteration of the GAIT GS software added the Navy standard ASTRAL 5.1 propagation loss model to PE 5.1. ASTRAL 5.1 is an updated version of the ASTRAL 5.0 propagation loss model implemented in late 2001 and early 2002 with the ASA based TL inversion software. The upgrade to ASTRAL 5.1 from ASTRAL 5.0 adds the ability to predict TL from areas where the ocean bottom is characterized using an N-layer bottom. However, the capability to invert measured TL data for an N-layer characterization of the ocean bottom was already handled by the PE 5.1 model and a decision was made to use ASTRAL 5.1 to invert just for a 10-parameter LFBL description of the ocean bottom.

As noted in the prior section of this summary on the Inversion Techniques Workshop, ASTRAL has a significant advantage over PE in terms of computational speed. However, this speed advantage comes at a price when evaluating the GAIT V&V test case results using ASTRAL 5.1. ASTRAL does not include the ability to predict the type of coherent (modal interference) structure observed in the synthetic test cases, and thus can not be expected to provide the type of detailed geoacoustic description that the PE 5.1 based inversion does. This is not to say that a computationally fast inversion has no value. An ability to estimate with a reasonable accuracy

one or two of the most important geoacoustic parameters in a very short run time (several minutes) would be an important tool in certain communities.

GAIT V&V Test Case 1

With range-independent bathymetry, test cases 1A, 1B and 1C were among the shortest run times (90, 88 and 98 seconds respectively) recorded using ASTRAL 5.1. The inversions using ASTRAL 5.1 were done using the 50, 100, 200, 400 and 500 Hz transmission loss data.[18] These run times work out to an average of roughly 35 milliseconds per iteration. For comparison, the fastest average iteration using PE 5.1 for test case 1 was roughly 100 milliseconds using a speeddial setting 4. It should also be noted that PE 5.3 is reported to be considerably faster and when implemented in GAIT GS may close that difference in run time.

The estimated sound speed ratio using ASTRAL 5.1 for test case 1A is 1.110 which compares favorably with the estimate of 1.110 using PE 5.1 and a fixed range step. The results for test case 1B show some difference as the ASTRAL 5.1 inversion estimates a sound speed ratio of 1.022 while PE 5.1 estimates 0.983. The ability of an ASTRAL 5.1 based inversion to accurately estimate sound speed ratios of less than 1.0 is certainly an issue that bears further examination beyond the limited number of test cases discussed in this report. The results for test case 1C show a sound speed ratio of 1.085 estimated by ASTRAL 5.1 and a sound speed ratio of 1.031 estimated by PE 5.1.

GAIT V&V Test Case 2

The results for test case 2 again show the trend that the ASTRAL 5.1 based inversion overestimates the sound speed ratio at the water-sediment interface. The sound speed ratio estimated using ASTRAL 5.1 was 1.067 while the sound speed ratio estimated using PE 5.1 was 1.012.

GAIT V&V Test Case 3

Test case 3 provides another comparison for an environment with a "slow" bottom. The inversion by GAIT GS using PE 5.1 estimated the sound speed ratio as 0.981 while the inversion

[18] The 25 Hz TL data was not used for the ASTRAL 5.1 based inversion due to the lower frequency limit of 50 Hz currently recommended by OAML.

by GAIT GS using ASTRAL 5.1 estimated the ratio to be 0.996. For this case the ASTRAL 5.1 inversion now correctly identifies the bottom as having a sound speed ratio of less than 1.0 but still overestimates the sound speed ratio. In comparison, only one of twenty-one inversions using PE 5.1 produced an estimated sound speed ratio greater than 0.996. This is not to imply that the inversion using ASTRAL has no value. The fastest inversion using PE 5.1 was done using a speeddial setting 3 and took just over 12 hours for a run using the full 25 km of acoustic data. The inversion using ASTRAL 5.1 ran in just over 7 minutes which is roughly 1% of the computational time of the fastest PE 5.1 inversion run.

GAIT V&V Test Case 4

The results for test case 4 show that the GAIT GS inversion using ASTRAL 5.1 can also be used effectively in cases where there is noise added. The estimated sound speed profile using ASTRAL 5.1 was 1.054 for test case 4A (no noise added) which compares favorably with PE 5.1 inversion result of 1.040. The results are only slightly different for the cases with added noise. The estimated sound speed ratio using ASTRAL 5.1 for test case 4B (15 dB SNR) is 1.066. The estimated sound speed ratio is relatively unchanged for test case 4C (5 dB SNR) with a value of 1.065 and for test case 4D (0 dB SNR) with a value of 1.068. These estimates are roughly 2% higher than the actual values and the values estimated by GAIT GS using PE 5.1. However, the run times for test cases 4A through 4D are all between 3 minutes 34 seconds and 3 minutes 41 seconds. This compares against run times for GAIT GS using PE 5.1 and a speeddial setting 4 that are between 15 minutes 22 seconds and 26 minutes 7 seconds. Once again it should be noted that this difference in run time may be reduced with PE 5.3.

GAIT V&V Test Case 6

Test case 6 with narrow-band TL data from the Gulf of Mexico represents the first comparison between inversions using PE 5.1 and ASTRAL 5.1 using measured acoustic data. Using the TL data from 53 to 503 Hz, the ASTRAL 5.1 based inversion was completed in 1 minute 10 seconds with an estimated sound speed ratio of 0.999. This value compares favorably with the PE 5.1 inversion which produced estimates for the sound speed ratio between 0.973 and 1.002. The fastest run time for a PE 5.1 inversion was 22 minutes 18 seconds for a speeddial setting 3.

GAIT V&V Test Case 10

Test case 10A, 10B and 10C provide third-octave band transmission loss data out to a maximum range of 36 km. This type of acoustic data is not handled well using a PE 5.1 based inversion due to its narrow-band transmission loss calculations. However, ASTRAL 5.1 is well-suited to the problem of broadband transmission loss computations and should perform well on these data sets. For both test case 10A and 10B the GAIT GS software using PE 5.1 overestimated the sound speed ratio while the GAIT GS software using ASTRAL 5.1 estimated the sound speed ratios for test cases 10A and 10B to be 1.087 and 1.139 respectively. The "ground-truth" geoacoustics for test case 10A can found in Figure 49 and in Figure 52 for test case 10B.

The geoacoustic characteristics of test case 10C (shown in Figure 55) have a large number of layers in the first 100 meters. The estimated sound speed profile generated by GAIT GS using PE 5.1 provides a reasonable approximation for this first 100 meters of sediment but misses a transition at 100 meters to a higher sound speed material. The GAIT GS inversion using ASTRLA 5.1 produced an estimate of the sound speed ratio of 1.047 (approximately 1562 m/s).

GAIT GS – ASPM 5.1

The addition of ASPM 5.1 to the GAIT GS software represents the first implementation of a Navy standard active sonar performance prediction model within GAIT. Whereas TL is required for inversions using ASTRAL or PE, ASPM provides GAIT with the ability to invert for geoacoustic bottom properties from monostatic reverberation data. Modeling reverberation data also allows for the inversion for bottom backscatter parameters. Finally, there is a significant advantage in using reverb data because it is much more easily collected by the Fleet in comparison to TL data.

ASPM 5.1 is a powerful active sonar prediction model. It can be set up to model a wide range of monostatic and bistatic tactical situations. Part of its power comes from the incorporation of environmental databases for the use by various parts of ASPM. The databases include classified high resolution databases and historical databases. If environmental data is collected at the location, that may also be incorporated.

Although ASPM can model many aspects of source-receiver-target scenarios, the part of ASPM of use by GAIT is the calculation of reverberation. ASPM calculates reverb after first using its own modified ASTRAL program to calculate two-way TL out along radials from the collocated source and receiver.

In the architecture of GAIT, ASPM was added in a different manner than the previous TL models, PE 5.1 and ASTRAL 5.1. Whereas GAIT employs the PE and ASTRAL TL models as callable subroutines, ASPM proved to make the resulting single program too large in memory requirements for the Fortran/C compilers used for GAIT development. This was true even though ASPM uses an architecture involving separate executables called by the either the Graphical User Interface or a command line program. This partly arose because PE and ASTRAL both require substantial array allocation at runtime.

In order to include ASPM 5.1 the interface between GAIT and ASPM was redesigned to generate ASPM input files for use by the standalone ASPM set of programs. GAIT copies an ASCII master template lacking the frequency and bottom scatter coefficient to a runtime file. GAIT then adds the current frequency and bottom scatter coefficient from the ASA algorithm to the runtime file. GAIT then writes the other bottom parameters to another runtime file referenced by the ASPM input file. This process is repeated at each GAIT fitting step.

The advantage of this GAIT/ASPM setup is that minimal changes are required to the ASPM software. One ASPM library I/O routine for reverberation has been modified to output a reverb data file in a format for GAIT to read. The only other changes have been to suppress screen writes in the ASPM programs related to obtaining environmental data, calculating TL radials and calculating the reverb. The ASPM screen writes interfered with reports generated by GAIT.

One problem did arise during the design and coding of the GAIT/ASPM program. ASPM is constrained to run single frequency scenarios. There is a batch multi-frequency mode but it simply reruns ASPM for each frequency and accumulates the TL data. The current ASPM implementation in GAIT requires running ASPM once for each frequency of the fit. This substantially impacts runtimes. ASTRAL is the TL model used by ASPM to calculate the two-way TL used by the reverb calculation. ASTRAL can be run in a multi-frequency mode with a minimal increase in run time compared to a single frequency calculation. However, substantial changes in ASPM will be required to run in a multi-frequency mode.

Other aspects of ASPM have been optimized for speed. The ranges for TL calculation are always tested beforehand to ensure that extra TL calculations do not take place. The restricted ranges also mean that the amount of environmental data extracted and read from the databases is optimized to be the minimum needed. Finally, the number or radials are restricted to 18 (20 degree spacing), the minimum number allowed by ASPM 5.1.

GAIT V&V Test Case 7

Test case 7 consists of Harsh Environments Program (HEP) data collected in the East China Sea. In addition to the Reverb data the only other data supplied were the source and receiver depths, the measured sound speed profile for the site and the water depth at the site. As the coordinates were not provided for the data the model runs were performed with the assumption of a flat bottom and the single sound speed profile. The site was run as a range independent environment.

An inversion run with 1500 steps required 12.5 hours of runtime on a 1.4 GHz Athlon XP 1600+ with 512 MB of RAM.[19] The curves with the GAIT GS 1.0 inversion results versus the HEP data are shown in Figure 58. Although the model curves fit the reverb data fairly closely for times after 8 seconds there is an increasing divergence from the data with higher frequencies. This is especially true at 400 and 800 Hz. What appears to be happening in the fitting process is that the structure in the data observable for the 400 and 800 Hz cases cannot be fitted with the range independent environment chosen for the run. The high frequency structure in the data is either a data collection artifact or there is some range dependence to the bottom. The data could indicate some shorter range discontinuity in bathymetry, sound speed profile or bottom properties.

The output parameters for the fitting of test case 7 are presented in Table 19. As with the TL runs for ASTRAL there is a general mismatch between the density and the ratio for the model fit. The density is unrealistically high for the value of the ratio. In general for the earlier TL tests the ratio is fit to a better degree than the density. Fluctuations in density for the same ratio cause relatively small changes in the reduced chi square.

The bottom backscatter coefficient is unusually low. There may be a coupling of the bottom backscatter parameter with the sound speed ratio parameter in the calculation of the reverb and the ASA software may not be splitting these two parameters adequately. It is possible that the monostatic reverb data alone does not have the necessary information for separating out the some of the associated parameters.

In general the running of the GAIT package for reverb setup with a range independent environment appears to yield an optimal fit according to the chi square statistics. The problem is that if the environment is not range independent the resulting parameters may not be reasonable.

---

[19] At the time this report was written, run time comparisons on the same P4 3.0 GHz PC used for the PE 5.1 and ASTRAL 5.1 inversions were not available.

GAIT V&V Test Case 8

Test case 8 was also comprised of HEP data from the Gulf of Mexico. The location is on the shallow water shelf west of the Florida Keys. In this case there are two sets of data labeled 8A and 8B. For this particular site the data is not actually monostatic as the source collocated with the receiver did not function. The source for case 8A was approximately one nautical mile away from the receiver and for case 8B the source was about nine nautical miles away from the receiver. Although these cases are clearly not monostatic they were run that way for testing the GAIT software.

For test case 8A, 1500 fitting steps required 13.5 hours on the same Athlon system as was used for test case 7. The increased runtime over test case 7 was primarily the result of using an ASCII text file of gridded bathymetry from DBDBV version 4.0 as input into the ASPM program. When GAIT makes a call to ASPM during each step of the fitting process ASPM reloads the environmental data. The bathymetry data does not add significant overhead as can be seen by the comparison of the test cases 7 and 8a runtimes. Substantially more overhead is involved when using historical sound speed profiles from the Generalized Digital Environmental Model (GDEM), which can be accessed through ASPM. In addition to the overhead of reading in the data the range dependence also slows the TL calculations performed by ASTRAL in ASPM. Since a measured sound speed profile from the experiment was provided, the GDEM database was not used.

The graphs of the model versus data reverb curves for test case 8A are shown in Figure 59. Visually, the curves pass through or near the data for all but the highest frequency of 800 Hz. In detail the model curves overestimate the Reverb slightly for the lower frequencies between 7 and 15 seconds and then underestimate the levels for times in excess of 24 seconds. There appears to also be some fine scale structure to 400 and 800 Hz data between 15 and 29 seconds that the model reverb curves do not match. This is not too surprising as the two-way TL for calculating the reverb uses ASTRAL uses significant range averaging.

Considering the deviation from a monostatic experiment the resulting chi square for test case 8A was still low enough to be a statistically valid fit, as shown in Table 19. For test case 8A in particular the chi square value from the fitting should be viewed as anomalously high but still statistically valid. For the model ASPM runs with the test case 8A environment the last time point represented a cutoff in the reverb level. The value for the last model point was uniformly 0 dB. This was not plotted on the graphs of Figure 59. This lack of a model value skews the

reduced chi square to a higher value than it would be otherwise. The fit reduced chi square would be much lower without this mismatch at the end of the reverb. The curves and parameters change very little if the final data and times are deleted before initializing the run but the chi square value drops by nearly a factor of 3.

The values for some of the parameters were consistent with the environment on the shelf off of Florida. The sediment TWTT (Two-Way Travel Time) suggests thin sediments less than 50 meters thick. The high basement reflectivity would correspond to the limestone reef basement structures prevalent on the Florida shelf.

Unlike test case 7 and most of the ASTRAL TL fitting runs, the usual relationship between the density and sound speed ratio is switched for test case 8A. The density is very low, essentially at the lowest value allowed by the GAIT software. The ratio, however, is abnormally high for sediment that is essentially clay according to the density results. At the same time the bottom backscatter parameter appears once again to be too low. GAIT may not be able to separate out the effects of the sound speed ratio versus the bottom backscatter on the reverb level curves, which was also observed for Test Case 7.

Test case 8B required approximately 13.6 hours to run, essentially the same timing as test case 8A. The results for test case 8B were also similar to the results for test case 8A. The graphs of the comparison between the data and model reverb curves are shown in Figure 60. In the case of test case 8B there was no model to data mismatch at the end of the reverb curve. The reverb model in ASPM produced reverb levels out to the final time of the recorded data.

Visual examination of the model versus data reverb curves for test case 8B indicates more deviation between the curves than for test case 8A. This is not surprising as the actual setup for the experiment involved the source being over 9 nautical miles distance from the receiver rather than a monostatic configuration of the model. Test case 8A had the source only one nautical mile away from the receiver. The model curves uniformly underestimate the reverb levels for the first 5 seconds and then overestimate the reverb levels between 5 and 15 seconds. Beyond 15 seconds there is a better match between the model and data curves.

Table 19 shows the parameter set and reduced chi square resulting from the fit for test case 8B. The reduced chi square is smaller than that for test case 8A by a factor of nearly 2. Test case 8A would have a lower reduced chi square than test case 8B without the model to data mismatch at the last reverb point.

The density for test case 8B is low, similar to the results for test case 8A. It does not reach the lower bounding value set by GAIT though. The value of 1.49 is reasonable, although perhaps still a bit low for the shelf environment west of the Florida Keys. In comparison, the sound speed ratio is once again higher than is reasonable for the model density or the environment. As in test case 8A the bottom backscatter coefficient is lower than expected.

Finally, as in test case 8A there are the same two parameters that do appear to fit the environment. The GAIT results for test case 8B also indicate relatively thin sediment overlying a reflecting basement.

GAIT GS – ASPM 5.1 Conclusions

ASPM 5.1 has successfully been implemented as a modified, standalone program that can be called by GAIT. The power of ASPM for reverberation modeling within GAIT comes from the incorporation of a complete prediction model, including necessary environmental databases for range dependent environments. Further, reverberation data is much easier to acquire with Fleet assets in comparison to TL data.

The results from test cases 7, 8A and 8B clearly show that GAIT with ASPM can produce statistically valid fits to the data. Problems have been identified primarily with the apparent inability of GAIT/ASPM to decouple the effects of the sound speed ratio and the bottom backscatter on the reverb curve. Other parameters, such as the two-way travel time and the basement reflectivity, can be adequately modeled, at least in one of the test cases.

Another question still to be addressed is how much the results have been degraded by model/experiment mismatch and lack of environmental information. The reverb data from test case 7 clearly show structure indicating range dependence while the model was run with no range dependence because of lack of information. ASPM incorporates worldwide databases that can be used for any experimental location and thus potentially solve the problem with test case 7.

Test cases 8A and 8B were not really monostatic. ASPM and therefore GAIT can be run with bistatic source and receiver geometries. It may be useful in future work to revisit test cases 8A and 8B with the correct bistatic geometry.

Finally, there is the problem of runtimes. GAIT/ASPM runs too slow in its current configuration to provide near real time inversion results for most computer systems. One possible solution is to revise ASPM to handle multiple frequencies during the ASPM run. ASTRAL, the TL model, can handle multiple frequencies with a minimum of increase in overhead. The reverb calculation is

actually a minor part of the ASPM run compared to the TL calculations. Such changes should and could only be undertaken by the ASPM authors (SAIC).

In addition to increasing the speed of ASPM with multiple frequencies another approach would include the Fleet farming the runs by satellite to onshore stations with more powerful computers. This, in conjunction with or even instead of the ASPM changes, possibly could yield near real time results.

GAIT GS – Nautilus 1.0

The addition of Nautilus 1.0 to the stable of models in GAIT GS will allow for the inversion of broadband time series for an N-layer estimate of the shallow water ocean bottom properties. The efficiency of the Nautilus normal code from ARL/UT allows the generation of a synthetic time series using a standard FFT approach without the onerous run times present when using a propagation loss model of the fidelity of PE 5.1. Nautilus 1.0 is currently limited to range-independent environments limiting its immediate utility but future versions of the Nautilus model will handle range-dependent environments.

Phase III Transitions of Phase II Products

The products from this Phase II SBIR are being transitioned as part of the GAIT (Geoacoustic Inversion Toolkit) product being proposed for acceptance as an OAML approved product by PMW-150 Operational Effects Program (OEP). As noted in this summary, the GAIT Version 1.0 product will use the ASTRAL 5.1, PE 5.1, ASPM 5.1 and Nautilus 1.0 OAML approved models for inversion of broadband transmission loss, narrowband transmission loss, broadband monostatic reverberation and broadband time series acoustic data. An upgrade from PE 5.1 to PE 5.3 is planned which will reduce the run times reported in this report generated using PE 5.1.

The GAIT V&V test case results will be documented in an upcoming NRL Memorandum Report slated for publication (likely on CD) in late 2004. This report will include the GAIT V&V committee's discussion of the test case results and a complete set of plots for all the test cases including many plots not shown in this report. It is also anticipated that the work done by the GAIT V&V committee will form the basis for the Software Test Description (STD) document for GAIT when it is submitted to OAML. The STD document will include a number of test cases that an end-user of GAIT would run to validate the correct installation and implementation of the GAIT software.

A proposed extension of the products developed under this SBIR has been submitted to NAVAIR as a Phase I SBIR proposal. PSI submitted the proposal in response to SBIR topic N04-247 titled "Littoral Environment Parameter Estimation from Bistatic and Multistatic Fleet Air Antisubmarine (ASW) Acoustic Reverberation Data" in mid-August 2004. PSI teamed with APL/UW for the Phase I SBIR proposal in an effort to leverage the experiences and products developed by each organization. PSI brings to the proposal the several years of experience in the development of the GAIT GS software and in the integration of the ASPM 5.1 model. APL/UW, represented by Robert Odom, K.Y. Moravan and Darrell Jackson, brings their experience in the development of GABIM (Geophysical Bottom Interaction Model). The goals of the SBIR proposal are the development of a bistatic reverberation inversion capability using ASPM and/or CASS and the GABIM bottom scatter kernel. The inversion would use the ASA algorithm and the intent is to integrate these modifications into a future version of GAIT with OAML acceptance being an important milestone for the work. The application for this type of product is in the air ASW community where sonobuoy fields are deployed with a focus on target detection and not on acoustic data collection. While transmission loss data provides an easy inversion problem, in many cases, transmission loss data is not easily collected during a standard air ASW mission. However, there is an abundance of reverberation data and far more bistatic than monostatic reverberation data available from a sonobuoy field. The Phase I tasking will integrate a monostatic version of the GABIM code into ASPM to provide a proof of concept demonstration. A continuation on to a Phase II will allow the integration of a bistatic version of the GABIM code into ASPM and CASS.

Acknowledgements

The authors of this report would like thank the manner individuals who contributed to the results presented in this summary report. The ONR program manager who managed this Phase I and Phase II SBIR were Ken Dial, David Armstrong and Larry Green. The SPAWAR PMW-150 program managers who endorsed this SBIR to proceed to a Phase II SBIR and are funding the transition of the ASA based inversion software into GAIT are Kim Koehler (Strategic Planning Senior Executive for PMW-150) and Marcus Speckhahn (Assistant Program Manager Undersea Warfare for PMW-150). The ITW (Inversion Technique Workshop) was organized by Ross Chapman (U. of Victoria), Stanley Chin-Bing (NRL-SSC) and David King (NRL-SSC). The GAIT V&V committee is chaired by John Perkins (NRL-DC) with David Knobles (ARL-UT), Martin Siderius (SAIC), David King (NRL-SSC) and Jim Fulford (NRL-SSC). The authors

would also like to recognize Lester Ingber who is the developer of the Adaptive Simulated Annealing (ASA) algorithm and made it publicly available.

Tables

Table 1: Summary of Inversion Results Using PE 5.0 (RAM) for ITW Synthetic Test Cases

Test Case (Description)	Frequencies (Hz)	Reduced Chi-Square Values			
		True Environment	ASA Inversion	# of Data Points	# of Unknowns
Test Case 0 – Calibration Case	25, 50,100 and 200	7.6703	1.394	4,776	11
	25, 50, 100, 200, 400 and 500	5.6142	2.0354	7,164	11
Test Case 1 – Monotonic Downslope	25, 50,100 and 200	9.034	2.0128	7,944	20
	25, 50, 100, 200, 400 and 500	8.387	7.5751	11,916	20
Test Case 2 – Shelf-break	50,100 and 200	9.4713	3.831	5,958	20
	25, 50, 100, 200, 400 and 500	6.7770	6.1846	11,916	20
Test Case 3 - Flat Bottom	50,100 and 200	6.332	5.0345	5,958	24
	25, 50, 100, 200, 400 and 500	6.0388	5.7115	11,916	24

Table 2: Summary of ASTRAL 5.0 and PE 5.0 Inversion Results for ITW Measured Test Cases

Test Case (Description)		Reduced Chi-Square Values						
		ASTRAL 5.0 (Inverted 50, 100, 200, 400 and 800 Hz TL Data)				PE 5.0 (Inverted 25, 50, 100, 200, and 400 Hz TL Data)		
		3,000 Steps	10,000 Steps	# of Data Points	# of Unknowns	10,000 Steps	# of Data Points	# of Unknowns
Test Case 4		10.737	10.181	325	8	15.518	260*	11
Test Case 5	TL Post 1	7.864	7.765	95	8	10.052	93	11
	TL Post 2	8.697	8.640	195	8	17.697	195	11
	TL Post 3	18.715	18.708	117	8	23.303	131	11
	TL Post 4	5.141	5.029	350	8	15.922	350	11

- *PE 5.0 inversion for test case 4 was done using 50, 100, 200 and 400 Hz TL data only.*

Table 3: Summary of ASTRAL 5.0 and PE 5.0 Inverted Geoacoustic Parameters for ITW Test Cases 4 and 5

Inverted Geoacoustic Parameter	Test Case 4		Test Case 5 – TL Post 1	
	ASTRAL 5.0	PE 5.0	ASTRAL 5.0	PE 5.0
Sediment Sound Speed Ratio	1.058	1.094	1.078	0.996
Sound Speed at Bottom of Sediment (m/s)	-	1,811.1	-	1,827.9
Sound Speed Gradient (m/s/m)	2.736	-	2.326	-
Density at Top of Sediment (g/cc)	3.929	1.460	1.338	1.864
Density at Bottom of Sediment (g/cc)	-	1.377	-	1.272
Attenuation (dB/λ)	0.678	0.303	2.323	0.098
Attenuation Gradient (dB/ λ /m)	0.019	-0.020	0.024	0.097
Frequency Exponent	1.498	-	1.750	-
Basement Reflectivity	0.301	-	0.066	-
Sound Speed in Basement (m/s)	-	1,659.6	-	1,973.2
Density in Basement (g/cc)	-	2.271	-	1.735
Attenuation in Basement (dB/ λ)	-	0.025	-	0.242
Two-way Travel Time (sec)	0.957	-	0.029	-
Sediment Thickness (m)	-	15.28	-	9.06

Table 4: Summary of GAIT V&V Test Case 1A inversion results using GAIT GS Version 1.0 (PE 5.1).

	Manual	Speeddial Settings			
	dR = 5.0 dZ = 0.1	1	2	3	4
Run Time (H:M:S)	8:45:17	2:30:56	0:33:28	0:15:15	0:08:22
Cost Function Value (Reduced Chi-Square with TL Data)	0.0282	0.0382	0.0714	0.0987	0.1905
Sediment Layer Thickness (m)	31.62	31.99	34.69	25.61	16.85
Sound Speed at Top of Sediment Layer (m/s)	1620.76	1617.36	1617.49	1597.00	1581.22
Sound Speed at Bottom of Sediment Layer (m/s)	1677.60	1684.43	1705.69	1673.35	1625.65
Sound Speed in Basement Half-Space (m/s)	1873.15	1879.31	1893.41	1729.99	1918.21
Density in Sediment Layer (g/cc)	1.8245	1.8159	1.7979	1.7702	1.4793
Density in Basement Half-Space (g/cc)	2.3065	2.2612	1.8040	1.9463	1.6107
Attenuation in Sediment Layer (dB/ λ)	0.4548	0.3901	0.4486	0.2890	0.2136
Attenuation in Basement Half-Space (dB/ λ)	0.8180	0.4010	0.1912	0.0410	0.7777

Table 5: Summary of GAIT V&V Test Case 1B inversion results using GAIT GS Version 1.0 (PE 5.1).

	Manual	Speeddial Settings			
	dR = 5.0 dZ = 0.1	1	2	3	4
Run Time (H:M:S)	28:59:39	10:50:15	2:19:36	1:24:13	0:38:51
Cost Function Value (Reduced Chi-Square with TL Data)	0.0232	0.0341	0.0569	0.0675	0.1655
Sediment Layer Thickness (m)	14.99	15.00	14.93	15.17	15.21
Sound Speed at Top of Sediment Layer (m/s)	1434.66	1438.42	1443.35	1440.23	1443.95
Sound Speed at Bottom of Sediment Layer (m/s)	1470.86	1469.99	1463.03	1467.82	1468.22
Sound Speed in Basement Half-Space (m/s)	1622.24	1636.14	1625.54	1625.59	1623.72
Density in Sediment Layer (g/cc)	1.5051	1.4296	1.4477	1.5154	1.4964
Density in Basement Half-Space (g/cc)	1.9059	1.5970	1.6008	1.6710	1.6084
Attenuation in Sediment Layer (dB/ λ)	0.0198	0.0165	0.0067	0.0150	0.0273
Attenuation in Basement Half-Space (dB/ λ)	0.3253	0.3621	0.4020	0.3190	0.2270

Table 6: Summary of GAIT V&V Test Case 1C inversion results using GAIT GS Version 1.0 (PE 5.1).

	Manual	Speeddial Settings			
	dR = 5.0 dZ = 0.1	1	2	3	4
Run Time (H:M:S)	8:56:58	2:29:13	0:32:07	0:15:01	0:08:26
Cost Function Value (Reduced Chi-Square with TL Data)	0.0222	0.0276	0.0386	0.0515	0.1522
Sediment Layer Thickness (m)	40.20	40.25	40.27	40.80	38.61
Sound Speed at Top of Sediment Layer (m/s)	1504.56	1506.45	1505.93	1505.91	1502.96
Sound Speed at Bottom of Sediment Layer (m/s)	1551.79	1547.24	1549.28	1548.05	1571.11
Sound Speed in Basement Half-Space (m/s)	1807.27	1817.07	1820.56	1830.12	1713.64
Density in Sediment Layer (g/cc)	1.6567	1.6699	1.6587	1.7065	1.5080
Density in Basement Half-Space (g/cc)	2.1632	1.7179	1.9274	1.8853	2.4245
Attenuation in Sediment Layer (dB/ λ)	0.1090	0.0975	0.1101	0.0884	0.1236
Attenuation in Basement Half-Space (dB/ λ)	0.1269	0.3188	0.0771	0.2678	0.2761

Table 7: Summary of GAIT V&V Test Case 2 inversion results using GAIT GS Version 1.0 (PE 5.1) for one-layer (N=1).

	Manual	Speeddial Settings		
	dR = 5.0 dZ = 0.1	1	2	3
Run Time (H:M:S)	27:56:11	30:09:47	2:04:21	0:52:20
Cost Function Value (Reduced Chi-Square with TL Data)	0.0473	0.0778	0.1051	0.0832
Sediment Layer Thickness (m)	4.29	4.12	4.63	4.45
Sound Speed at Top of Sediment Layer (m/s)	1507.55	1500.24	1508.45	1505.44
Sound Speed at Bottom of Sediment Layer (m/s)	1513.89	1512.56	1516.07	1518.18
Sound Speed in Basement Half-Space (m/s)	1769.02	1718.15	1778.25	1749.37
Density at Top of Sediment Layer (g/cc)	1.5455	1.7404	1.6828	1.6200
Density at Bottom of Sediment Layer (g/cc)	1.5891	1.7444	1.7188	1.6809
Density in Basement Half-Space (g/cc)	1.9715	1.8833	1.8077	1.7285
Attenuation at Top of Sediment Layer (dB/ λ)	0.1222	0.1695	0.1690	0.1426
Attenuation at Bottom of Sediment Layer (dB/ λ)	0.1228	0.1683	0.1893	0.1214
Attenuation in Basement Half-Space (dB/ λ)	0.5383	0.1102	0.4955	0.2268

Table 8: Summary of GAIT V&V Test Case 3 inversion results using GAIT GS Version 1.0 (PE 5.1) for one-layer (N=1) and TL from 0 to 5,000 meters.

	Manual	Speeddial Settings		
	dR = 5.0 dZ = 0.1	1	2	3
Run Time (H:M:S)	162:03:59	30:18:51	10:32:38	5:16:31
Cost Function Value (Reduced Chi-Square)	0.0977	0.0704	0.0959	0.1494
Sediment Layer Thickness (m)	50.35	50.11	50.35	50.65
Sound Speed at Top of Sediment Layer (m/s)	1461.29	1460.41	1459.52	1456.34
Sound Speed at Bottom of Sediment Layer (m/s)	1511.96	1513.56	1514.50	1517.41
Sound Speed in Basement Half-Space (m/s)	1783.87	1746.84	1774.08	1758.62
Density at Top of Sediment Layer (g/cc)	1.3283	1.3724	1.5386	1.6064
Density at Bottom of Sediment Layer (g/cc)	1.5081	1.5184	1.8510	1.6379
Density in Basement Half-Space (g/cc)	2.2263	2.2782	2.7318	1.7117
Attenuation at Top of Sediment Layer (dB/ λ)	0.1241	0.0232	0.0410	0.1823
Attenuation at Bottom of Sediment Layer (dB/ λ)	0.0382	0.1397	0.1258	0.0010
Attenuation in Basement Half-Space (dB/ λ)	0.1960	0.0255	0.2879	0.0010

Table 9: Summary of GAIT V&V Test Case 4A (no added noise) inversion results using GAIT GS Version 1.0 (PE 5.1) for one-layer (N=1).

	Manual	Speeddial Settings			
	dR = 5.0 dZ = 0.1	1	2	3	4
Run Time (H:M:S)	21:48:18	6:25:07	1:11:49	0:32:13	0:17:04
Cost Function Value (Reduced Chi-Square)	0.0163	0.1559	0.0432	0.0814	0.1600
Sediment Layer Thickness (m)	18.04	95.58	18.17	18.36	17.95
Sound Speed at Top of Sediment Layer (m/s)	1549.49	1549.87	1549.85	1548.32	1543.34
Sound Speed at Bottom of Sediment Layer (m/s)	1598.79	1831.46	1597.24	1598.96	1596.79
Sound Speed in Basement Half-Space (m/s)	1858.19	2645.74	1873.32	1867.77	1895.33
Density at Top of Sediment Layer (g/cc)	1.6811	1.8278	1.7001	1.6907	1.7428
Density at Bottom of Sediment Layer (g/cc)	1.7796	2.0298	1.9218	1.7582	1.8534
Density in Basement Half-Space (g/cc)	2.0768	2.1915	1.9750	1.8334	1.9760
Attenuation at Top of Sediment Layer (dB/ λ)	0.2117	0.2148	0.2041	0.1929	0.1381
Attenuation at Bottom of Sediment Layer (dB/ λ)	0.1422	0.3208	0.1759	0.1395	0.1716
Attenuation in Basement Half-Space (dB/ λ)	0.0711	0.0461	0.0525	0.0445	0.3487

Table 10: Summary of GAIT V&V Test Case 4B (15 dB SNR) inversion results using GAIT GS Version 1.0 (PE 5.1) for one-layer (N=1).

	Manual	Speeddial Settings			
	dR = 5.0 dZ = 0.1	1	2	3	4
Run Time (H:M:S)	21:53:02	5:40:30	1:10:56	0:34:45	0:16:00
Cost Function Value (Reduced Chi-Square)	0.0537	0.0798	0.0707	0.1025	0.1720
Sediment Layer Thickness (m)	18.01	18.49	17.97	18.57	18.35
Sound Speed at Top of Sediment Layer (m/s)	1554.64	1551.28	1549.48	1547.85	1544.69
Sound Speed at Bottom of Sediment Layer (m/s)	1594.72	1600.69	1596.13	1601.01	1596.99
Sound Speed in Basement Half-Space (m/s)	1854.36	1881.18	1840.46	1861.08	1888.50
Density at Top of Sediment Layer (g/cc)	1.7544	1.7428	1.6977	1.7534	1.7080
Density at Bottom of Sediment Layer (g/cc)	1.8229	1.7550	1.7814	1.9020	1.7822
Density in Basement Half-Space (g/cc)	2.0956	1.7798	1.8790	1.9973	1.8100
Attenuation at Top of Sediment Layer (dB/ λ)	0.1954	0.2083	0.1922	0.1506	0.1645
Attenuation at Bottom of Sediment Layer (dB/ λ)	0.1465	0.1350	0.1761	0.1711	0.1753
Attenuation in Basement Half-Space (dB/ λ)	0.1426	0.4115	0.0736	0.1193	0.0264

Table 11: Summary of GAIT V&V Test Case 4C (5 dB SNR) inversion results using GAIT GS Version 1.0 (PE 5.1) for one-layer (N=1).

	Manual	Speeddial Settings			
	dR = 5.0 dZ = 0.1	1	2	3	4
Run Time (H:M:S)	35:28:16	6:14:40	1:40:15	0:31:16	0:15:22
Cost Function Value (Reduced Chi-Square)	0.4424	0.3130	0.2151	0.2363	0.3263
Sediment Layer Thickness (m)	142.84	18.85	17.95	18.18	18.21
Sound Speed at Top of Sediment Layer (m/s)	1555.88	1549.39	1550.67	1549.60	1543.92
Sound Speed at Bottom of Sediment Layer (m/s)	1947.87	1604.26	1596.14	1591.05	1598.07
Sound Speed in Basement Half-Space (m/s)	3744.34	2475.79	1840.69	1850.93	1881.00
Density at Top of Sediment Layer (g/cc)	1.8281	1.8027	1.6935	1.7292	1.7514
Density at Bottom of Sediment Layer (g/cc)	2.1006	1.8461	1.8872	1.8763	1.7821
Density in Basement Half-Space (g/cc)	2.2810	2.3244	2.0648	1.9115	1.8495
Attenuation at Top of Sediment Layer (dB/ λ)	0.0841	0.1871	0.1967	0.1951	0.1458
Attenuation at Bottom of Sediment Layer (dB/ λ)	0.5311	0.2748	0.1097	0.1564	0.1550
Attenuation in Basement Half-Space (dB/ λ)	0.8843	0.3549	0.0509	0.0704	0.0535

Table 12: Summary of GAIT V&V Test Case 4D (0 dB SNR) inversion results using GAIT GS Version 1.0 (PE 5.1) for one-layer (N=1).

	Manual	Speeddial Settings			
	dR = 5.0 dZ = 0.1	1	2	3	4
Run Time (H:M:S)	25:07:19	8:04:35	1:12:03	0:30:58	0:26:07
Cost Function Value (Reduced Chi-Square)	0.4397	0.5292	0.3915	0.4097	0.4668
Sediment Layer Thickness (m)	17.99	169.48	18.44	18.61	176.78
Sound Speed at Top of Sediment Layer (m/s)	1562.76	1556.99	1549.53	1551.97	1544.02
Sound Speed at Bottom of Sediment Layer (m/s)	1583.31	1870.55	1604.16	1591.73	1733.23
Sound Speed in Basement Half-Space (m/s)	1865.69	4832.48	1837.24	1886.75	5182.65
Density at Top of Sediment Layer (g/cc)	1.7862	1.8238	1.7902	1.8005	1.6662
Density at Bottom of Sediment Layer (g/cc)	1.8316	2.0162	1.8927	1.8410	1.8062
Density in Basement Half-Space (g/cc)	1.9955	2.3988	1.9006	1.9133	1.8527
Attenuation at Top of Sediment Layer (dB/ λ)	0.0429	0.0479	0.1398	0.1218	0.0326
Attenuation at Bottom of Sediment Layer (dB/ λ)	0.0723	0.2674	0.1107	0.0788	0.0010
Attenuation in Basement Half-Space (dB/ λ)	0.0354	0.0250	0.0454	0.0519	0.5400

Table 13: Summary of GAIT V&V Test Case 6 inversion results using GAIT GS Version 1.0 (PE 5.1) for one-layer (N=1) and 53 to 503 Hz TL data.

	Speeddial Settings				
	1	2	3	4	5
Run Time (H:M:S)	37:10:01	8:22:48	4:16:07	2:24:58	1:14:06
Cost Function Value (Reduced Chi-Square)	0.4350	0.4903	0.4344	0.4338	0.4647
Sediment Layer Thickness (m)	36.27	53.74	84.40	96.13	86.30
Sound Speed at Top of Sediment Layer (m/s)	1477.80	1507.38	1478.32	1476.71	1478.31
Sound Speed at Bottom of Sediment Layer (m/s)	1536.59	1597.06	1639.61	1665.60	1646.54
Sound Speed in Basement Half-Space (m/s)	1570.07	1619.21	1890.17	2186.39	2583.13
Density at Top of Sediment Layer (g/cc)	1.6892	1.4300	1.4704	1.6081	1.5577
Density at Bottom of Sediment Layer (g/cc)	1.7666	1.5501	1.5569	1.8320	1.9108
Density in Basement Half-Space (g/cc)	1.8167	1.7769	1.6211	2.0743	2.3056
Attenuation at Top of Sediment Layer (dB/ λ)	0.0913	0.1454	0.0967	0.1004	0.0909
Attenuation at Bottom of Sediment Layer (dB/ λ)	0.0010	0.0010	0.0010	0.0010	0.0010
Attenuation in Basement Half-Space (dB/ λ)	0.0010	0.3028	0.0010	0.2706	0.0010

Table 14: Summary of GAIT V&V Test Case 6 inversion results (10-parameter LFBL geoacoustic parameter format) using GAIT GS Version 1.0 (ASTRAL 5.1).

Inverted Geoacoustic Parameter	53 – 503 Hz TL Data	53 – 953 Hz TL Data
Sediment Sound Speed Ratio	0.999	1.004
Sound Speed Gradient (m/s/m)	2.438	2.219
Sound Speed Curvature (Beta)	-0.97	-0.97
Density at Top of Sediment (g/cc)	1.332	1.443
Attenuation (dB/m/kHz)	0.120	0.269
Attenuation Gradient (dB/m/kHz/m)	0.010	0.019
Frequency Exponent	1.750	1.734
Basement Reflectivity	0.017	0.023
Two-way Travel Time (sec)	0.054	0.653

Table 15: Summary of GAIT V&V Test Case 10A inversion results using GAIT GS Version 1.0 (PE 5.1) for one-layer (N=1) using 20, 40, 80, 160, 315 and 630 Hz TL data.

	Speeddial Settings		
	3	**4**	**5**
Run Time (H:M:S)	4:48:53	2:35:39	0:54:28
Cost Function Value (Reduced Chi-Square)	0.3034	0.2804	0.3096
Sediment Layer Thickness (m)	58.05	150.06	22.39
Sound Speed at Top of Sediment Layer (m/s)	1921.69	1975.87	2259.82
Sound Speed at Bottom of Sediment Layer (m/s)	1922.88	1977.88	2266.93
Sound Speed in Basement Half-Space (m/s)	2231.32	3587.91	2437.16
Density at Top of Sediment Layer (g/cc)	1.3017	1.3687	1.5769
Density at Bottom of Sediment Layer (g/cc)	2.0833	1.8397	1.6481
Density in Basement Half-Space (g/cc)	2.1495	2.2087	2.3411
Attenuation at Top of Sediment Layer (dB/ λ)	0.4871	0.5713	0.9479
Attenuation at Bottom of Sediment Layer (dB/ λ)	0.7245	0.3329	0.8373
Attenuation in Basement Half-Space (dB/ λ)	0.0375	0.7199	0.8956

Table 16: Summary of GAIT V&V Test Case 10B inversion results using GAIT GS Version 1.0 (PE 5.1) for one-layer (N=1) using 20, 40, 80, 160, 315 and 630 Hz TL data.

	Speeddial Settings		
	3	**4**	**5**
Run Time (H:M:S)	3:48:33	1:27:15	0:53:40
Cost Function Value (Reduced Chi-Square)	0.2918	0.2822	0.3000
Sediment Layer Thickness (m)	59.40	15.86	175.82
Sound Speed at Top of Sediment Layer (m/s)	2013.69	2039.04	2056.23
Sound Speed at Bottom of Sediment Layer (m/s)	2017.29	2081.36	2581.27
Sound Speed in Basement Half-Space (m/s)	2864.54	2082.24	5286.71
Density at Top of Sediment Layer (g/cc)	1.3262	1.5656	1.6271
Density at Bottom of Sediment Layer (g/cc)	1.9633	1.8044	1.6404
Density in Basement Half-Space (g/cc)	2.4946	1.9135	2.8974
Attenuation at Top of Sediment Layer (dB/ λ)	0.6696	0.7388	0.7604
Attenuation at Bottom of Sediment Layer (dB/ λ)	0.8226	0.6746	0.9498
Attenuation in Basement Half-Space (dB/ λ)	0.5063	0.8479	0.0128

Table 17: Summary of GAIT V&V Test Case 10C inversion results using GAIT GS Version 1.0 (PE 5.1) for one-layer (N=1) using 20, 40, 80, 160, 315 and 630 Hz TL data.

	Speeddial Settings		
	3	**4**	**5**
Run Time (H:M:S)	3:20:01	1:47;23	0:55:24
Cost Function Value (Reduced Chi-Square)	0.3377	0.3286	0.3306
Sediment Layer Thickness (m)	69.50	110.79	189.85
Sound Speed at Top of Sediment Layer (m/s)	1638.96	1645.12	1739.32
Sound Speed at Bottom of Sediment Layer (m/s)	1686.05	1748.27	1768.04
Sound Speed in Basement Half-Space (m/s)	1742.88	1748.65	5394.04
Density at Top of Sediment Layer (g/cc)	1.8426	1.7295	1.7905
Density at Bottom of Sediment Layer (g/cc)	1.8441	1.9074	1.8144
Density in Basement Half-Space (g/cc)	1.8925	2.0196	1.9150
Attenuation at Top of Sediment Layer (dB/ λ)	0.3449	0.3264	0.7068
Attenuation at Bottom of Sediment Layer (dB/ λ)	0.0156	0.0825	0.1421
Attenuation in Basement Half-Space (dB/ λ)	0.8285	0.2254	0.3332

Table 18: Summary of GAIT V&V Test Case 10A, 10B and 10C inversion results (10-parameter LFBL geoacoustic parameter format) using GAIT GS Version 1.0 (ASTRAL 5.1) using 20, 40, 80, 160, 315 and 630 Hz TL data.

Inverted Geoacoustic Parameter	Test Case 10A	Test Case 10B	Test Case 10C
Sediment Sound Speed Ratio	1.078	1.139	1.047
Sound Speed Gradient (m/s/m)	2.342	1.993	0.503
Sound Speed Curvature (Beta)	-0.970	0.86	0.010
Density at Top of Sediment (g/cc)	2.797	2.123	1.670
Attenuation (dB/m/kHz)	0.117	0.381	0.454
Attenuation Gradient (dB/m/kHz/m)	0.015	0.001	0.010
Frequency Exponent	1.386	1.360	1.750
Basement Reflectivity	0.114	0.066	0.024
Two-way Travel Time (sec)	0.006	0.028	0.133

Table 19: Summary of GAIT V&V Test Cases 7, 8A and 8B inversion results (10-parameter LFBL geoacoustic parameter format with a bottom backscatter coefficient) using GAIT GS Version 1.0 (ASPM 5.1).

Inverted Geoacoustic Parameter	Test Case 7	Test Case 8A	Test Case 8B
Sediment Sound Speed Ratio	1.163	1.330	1.168
Sound Speed Gradient (m/s/m)	0.501	0.504	2.305
Sound Speed Curvature (Beta)	0.01	0.01	-0.97
Density at Top of Sediment (g/cc)	2.23	1.33	1.49
Attenuation (dB/m/kHz)	0.1434	0.7314	0.0001
Attenuation Gradient (dB/m/kHz/m)	0.0148	0.0174	0.0004
Frequency Exponent	1.21	1.02	1.13
Basement Reflectivity	0.91	0.75	0.93
Two-way Travel Time (sec)	0.3822	0.0173	0.0221
Bottom Backscatter Coefficient	-49 dB	-41 dB	-44 dB
Reduced Chi-Square	0.2140	0.1124	0.0595

Figures

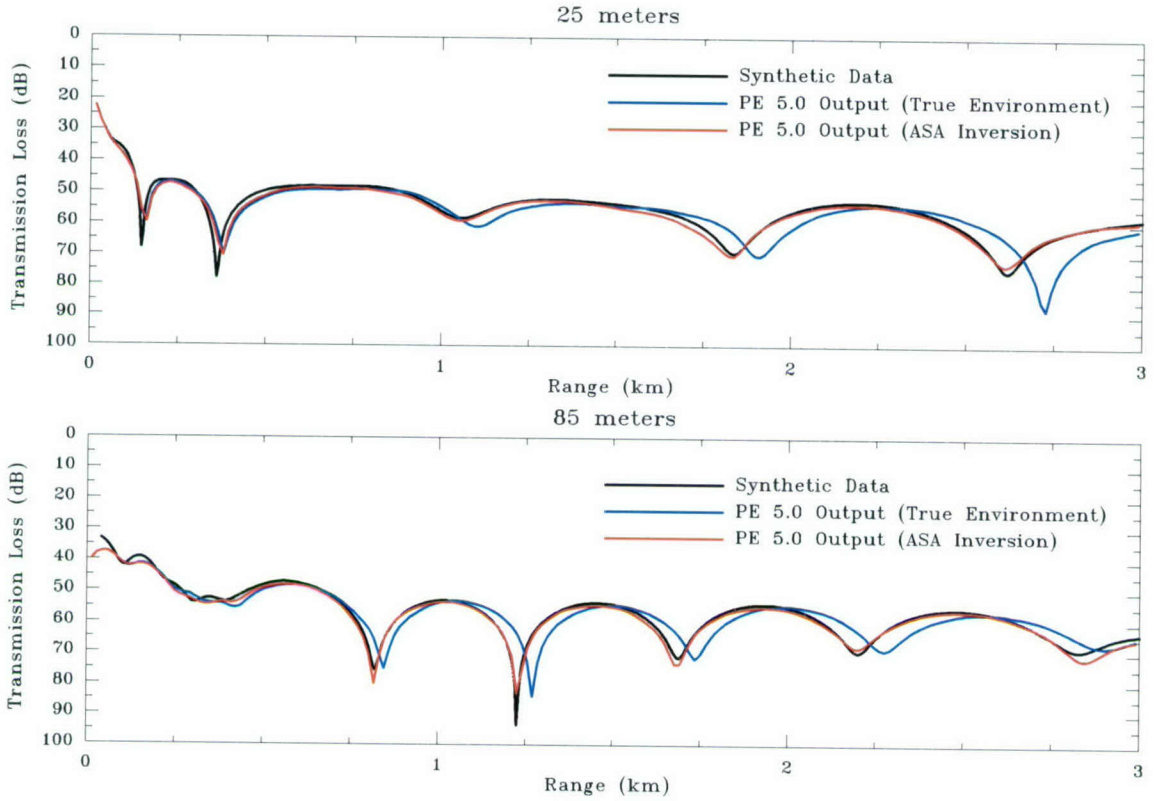

Figure 1: ITW Test Case 0 (25 Hz data) - Comparison between synthetic data (black line), PE 5.0 output using true environment and PE 5.0 output using ASA inversion environment. Top plot shows 25 meter receiver depth and bottom plot shows 85 meter receiver depth.

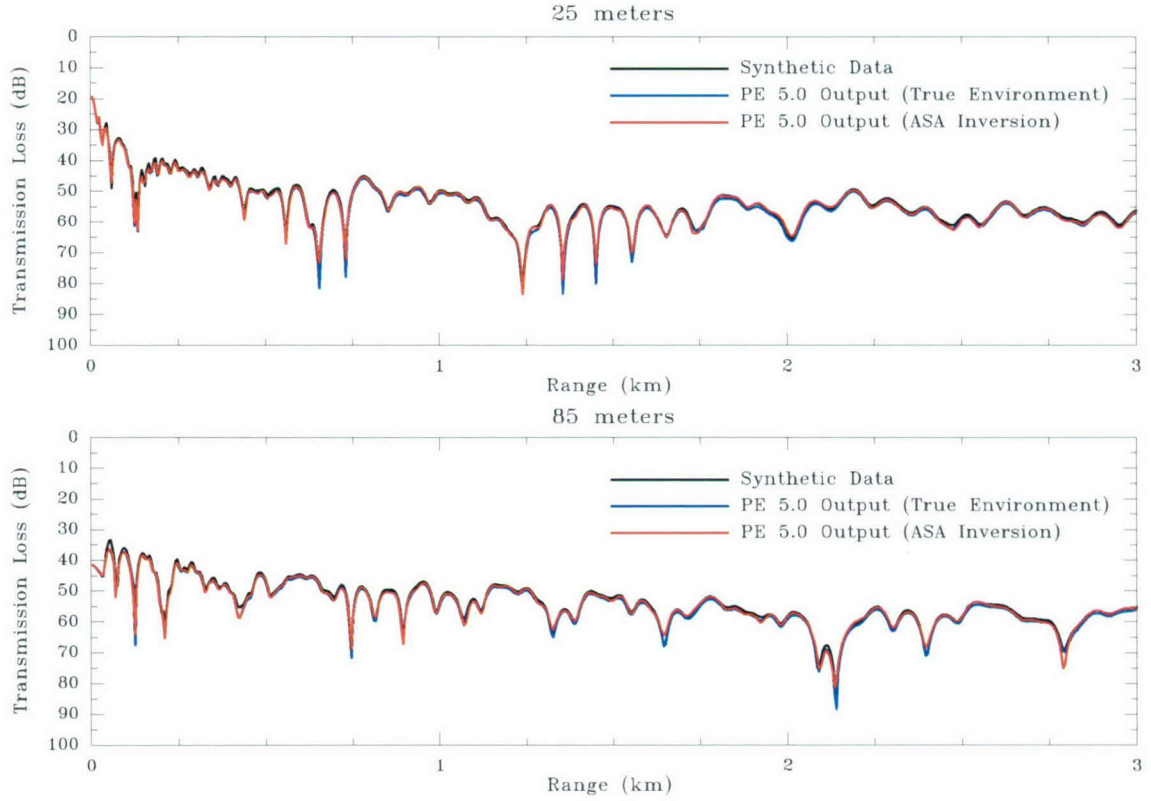

Figure 2: ITW Test Case 0 (200 Hz data) - Comparison between synthetic data (black line), PE 5.0 output using true environment and PE 5.0 output using ASA inversion environment. Top plot shows 25 meter receiver depth and bottom plot shows 85 meter receiver depth.

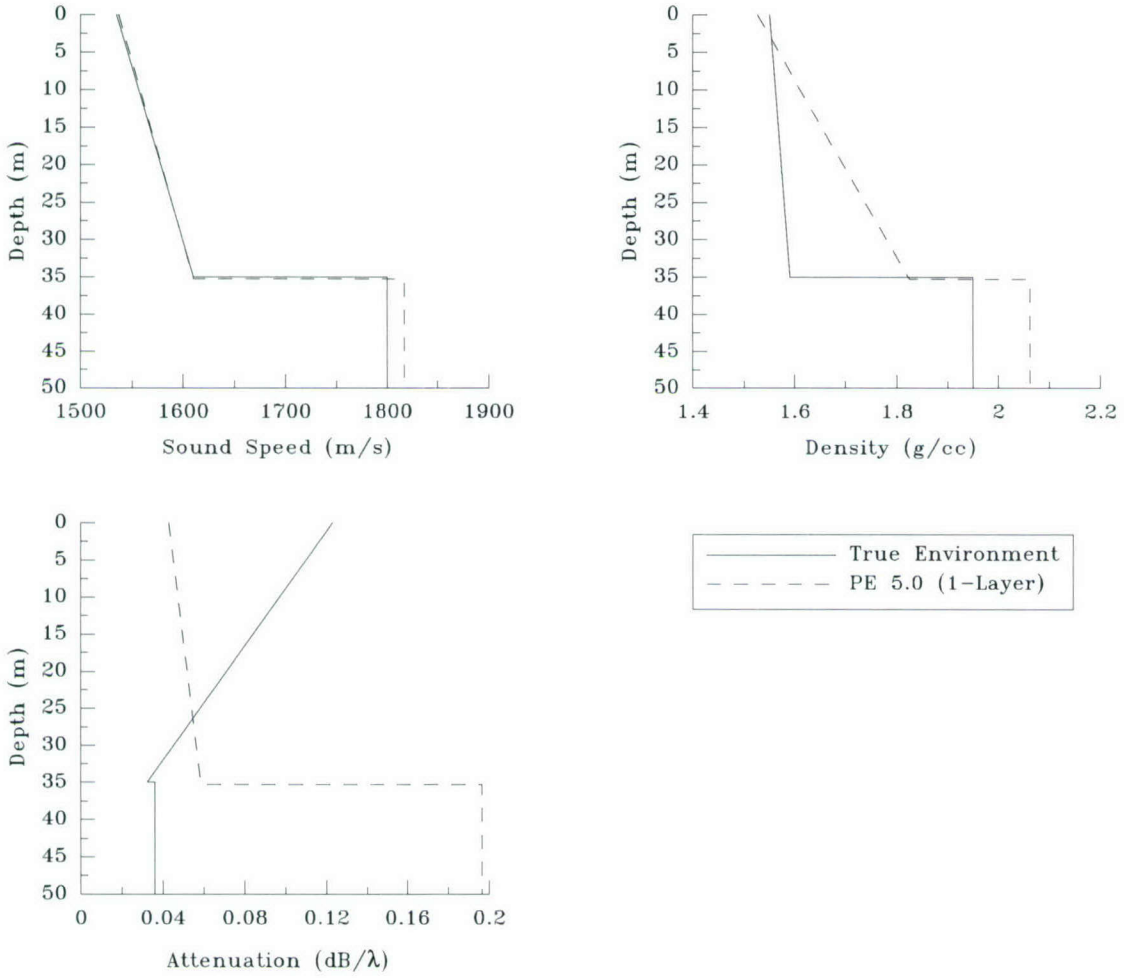

Figure 3: Comparison between true geoacoustics (solid black line) and best-fit (25, 50, 100 and 200 Hz) inverted parameters (dashed black line) for test case 0 (calibration case).

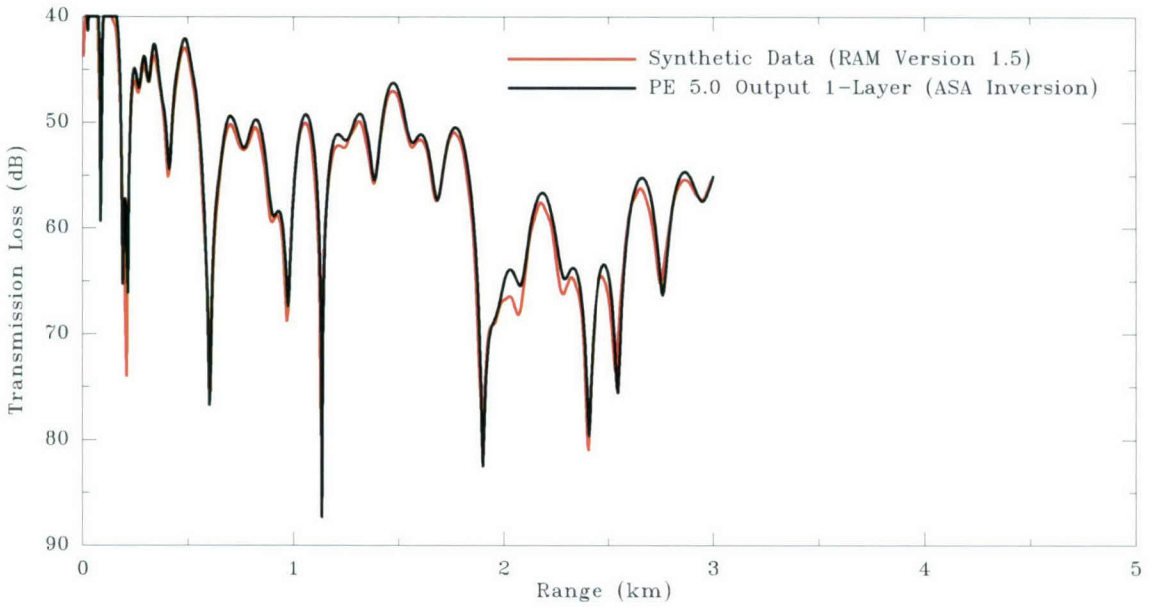

Figure 4: ITW Test Case 0 (80 Hz data) - Comparison between synthetic data (red line) and PE 5.0 output using ASA inversion environment (black line).

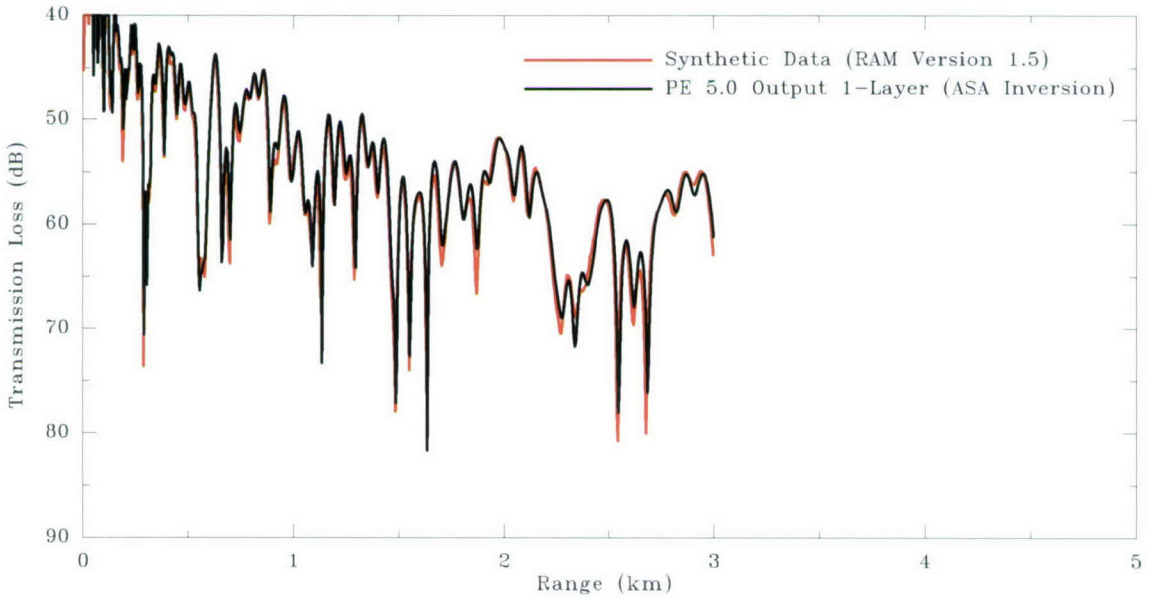

Figure 5: ITW Test Case 0 (220 Hz data) - Comparison between synthetic data (red line) and PE 5.0 output using ASA inversion environment (black line).

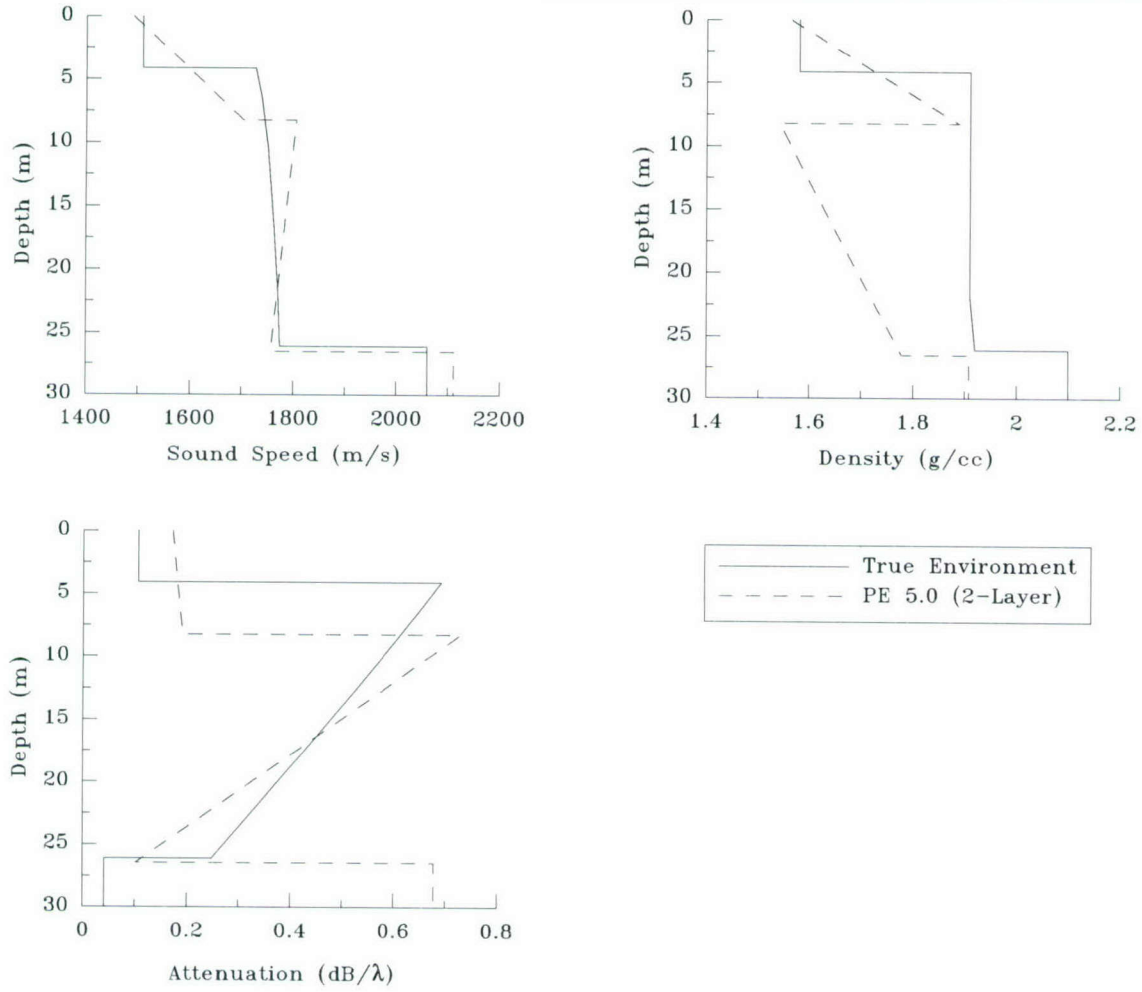

Figure 6: Comparison between true geoacoustics (solid black line) and best-fit (25, 50, 100 and 200 Hz) inverted parameters (dashed black line) for test case 1 (monotonic downslope).

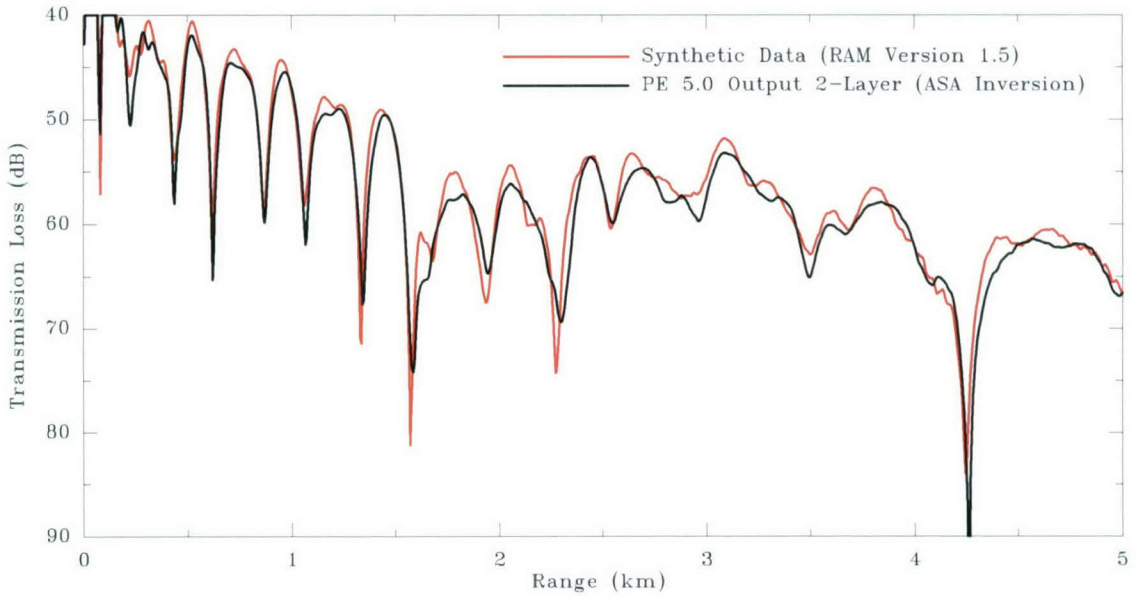

Figure 7: ITW Test Case 1 (80 Hz data) - Comparison between synthetic data (red line) and PE 5.0 output using ASA inversion environment (black line).

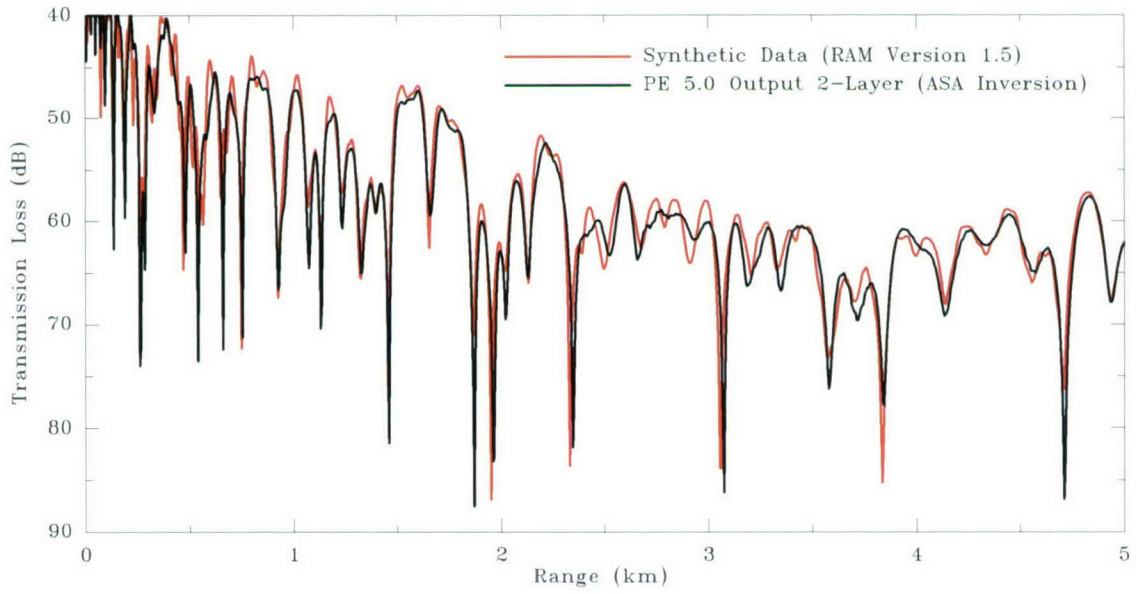

Figure 8: ITW Test Case 1 (220 Hz data) - Comparison between synthetic data (red line) and PE 5.0 output using ASA inversion environment (black line).

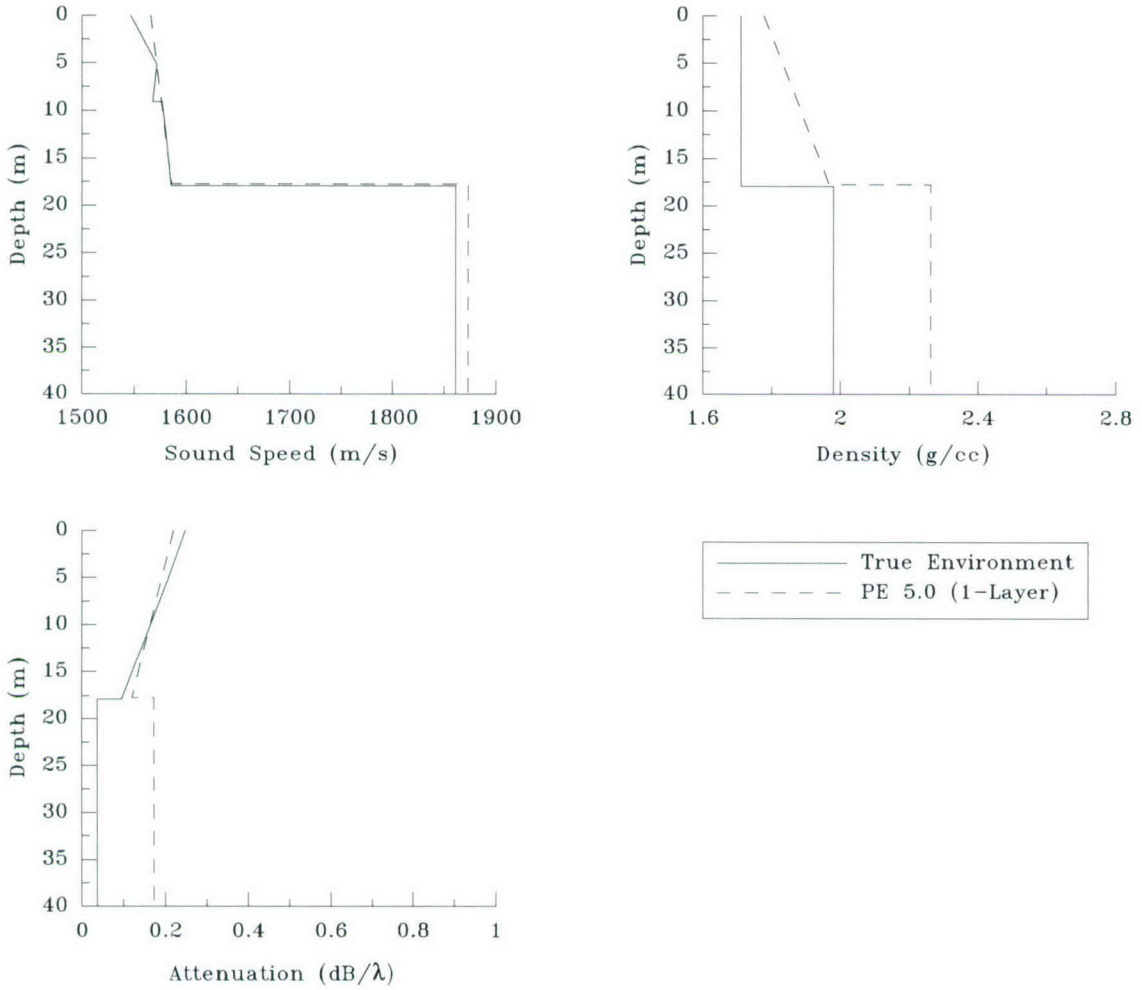

Figure 9: Comparison between true geoacoustics (solid black line) and best-fit (50, 100 and 200 Hz) inverted parameters (dashed black line) for test case 2 (shelfbreak).

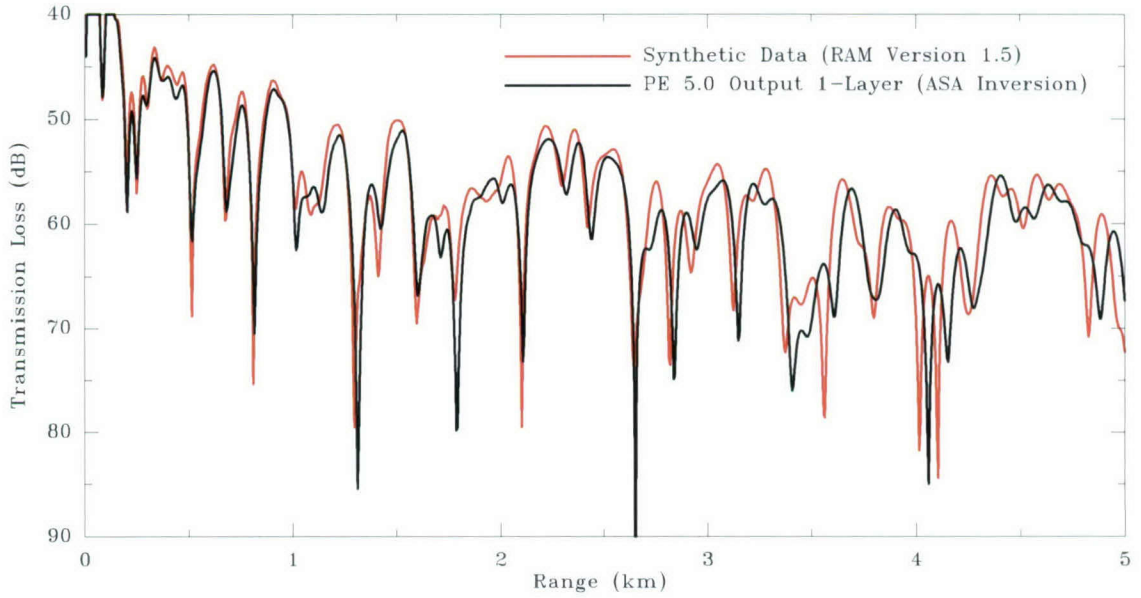

Figure 10: ITW Test Case 2 (80 Hz data) - Comparison between synthetic data (red line) and PE 5.0 output using ASA inversion environment (black line).

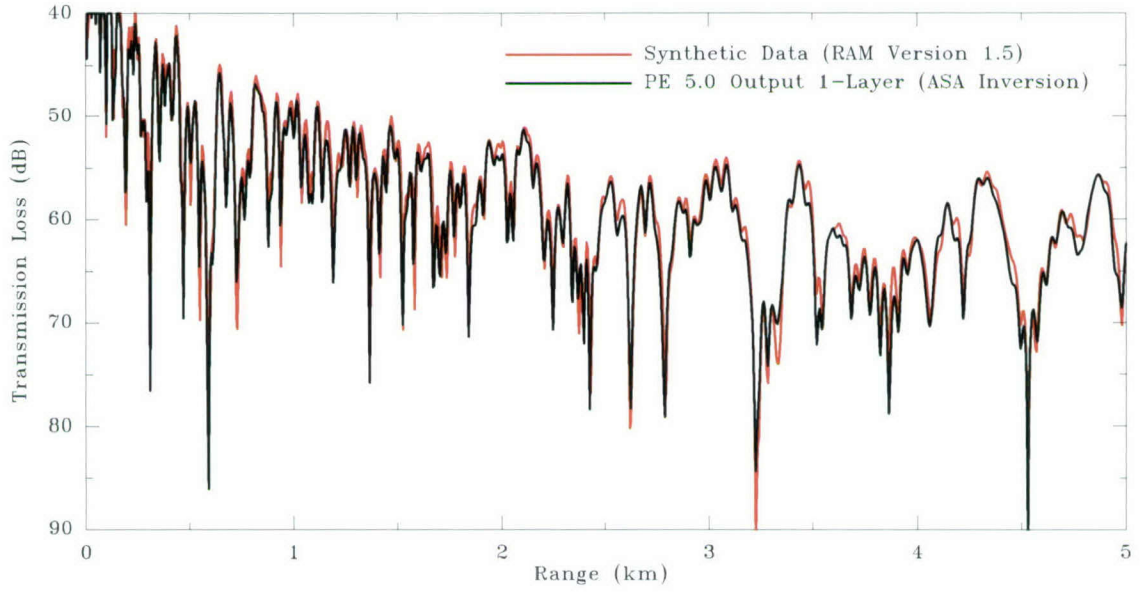

Figure 11: ITW Test Case 2 (220 Hz data) - Comparison between synthetic data (red line) and PE 5.0 output using ASA inversion environment (black line).

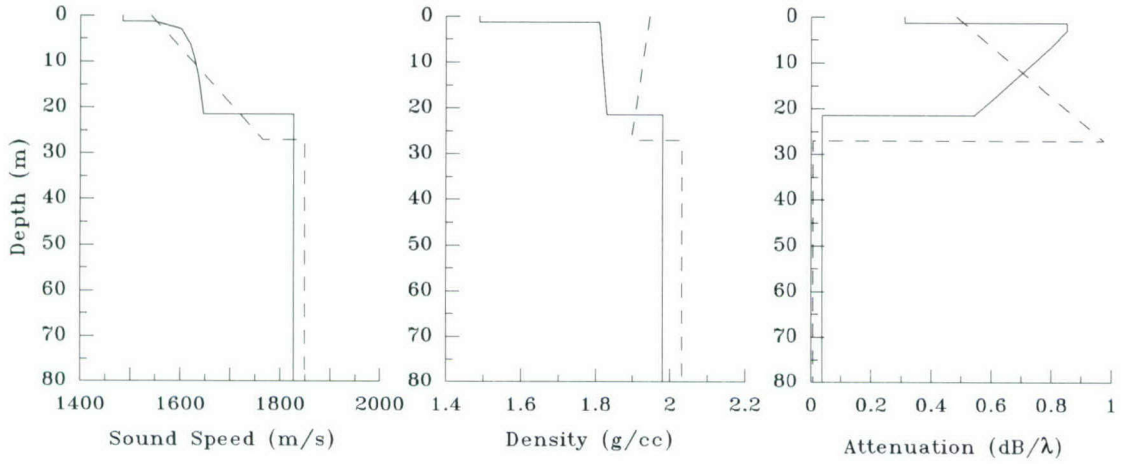

Figure 12: Comparison between true geoacoustics (solid black line) and best-fit inverted parameters (dashed line) for test case 3 background environment (0 - 1,100 meters and 2,900 – 5,000 meters).

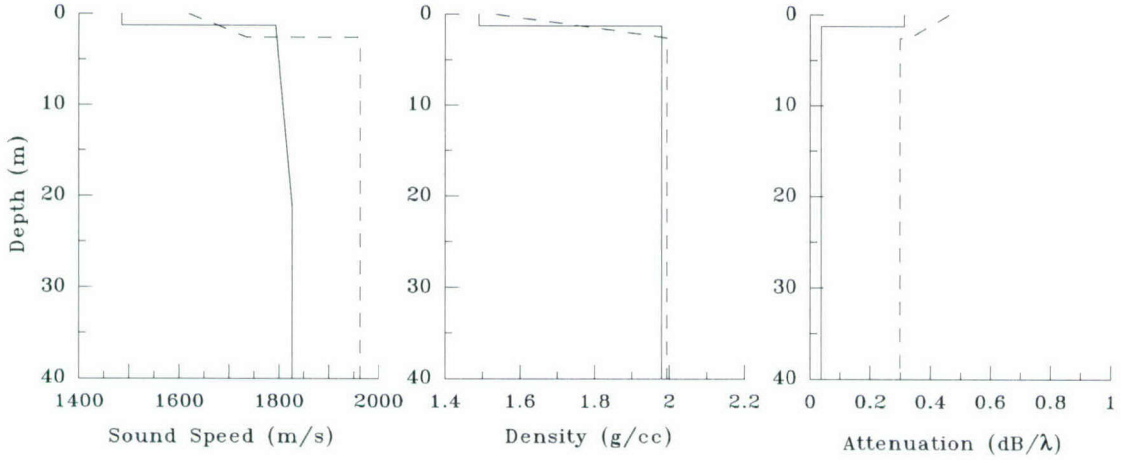

Figure 13: Comparison between true geoacoustics (solid black line) and best-fit inverted parameters (dashed line) for test case 3 intrusion environment (1,100 - 2,900 meters).

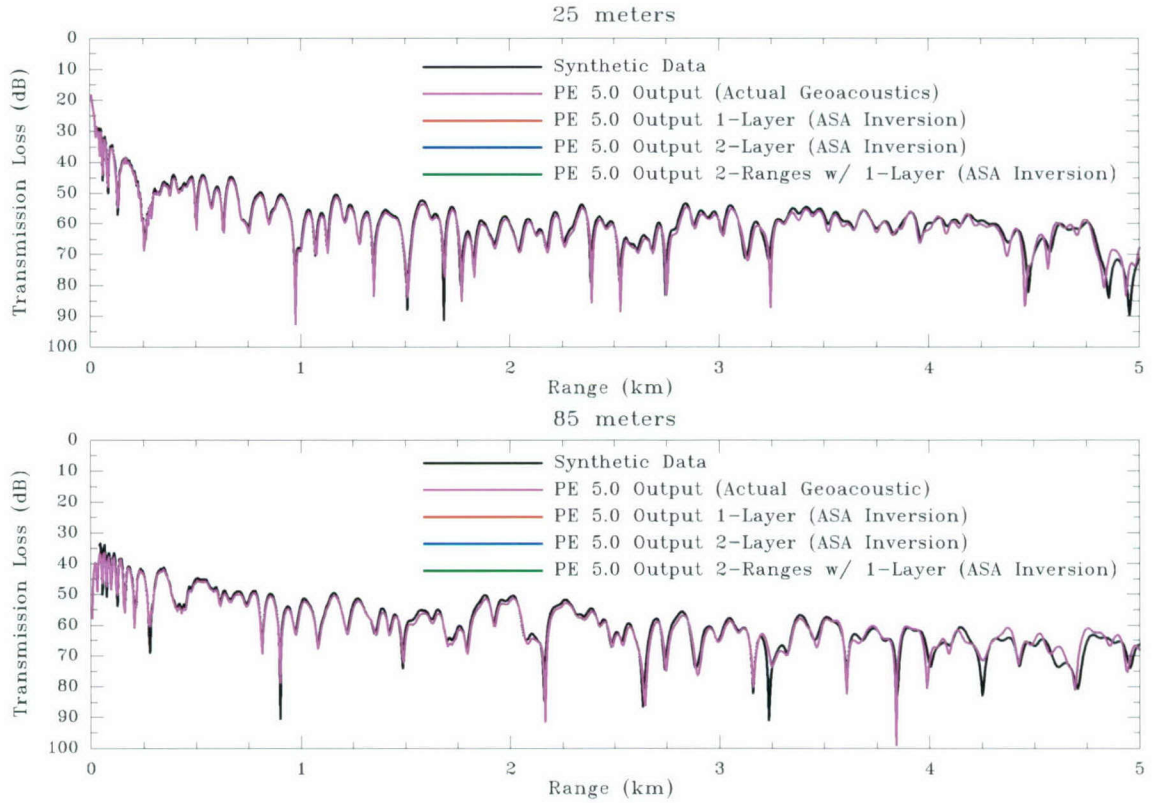

Figure 14: ITW Test Case 3 (400 Hz data) - Comparison between synthetic data (black line), PE 5.0 output using true environment (purple line), PE 5.0 output using inverted fit for 1-layer range-independent (red line), PE 5.0 output using inverted fit for 2-layer range-independent (blue line) and PE 5.0 output using inverted fit for 1-layer range-dependent (green line). Top plot shows 25 meter receiver depth and bottom plot shows 85 meter receiver depth.

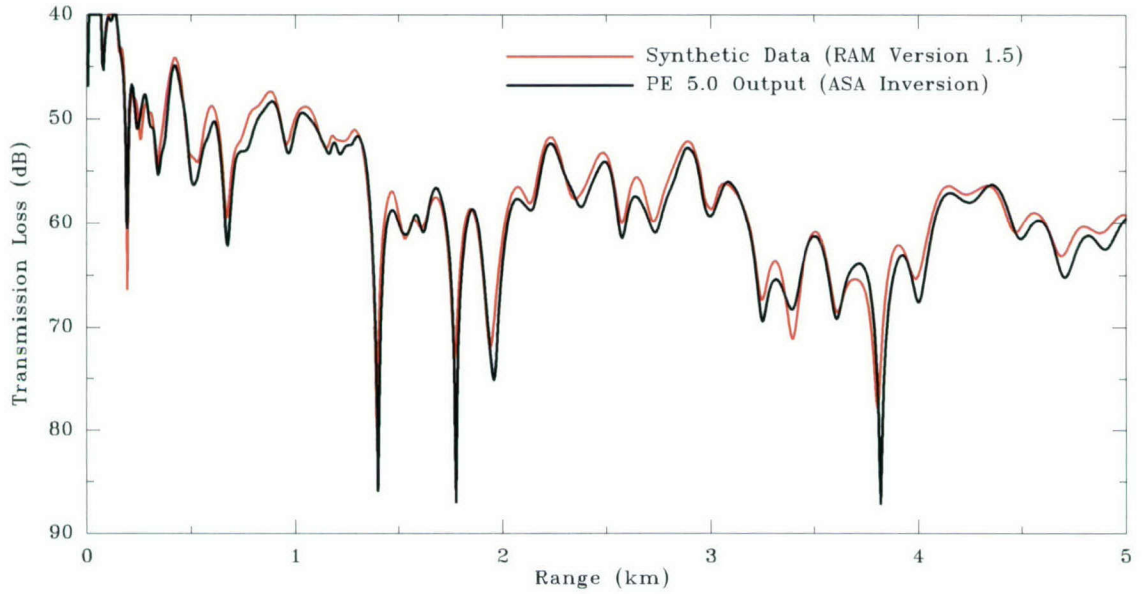

Figure 15: ITW Test Case 3 (80 Hz data) - Comparison between synthetic data (red line) and PE 5.0 output using ASA inversion environment (black line).

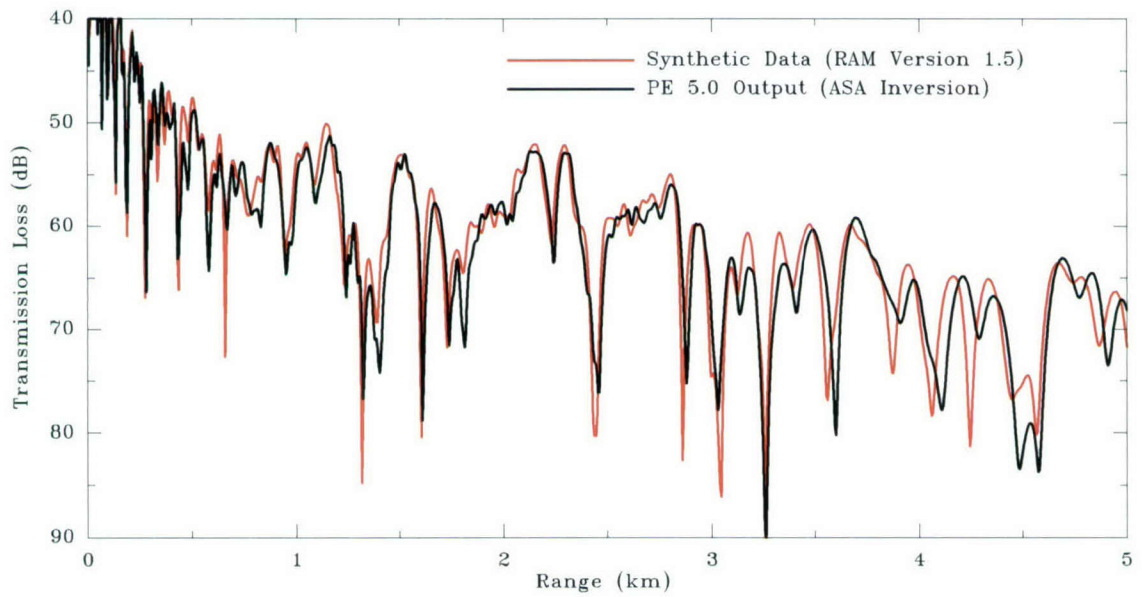

Figure 16: ITW Test Case 3 (220 Hz data) - Comparison between synthetic data (red line) and PE 5.0 output using ASA inversion environment (black line).

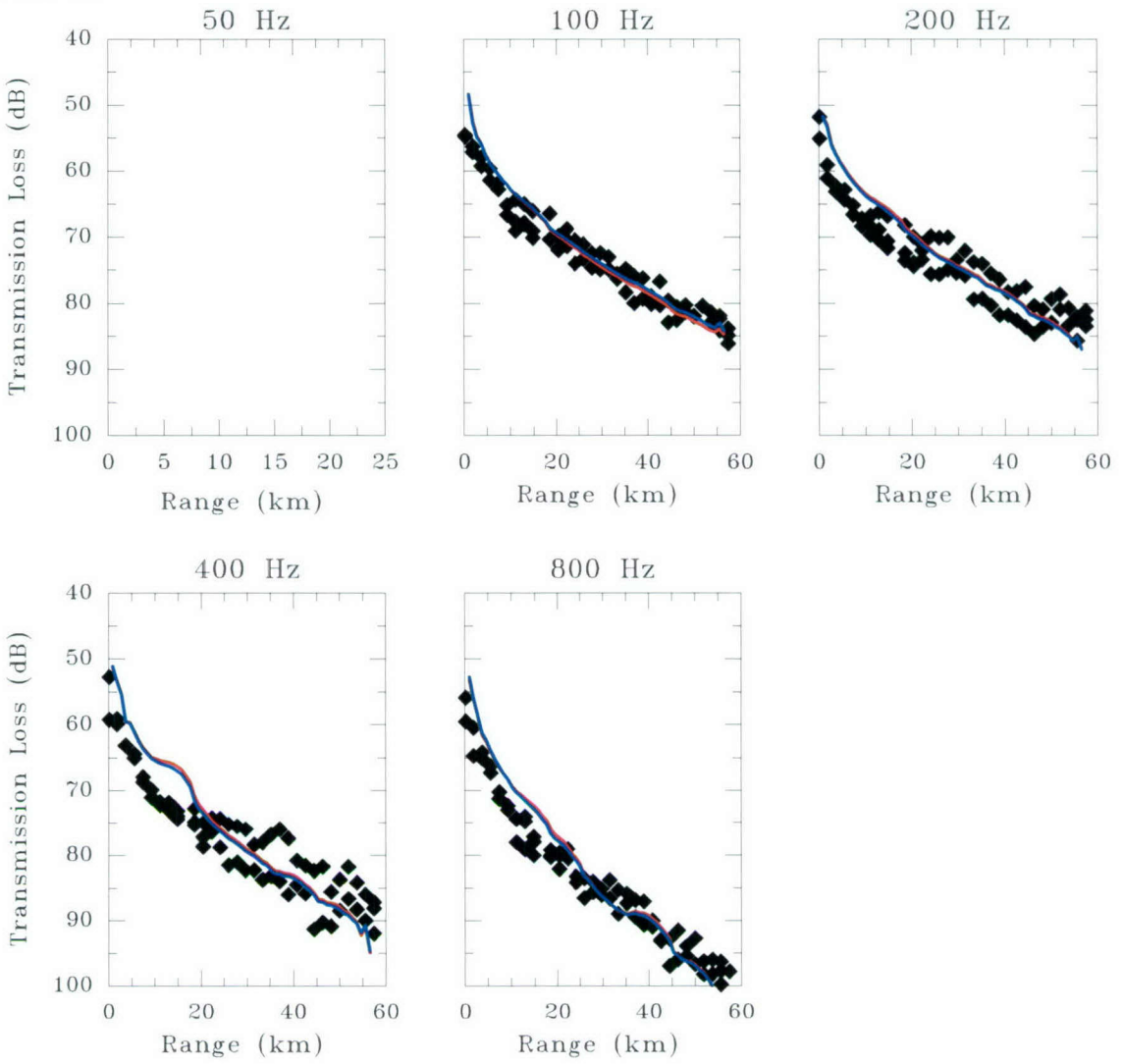

Figure 17: ITW Test Case 4 – Comparison of measured octave band TL data (black diamonds) with inversion using ASTRAL 5.0 with 3,000 iterations (red line) and 10,000 iterations (blue line).

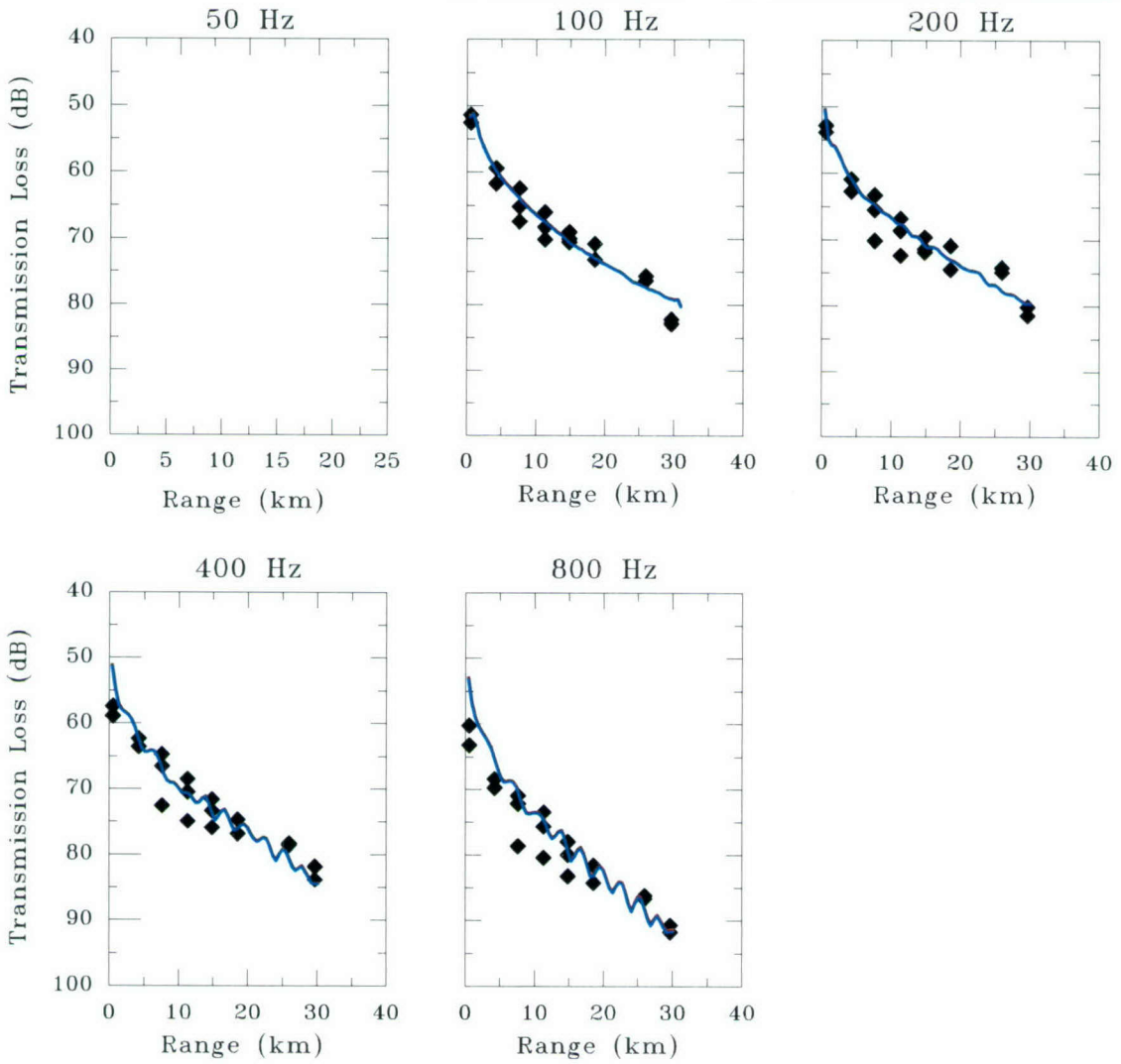

Figure 18: ITW Test Case 5 – Comparison of measured octave band TL data (black diamonds) with inversion using ASTRAL 5.0 with 3,000 iterations (red line) and 10,000 iterations (blue line).

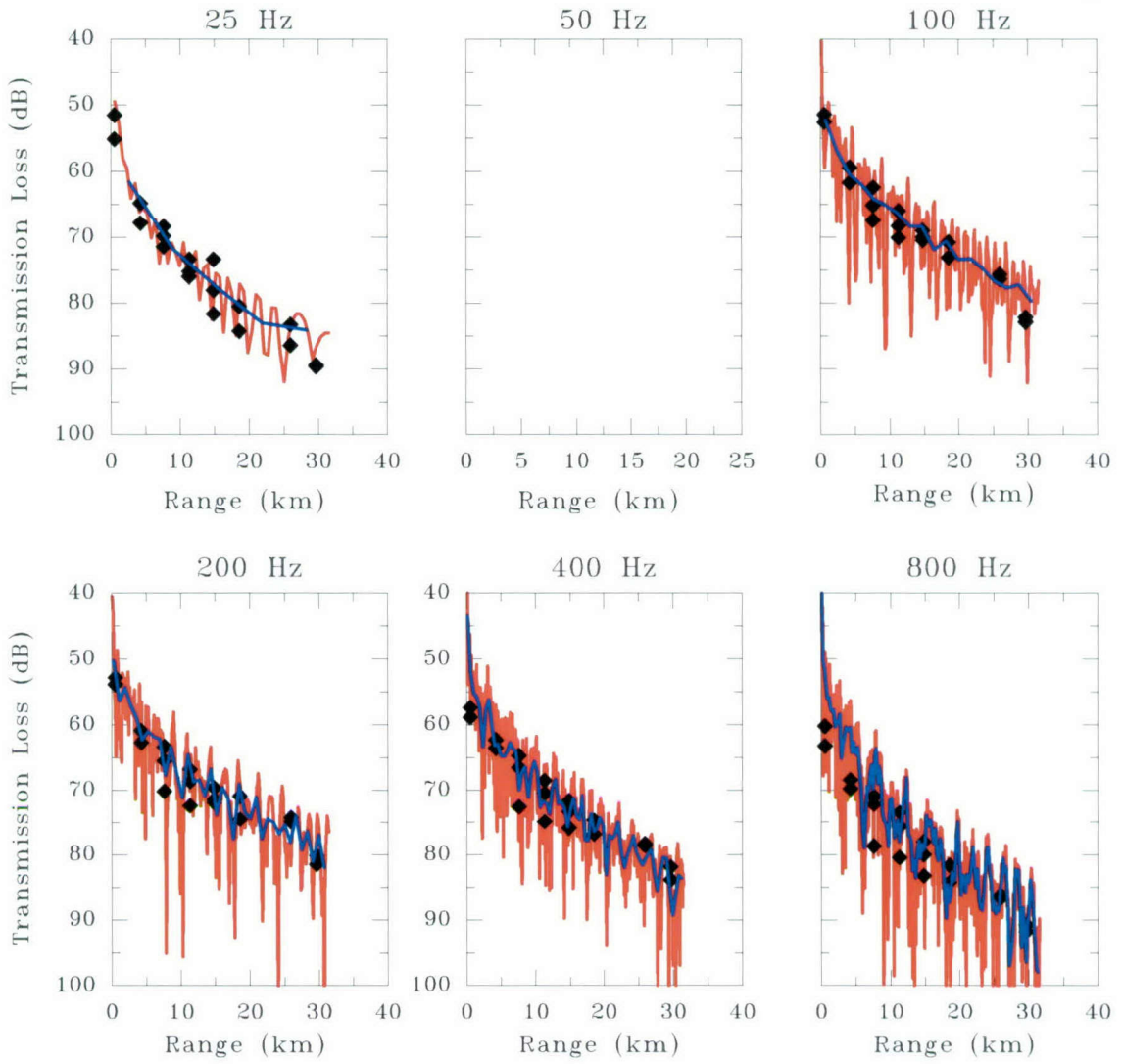

Figure 19: ITW Test Case 5 – Comparison of measured octave band TL data (black diamonds) with inversion using PE 5.0 with 10,000 iterations (red line) and the range-average output of PE 5.0 (blue line).

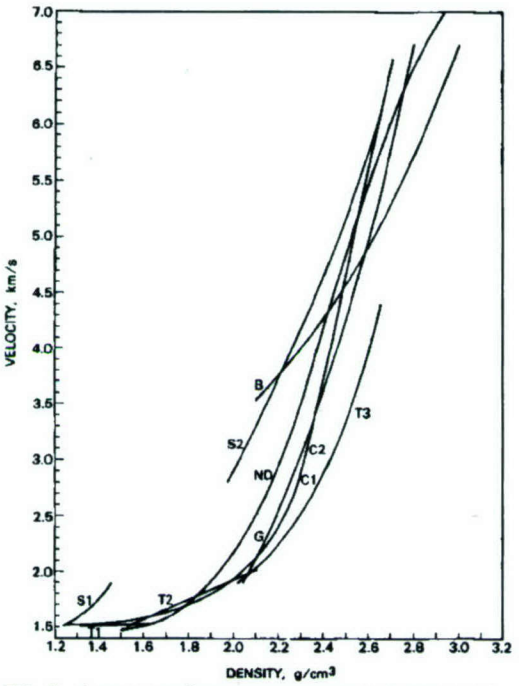

FIG. 7. A summary of compressional-wave velocity versus density in Figs. 1–4: S1–diatomaceous sediments (0–500 m), S2–siliceous rocks, T1–terrigenous surface sediments, T2–turbidites (0–500 m), T3–mudstones, shales, C1–chalk, limestone, C2–limestone, curve B (from Christensen and Salisbury[17]) represents basalt. The general curves of Nafe and Drake[11] (labeled ND) and Gardner *et al.*[12] (labeled G) are included for comparisons. The equation for the curve of Gardner *et al.*[12] (p. 779) is $\rho = 0.23 V_p^{0.25}$, where ρ is density in g/cm³, and V_p is compressional-wave velocity in ft/s.

Figure 20: Figure 7 from Edwin L. Hamilton, "Sound velocity-density relations in sea floor sediments and rock," Journal of Acoustical Society of America, 63 (2), pp. 366-377 (1978).

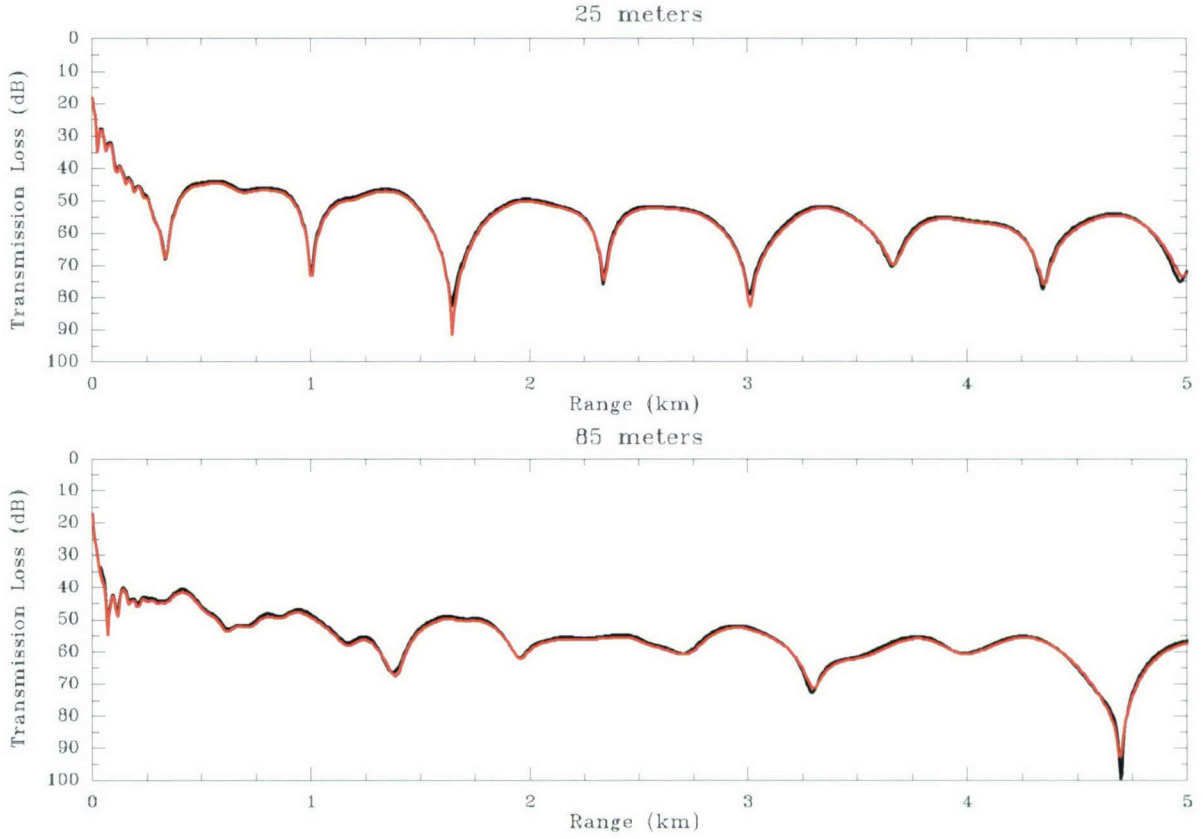

Figure 21: GAIT V&V Test Case 1A (50 Hz data) - Comparison between synthetic data (black line) and PE 5.1 output using geoacoustic parameters from GAIT GS Version 1.0. Top plot shows 25 meter receiver depth and bottom plot shows 85 meter receiver depth.

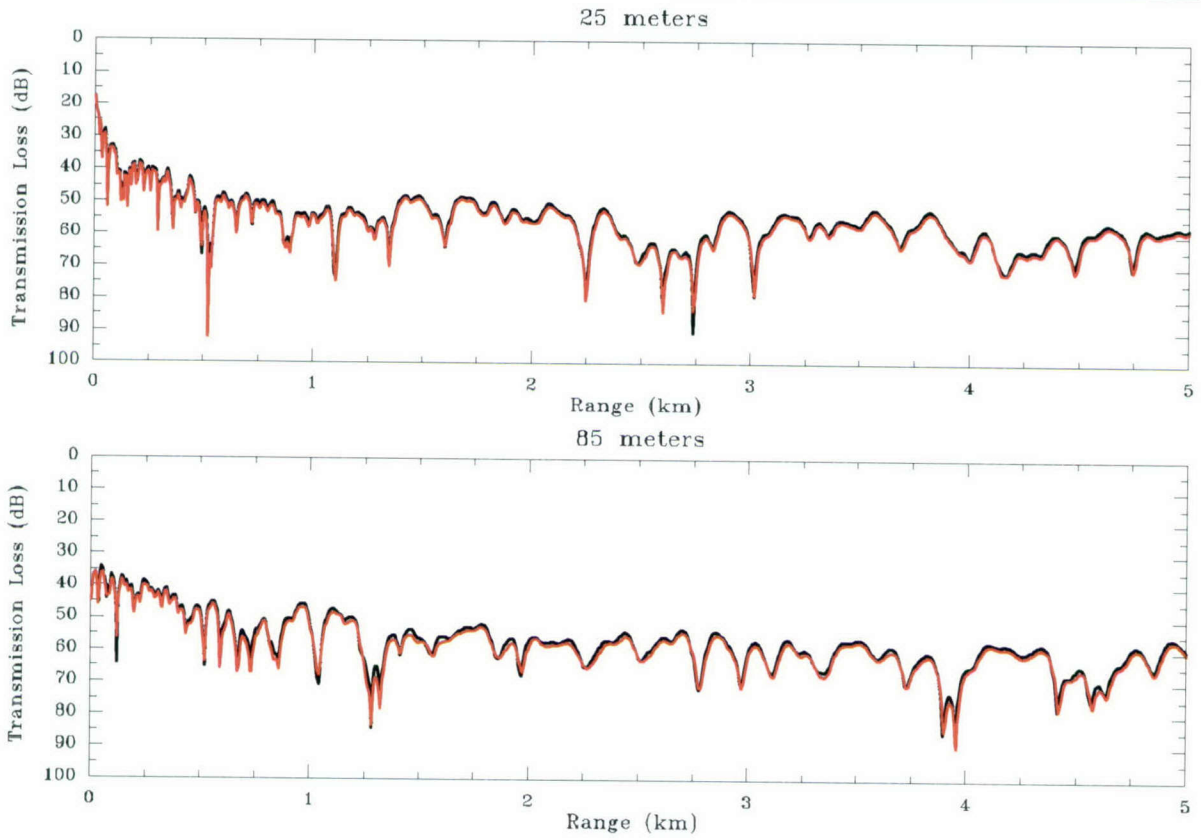

Figure 22: GAIT V&V Test Case 1A (200 Hz data) - Comparison between synthetic data (black line) and PE 5.1 output using geoacoustic parameters from GAIT GS Version 1.0. Top plot shows 25 meter receiver depth and bottom plot shows 85 meter receiver depth.

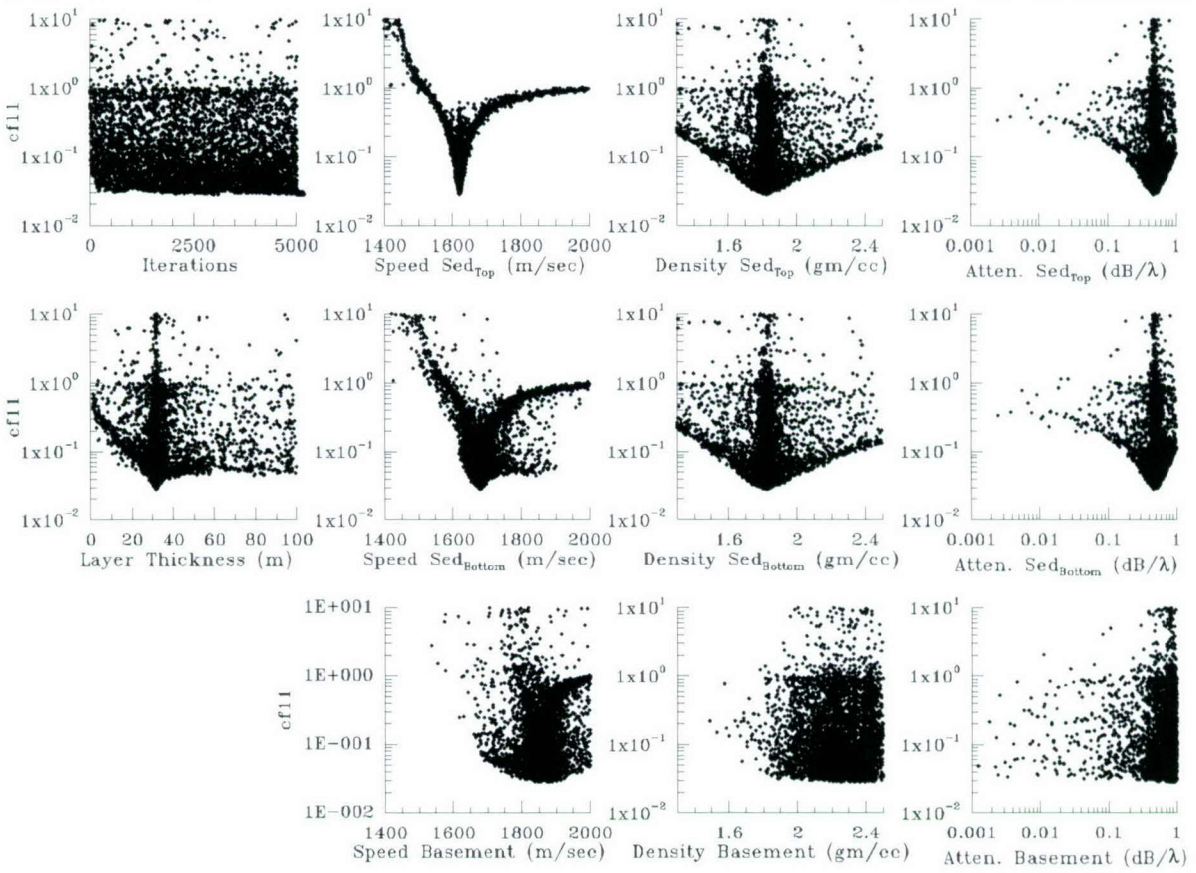

Figure 23: GAIT V&V Test Case 1A (5 meter range step for PE 5.1 with reduced chi-square cost function using TL data) – Plot of cost function values versus unknown parameters with left column – layer thickness, second column– sound speed, third column – density and fourth column – attenuation.

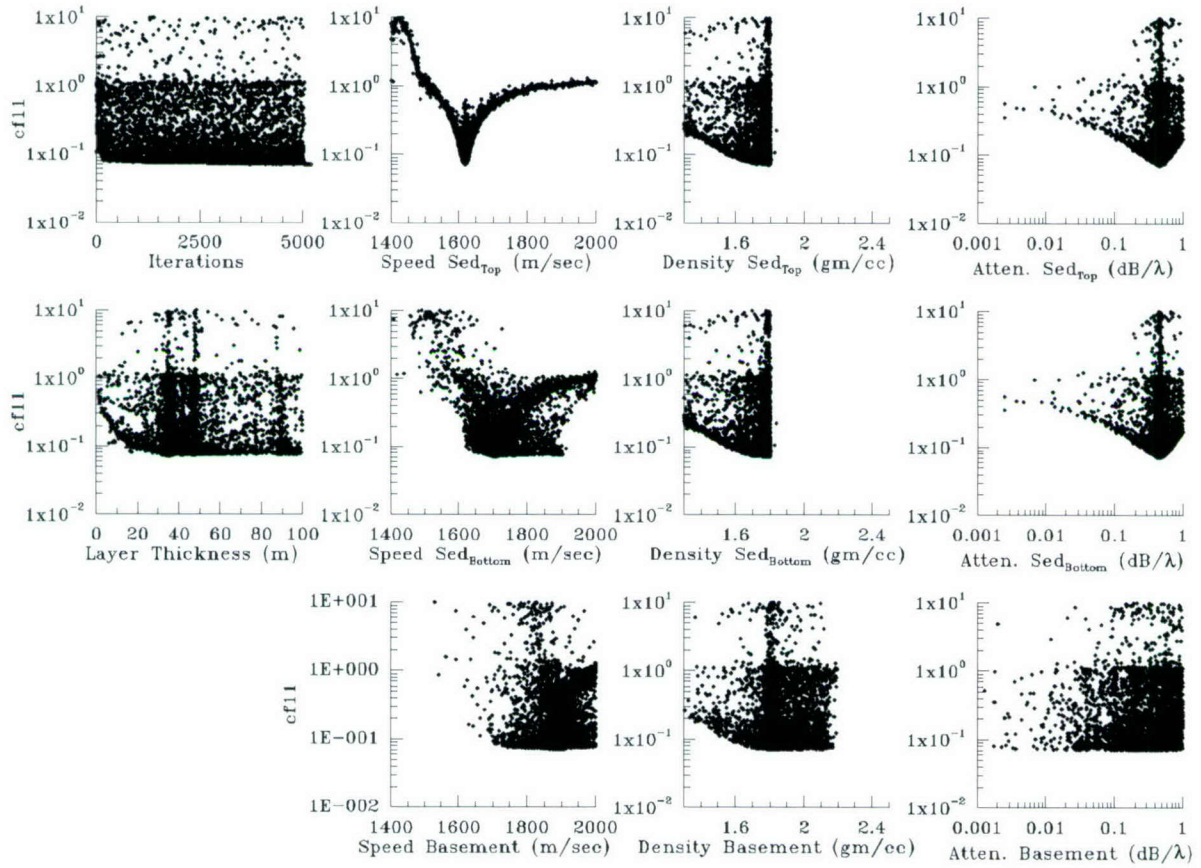

Figure 24: GAIT V&V Test Case 1A (speeddial = 2 for PE 5.1 with reduced chi-square cost function using TL data) – Plot of cost function values versus unknown parameters with left column – layer thickness, second column– sound speed, third column – density and fourth column – attenuation.

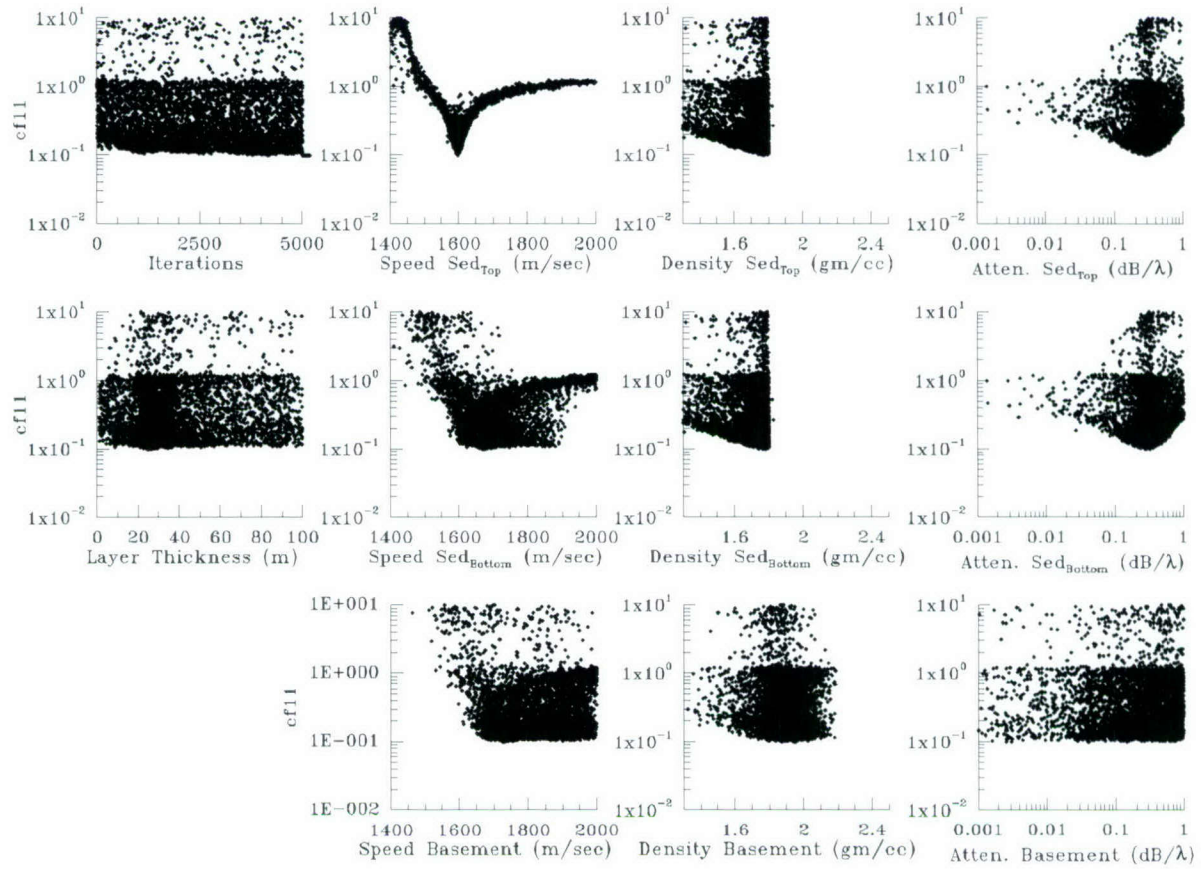

Figure 25: GAIT V&V Test Case 1A (speeddial = 3 for PE 5.1 with reduced chi-square cost function using TL data) – Plot of cost function values versus unknown parameters with left column – layer thickness, second column– sound speed, third column – density and fourth column – attenuation.

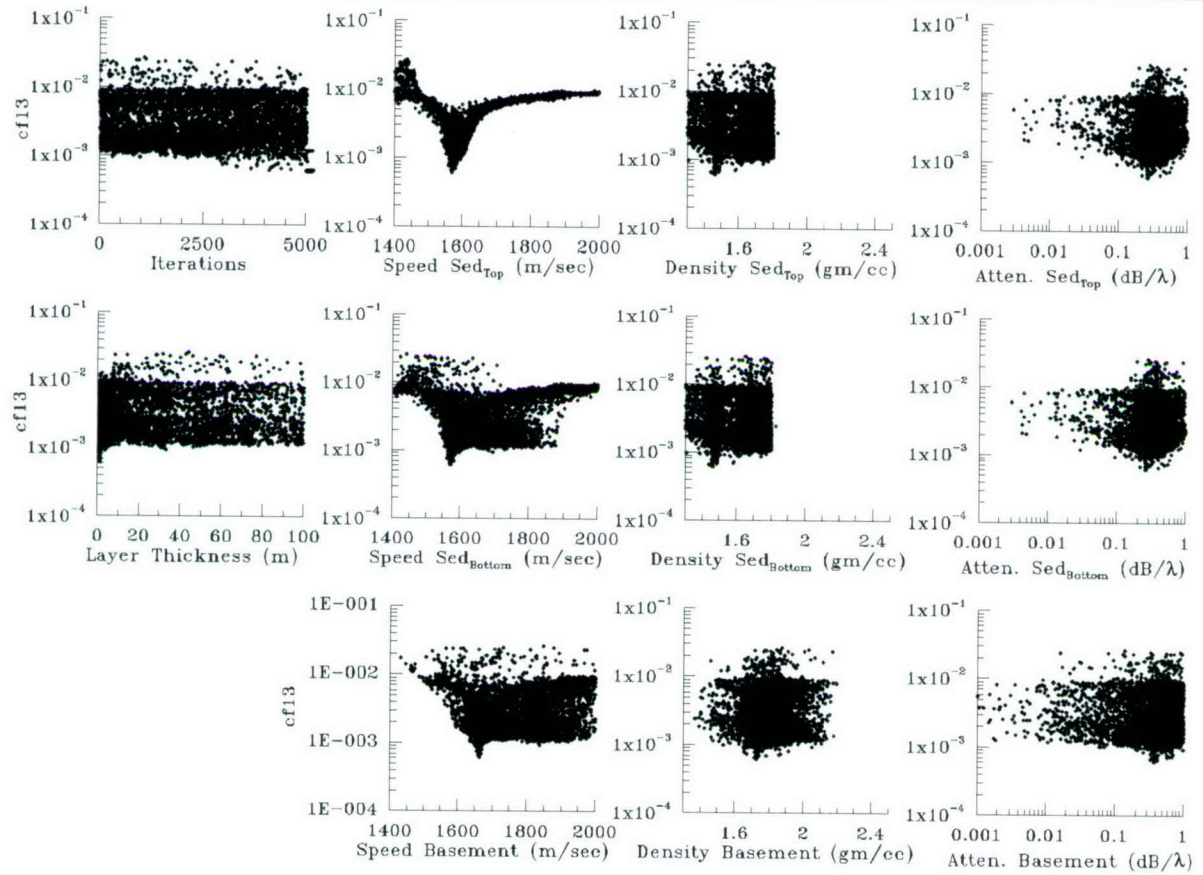

Figure 26: GAIT V&V Test Case 1A (speeddial = 3 for PE 5.1 with correlation cost function using TL data) – Plot of cost function values versus unknown parameters with left column – layer thickness, second column– sound speed, third column – density and fourth column – attenuation.

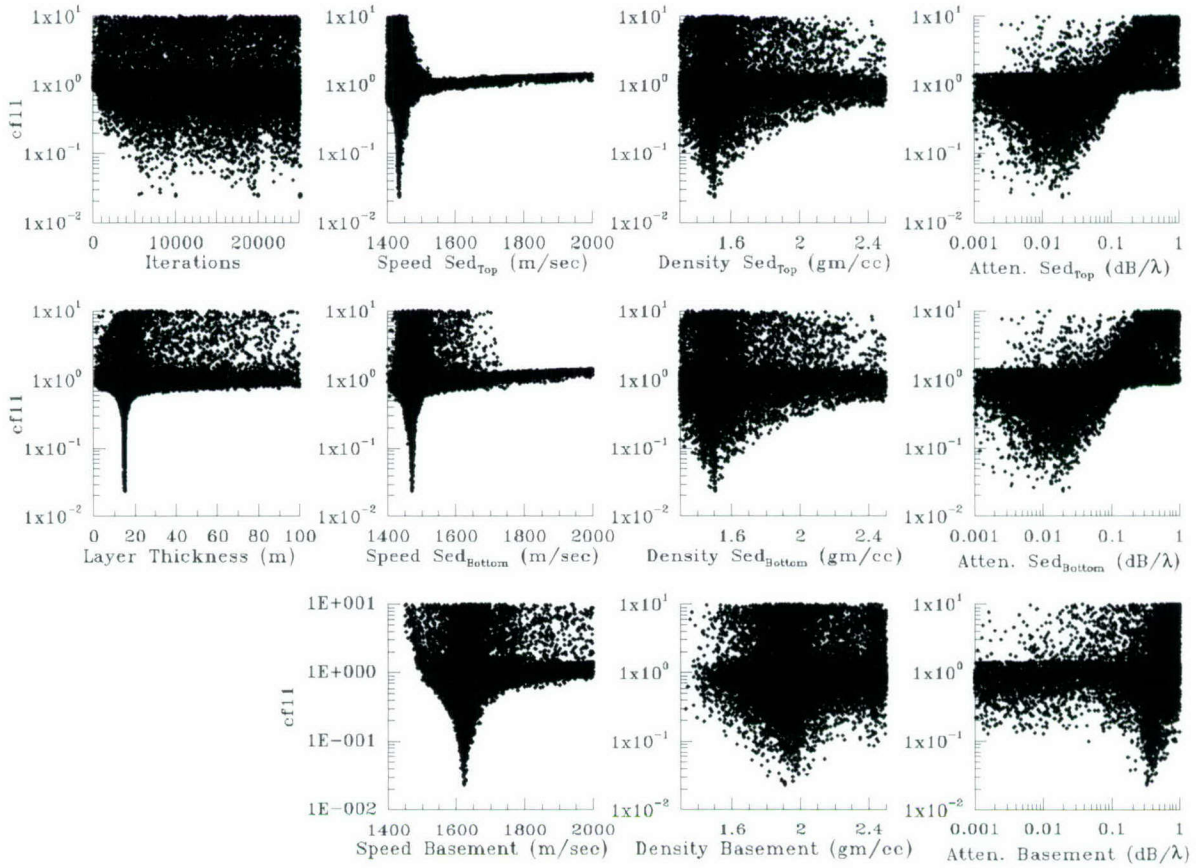

Figure 27: GAIT V&V Test Case 1B (5 meter range step for PE 5.1 with reduced chi-square cost function using TL data) – Plot of cost function values versus unknown parameters with left column – layer thickness, second column– sound speed, third column – density and fourth column – attenuation.

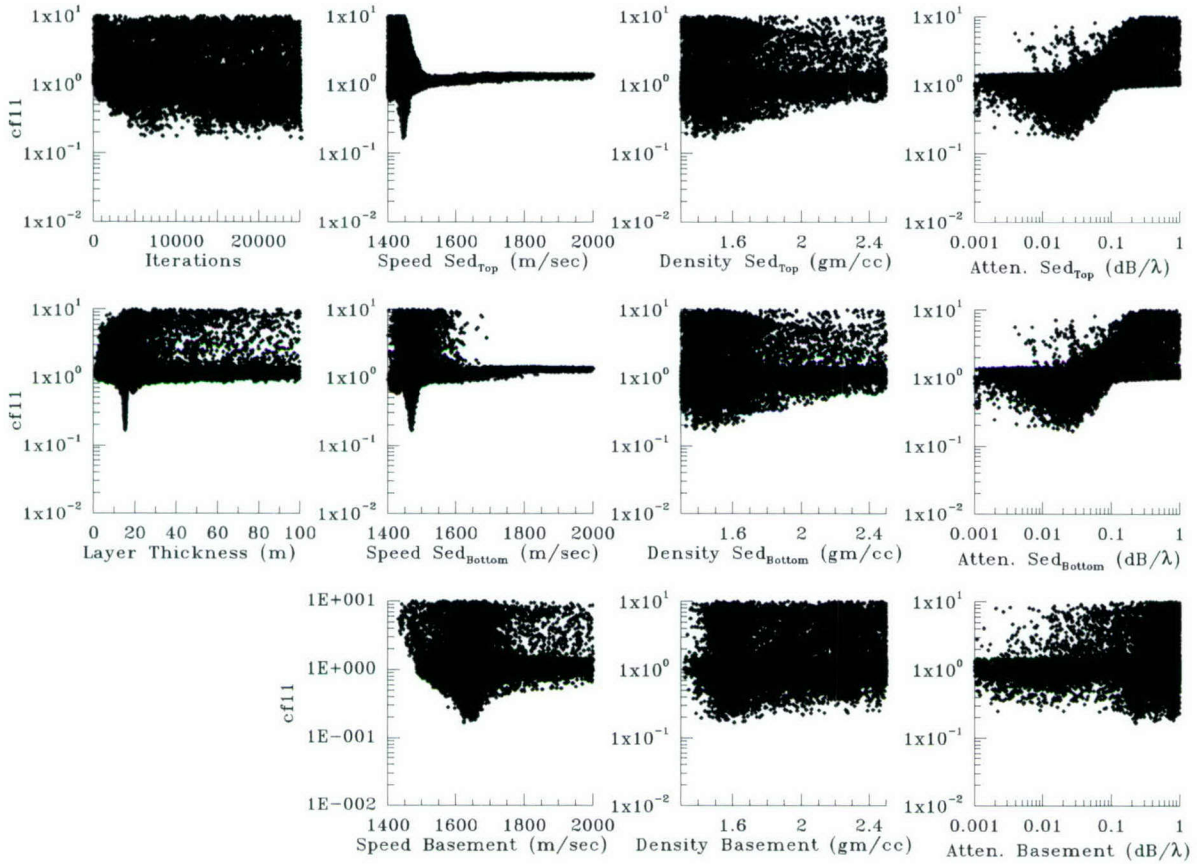

Figure 28: GAIT V&V Test Case 1B (speeddial = 4 for PE 5.1 with reduced chi-square cost function using TL data) – Plot of cost function values versus unknown parameters with left column – layer thickness, second column– sound speed, third column – density and fourth column – attenuation.

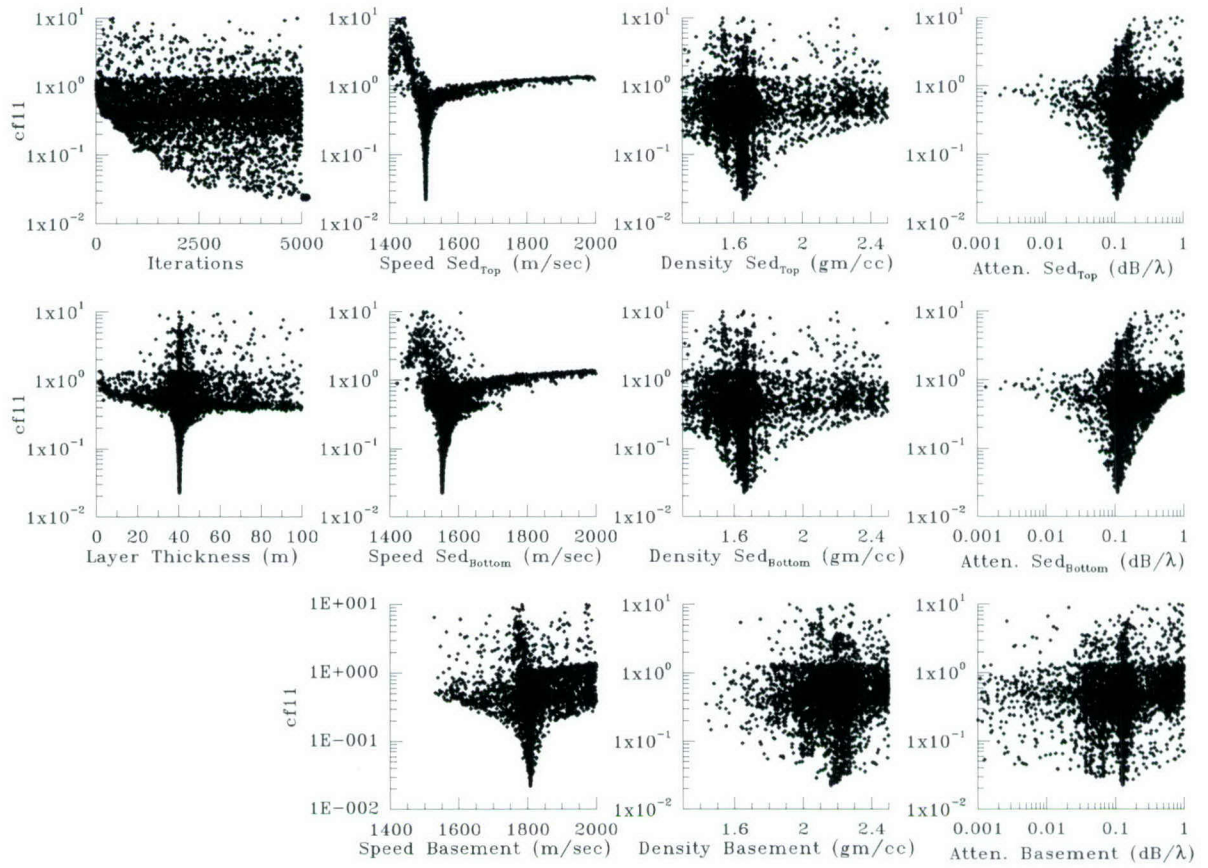

Figure 29: GAIT V&V Test Case 1C (5 meter range step for PE 5.1 with reduced chi-square cost function using TL data) – Plot of cost function values versus unknown parameters with left column – layer thickness, second column– sound speed, third column – density and fourth column – attenuation.

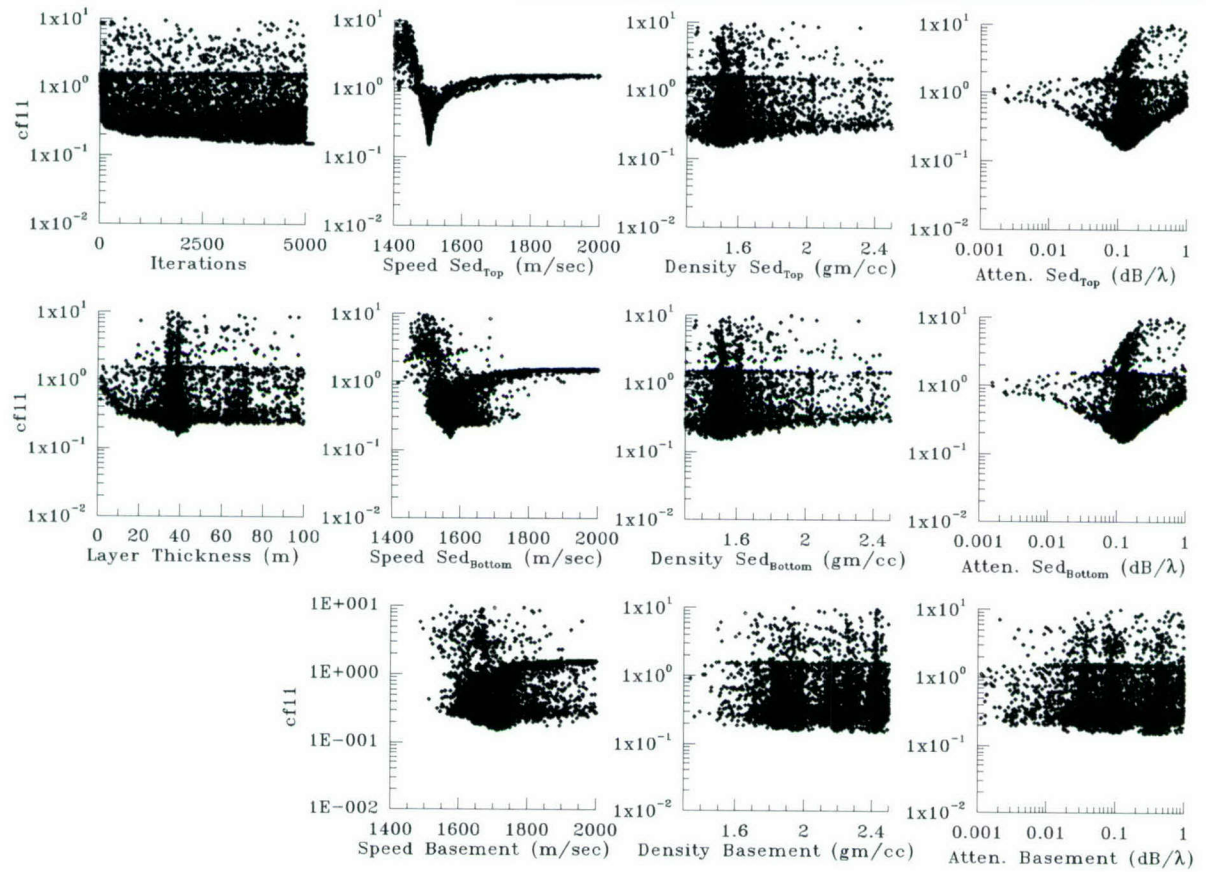

Figure 30: GAIT V&V Test Case 1C (speeddial = 4 for PE 5.1 with reduced chi-square cost function using TL data) – Plot of cost function values versus unknown parameters with left column – layer thickness, second column– sound speed, third column – density and fourth column – attenuation.

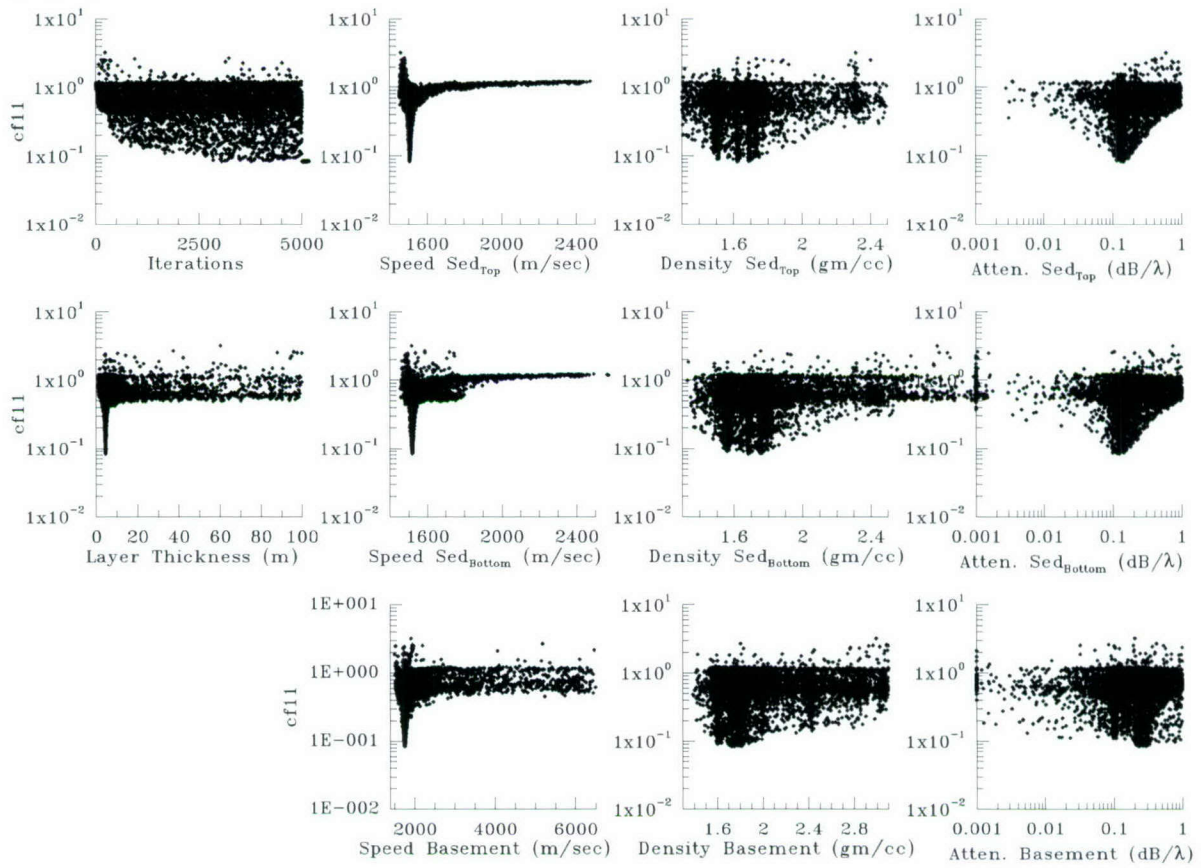

Figure 31: GAIT V&V Test Case 2 (speeddial = 3 for PE 5.1 with reduced chi-square cost function using TL data) – Plot of cost function values versus unknown parameters with left column – layer thickness, second column– sound speed, third column – density and fourth column – attenuation.

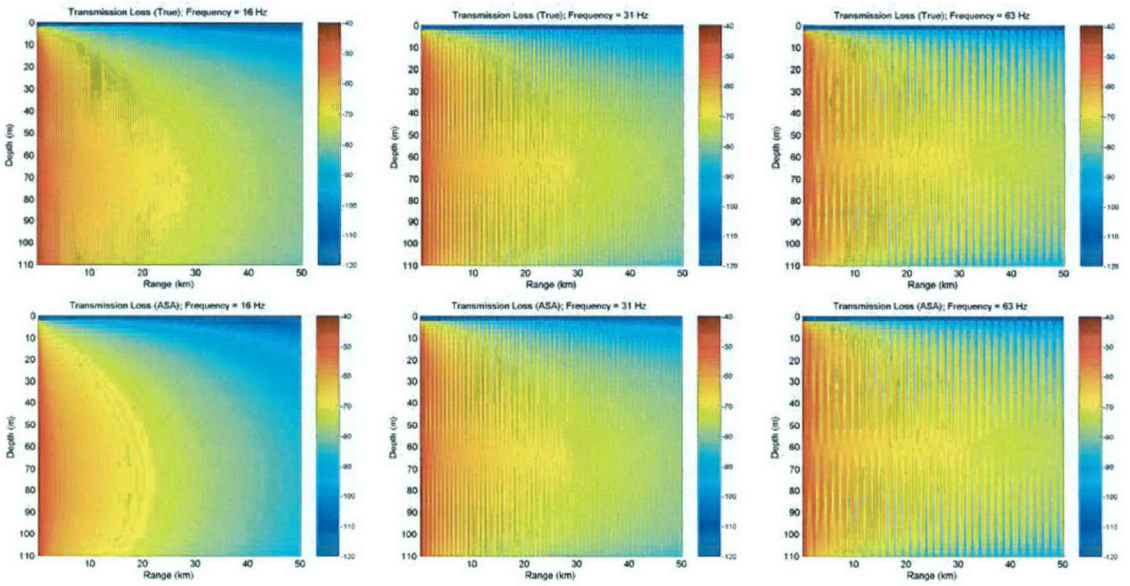

Figure 32: GAIT V&V Test Case 2 full-field transmission loss plots (source depth 20 m) for 16 Hz (left column), 31 Hz (middle column) and 63 Hz (right column). The top row is the ground-truth TL. The bottom row is the GAIT GS TL. (Graphics courtesy of Martin Siderius – SAIC)

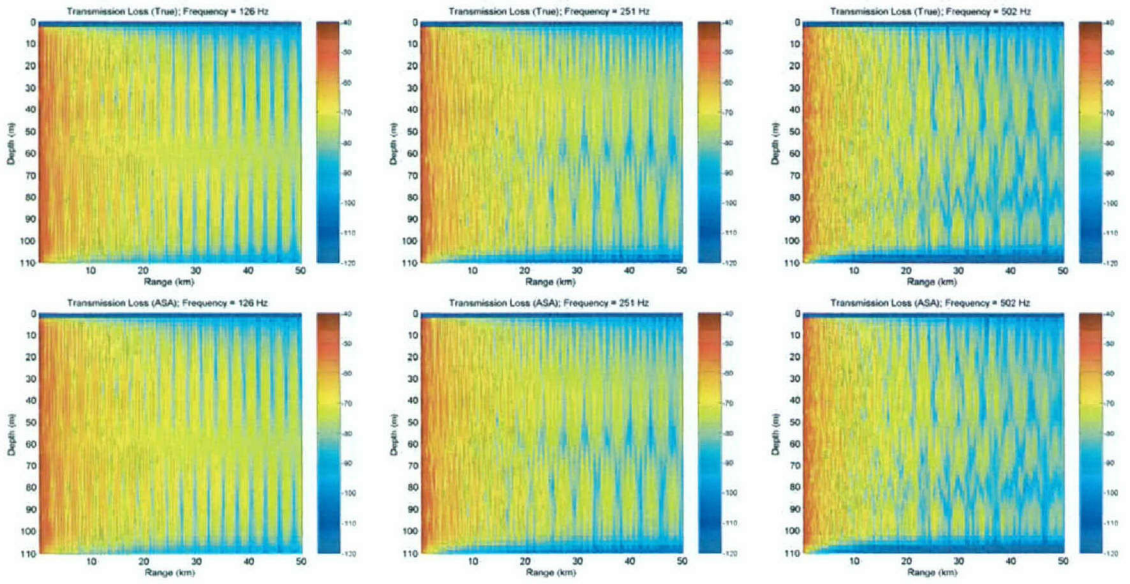

Figure 33: GAIT V&V Test Case 2 full-field transmission loss plots (source depth 20 m) for 126 Hz (left column), 251 Hz (middle column) and 502 Hz (right column). The

top row is the ground-truth TL. The bottom row is the GAIT GS TL. (Graphics courtesy of Martin Siderius – SAIC)

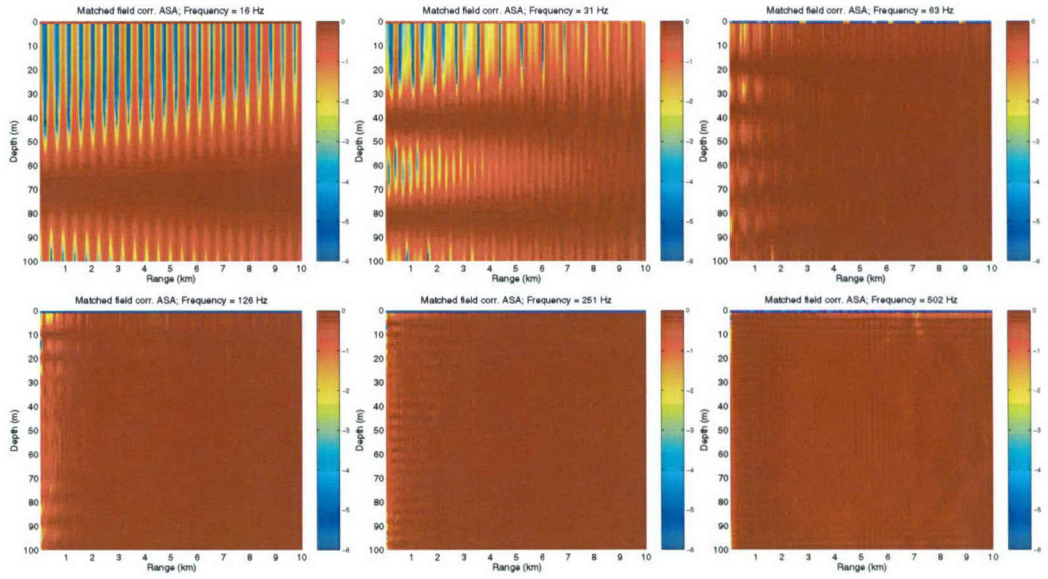

Figure 34: GAIT V&V Test Case 2 – Targets are generated at each range/depth cell on a 60 m vertical array using the ground-truth seabed properties. These are correlated with the same range-depth cell calculated using the geoacoustic properties from the GAIT GS inversion. Perfect agreement is red (0 dB) and blue indicates poorer agreement. The top left is 16 Hz, middle top is 31 Hz, top right is 63 Hz, bottom left is 126 Hz, middle bottom is 251 Hz and bottom right is 502 Hz. (Graphics courtesy of Martin Siderius – SAIC)

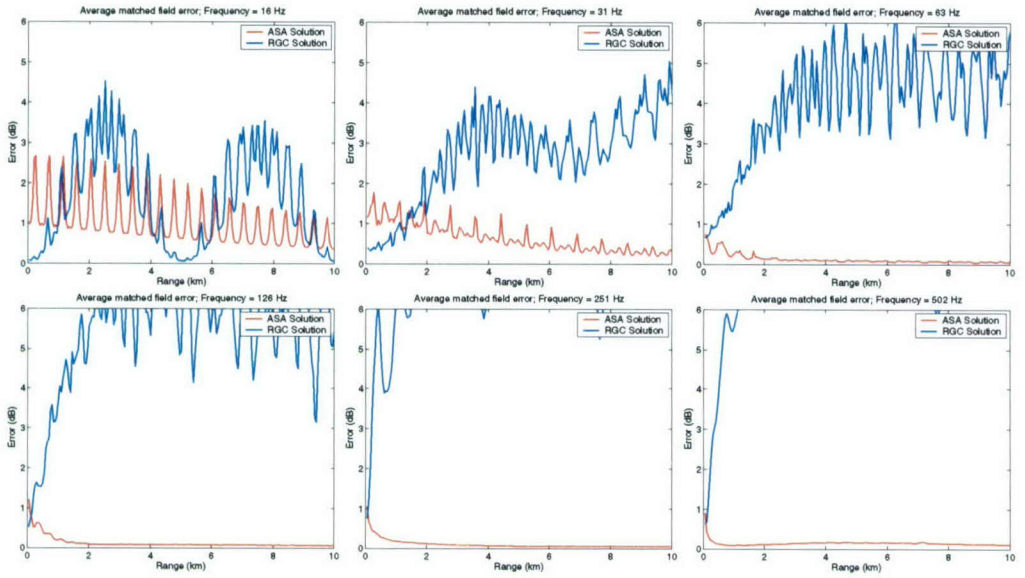

Figure 35: GAIT V&V Test Case 2 – Depth averaged matched field error showing the GAIT GS solution as the red line. The blue line denotes another inversion algorithm (RGC) also evaluated by the GAIT V&V committee. The top left is 16 Hz, middle top is 31 Hz, top right is 63 Hz, bottom left is 126 Hz, middle bottom is 251 Hz and bottom right is 502 Hz. (Graphics courtesy of Martin Siderius – SAIC)

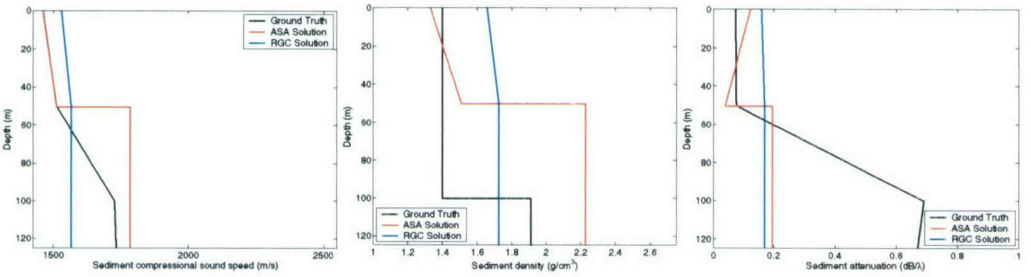

Figure 36: GAIT V&V Test Case 3 – Ground truth geoacoustic properties plotted against the inversion results from GAIT GS (red line). The blue line denotes the inversion results from the RGC algorithm also evaluated by the GAIT V&V committee. (Graphics courtesy of Martin Siderius – SAIC)

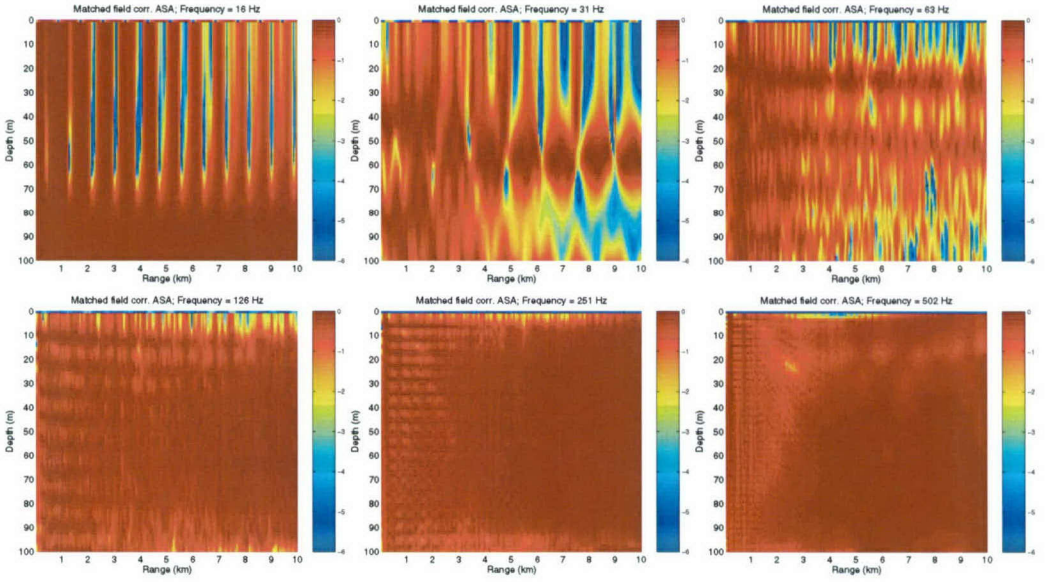

Figure 37: GAIT V&V Test Case 3 – Targets are generated at each range/depth cell on a 60 m vertical array using the ground-truth seabed properties. These are correlated with the same range-depth cell calculated using the geoacoustic properties from the GAIT GS inversion. Perfect agreement is red (0 dB) and blue indicates poorer agreement. The top left is 16 Hz, middle top is 31 Hz, top right is 63 Hz, bottom left is 126 Hz, middle bottom is 251 Hz and bottom right is 502 Hz. (Graphics courtesy of Martin Siderius – SAIC)

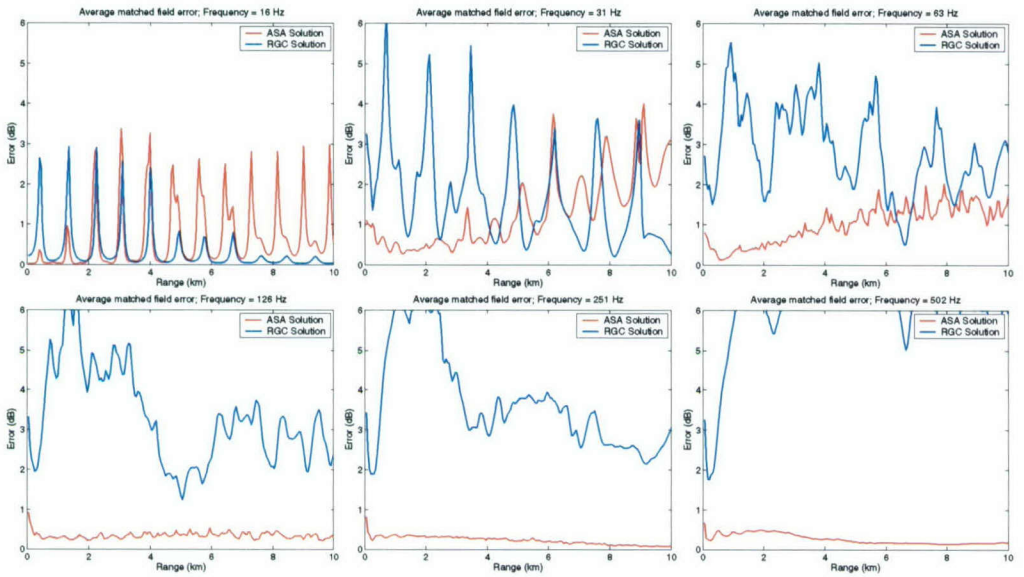

Figure 38: GAIT V&V Test Case 3 – Depth averaged matched field error showing the GAIT GS solution as the red line. The blue line denotes the RGC inversion algorithm also evaluated by the GAIT V&V committee. The top left is 16 Hz, middle top is 31 Hz, top right is 63 Hz, bottom left is 126 Hz, middle bottom is 251 Hz and bottom right is 502 Hz. (Graphics courtesy of Martin Siderius – SAIC)

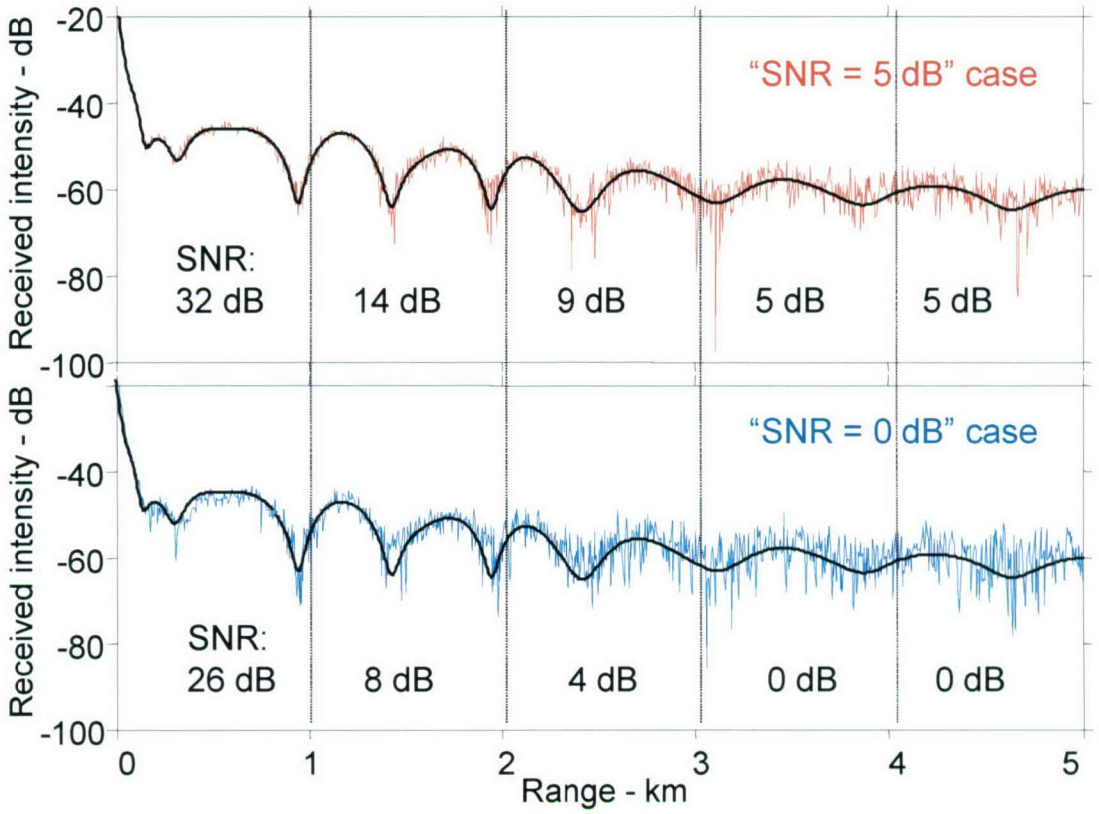

Figure 39: GAIT V&V Test Case 4 – Actual SNR values for 1 km segments at 25 Hz for the 25 meter receiver depth. Test case 4c (5 dB SNR) is shown in the top plot in red and test case 4d (0 dB SNR) is shown in the bottom plot in blue. The acoustic before the noise was added is shown as a black line in each plot. (Graphics courtesy of Tracianne Neilsen – ARL/UT)

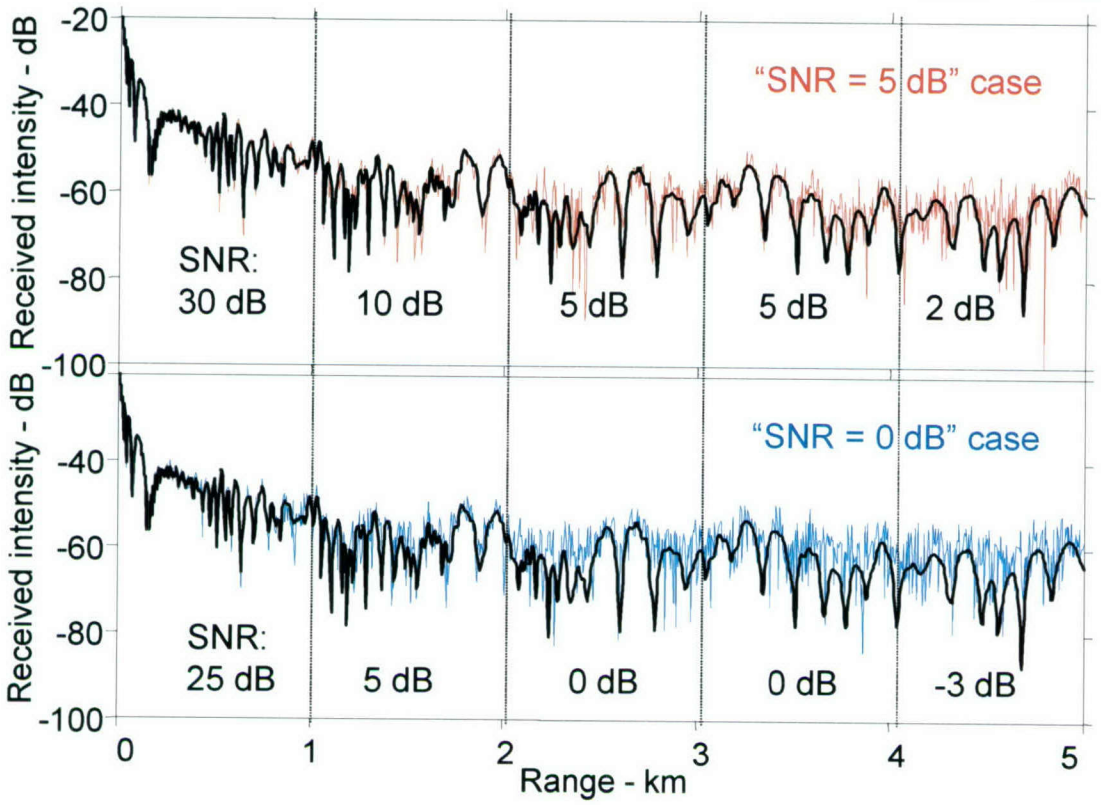

Figure 40: GAIT V&V Test Case 4 – Actual SNR values for 1 km segments at 250 Hz for the 25 meter receiver depth. Test case 4c (5 dB SNR) is shown in the top plot in red and test case 4d (0 dB SNR) is shown in the bottom plot in blue. The acoustic before the noise was added is shown as a black line in each plot. (Graphics courtesy of Tracianne Neilsen – ARL/UT)

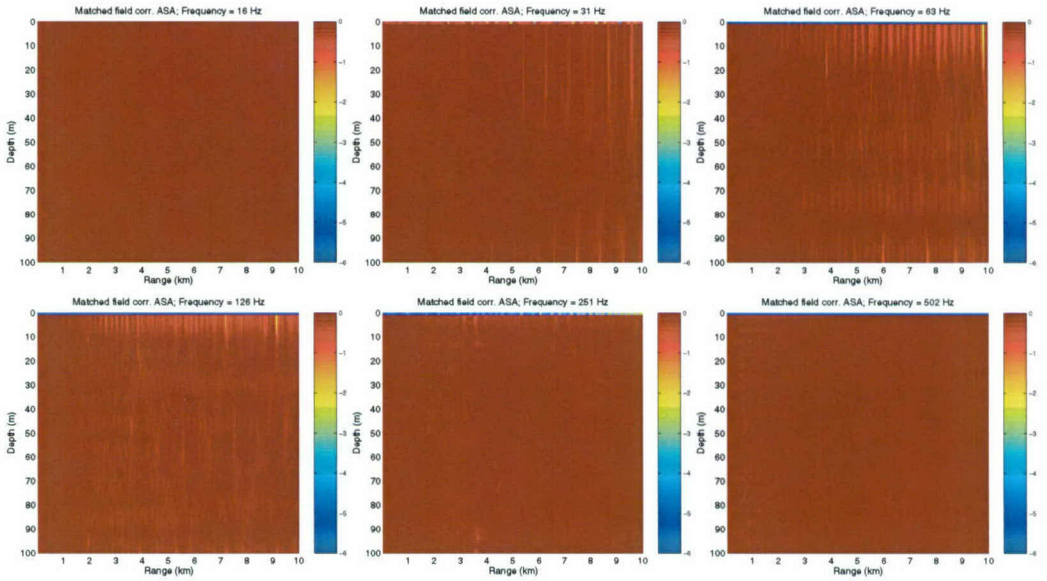

Figure 41: GAIT V&V Test Case 4A (no added noise) – Targets are generated at each range/depth cell on a 60 m vertical array using the ground-truth seabed properties. These are correlated with the same range-depth cell calculated using the geoacoustic properties from the GAIT GS inversion. Perfect agreement is red (0 dB) and blue indicates poorer agreement. The top left is 16 Hz, middle top is 31 Hz, top right is 63 Hz, bottom left is 126 Hz, middle bottom is 251 Hz and bottom right is 502 Hz. (Graphics courtesy of Martin Siderius – SAIC)

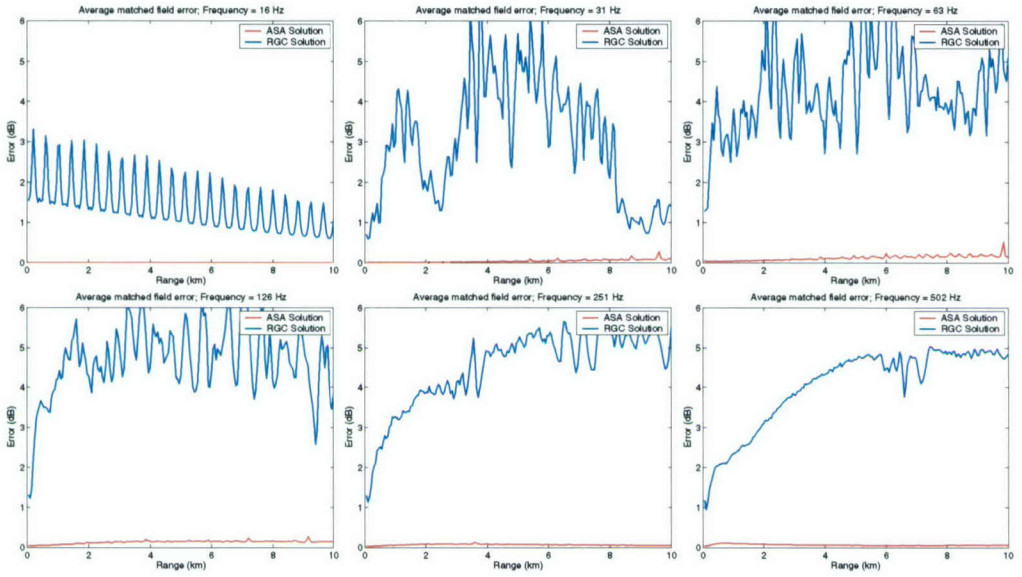

Figure 42: GAIT V&V Test Case 4A (no added noise) – Depth averaged matched field error showing the GAIT GS solution as the red line. The blue line denotes the RGC inversion algorithm also evaluated by the GAIT V&V committee. The top left is 16 Hz, middle top is 31 Hz, top right is 63 Hz, bottom left is 126 Hz, middle bottom is 251 Hz and bottom right is 502 Hz. (Graphics courtesy of Martin Siderius – SAIC)

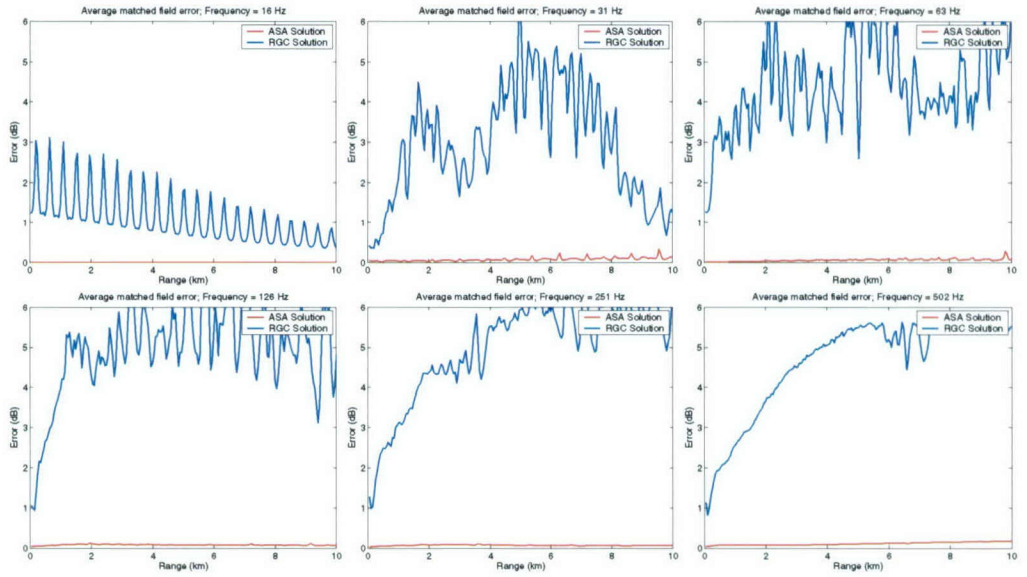

Figure 43: GAIT V&V Test Case 4B (15 dB SNR) – Depth averaged matched field error showing the GAIT GS solution as the red line. The blue line denotes the RGC inversion algorithm also evaluated by the GAIT V&V committee. The top left is 16 Hz, middle top is 31 Hz, top right is 63 Hz, bottom left is 126 Hz, middle bottom is 251 Hz and bottom right is 502 Hz. (Graphics courtesy of Martin Siderius – SAIC)

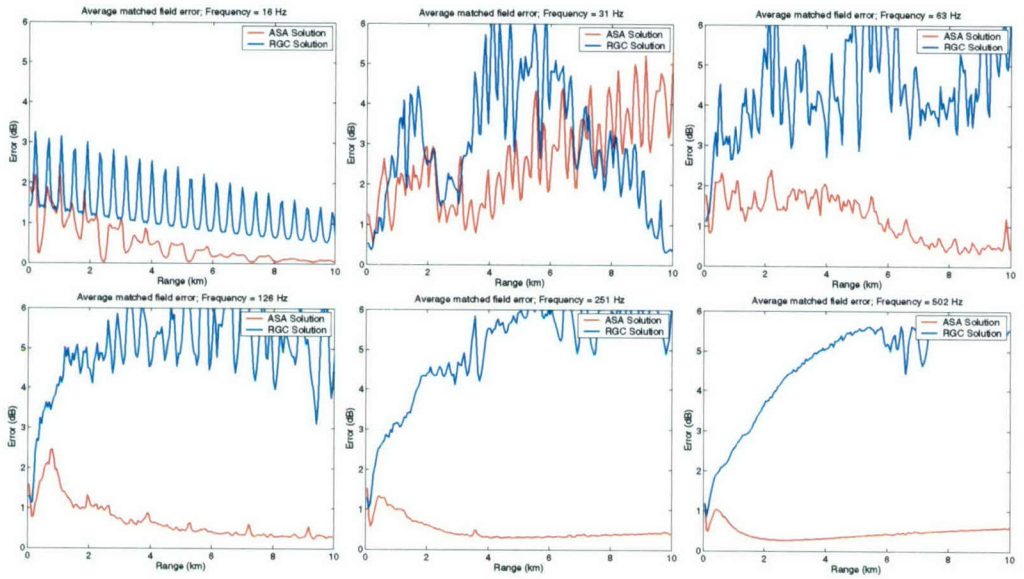

Figure 44: GAIT V&V Test Case 4C (5 dB SNR) – Depth averaged matched field error showing the GAIT GS solution as the red line. The blue line denotes the RGC inversion algorithm also evaluated by the GAIT V&V committee. The top left is 16 Hz, middle top is 31 Hz, top right is 63 Hz, bottom left is 126 Hz, middle bottom is 251 Hz and bottom right is 502 Hz. (Graphics courtesy of Martin Siderius – SAIC)

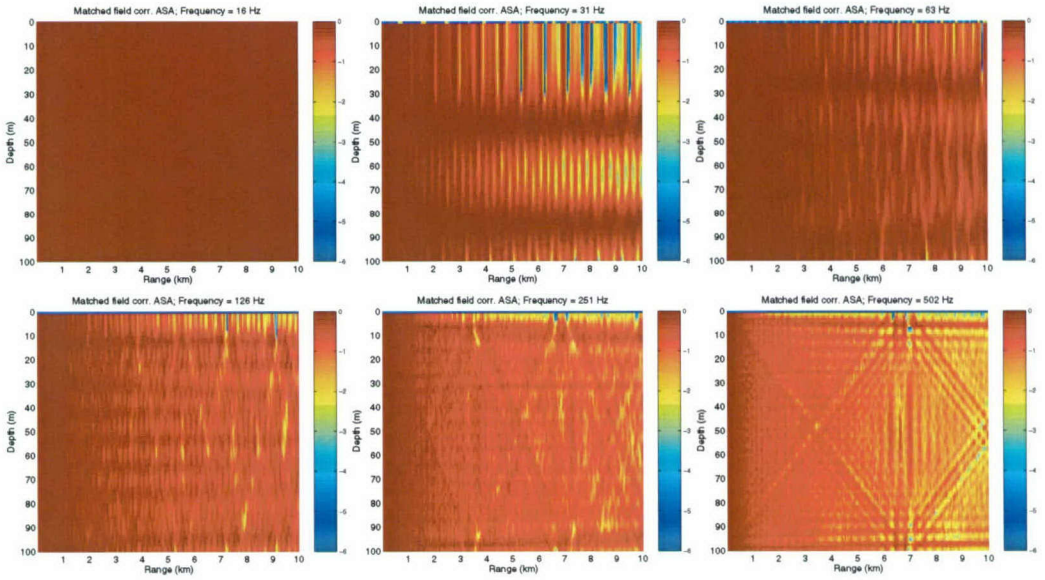

Figure 45: GAIT V&V Test Case 4D (0 dB SNR) – Targets are generated at each range/depth cell on a 60 m vertical array using the ground-truth seabed properties. These are correlated with the same range-depth cell calculated using the geoacoustic properties from the GAIT GS inversion. Perfect agreement is red (0 dB) and blue indicates poorer agreement. The top left is 16 Hz, middle top is 31 Hz, top right is 63 Hz, bottom left is 126 Hz, middle bottom is 251 Hz and bottom right is 502 Hz. (Graphics courtesy of Martin Siderius – SAIC)

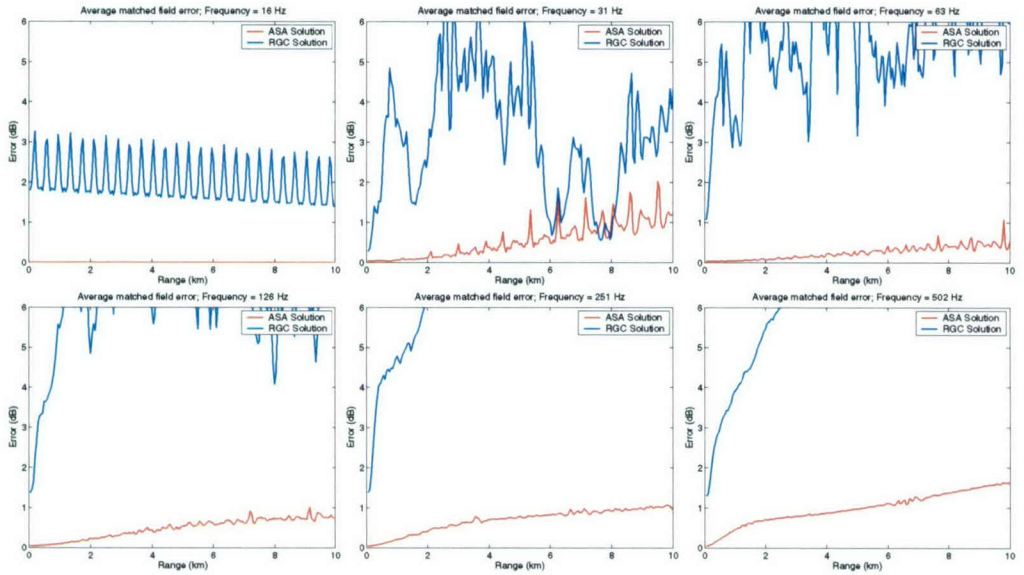

Figure 46: GAIT V&V Test Case 4D (0 dB SNR) – Depth averaged matched field error showing the GAIT GS solution as the red line. The blue line denotes the RGC inversion algorithm also evaluated by the GAIT V&V committee. The top left is 16 Hz, middle top is 31 Hz, top right is 63 Hz, bottom left is 126 Hz, middle bottom is 251 Hz and bottom right is 502 Hz. (Graphics courtesy of Martin Siderius – SAIC)

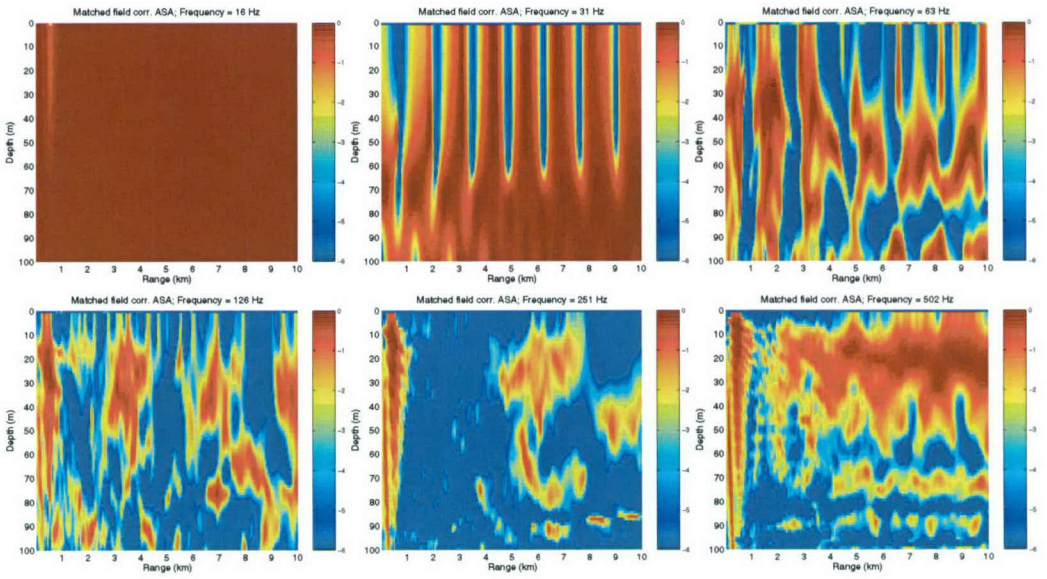

Figure 47: GAIT V&V Test Case 6 – Targets are generated at each range/depth cell on a 60 m vertical array using the ground-truth seabed properties. These are correlated with the same range-depth cell calculated using the geoacoustic properties from the GAIT GS inversion. Perfect agreement is red (0 dB) and blue indicates poorer agreement. The top left is 16 Hz, middle top is 31 Hz, top right is 63 Hz, bottom left is 126 Hz, middle bottom is 251 Hz and bottom right is 502 Hz. (Graphics courtesy of Martin Siderius – SAIC)

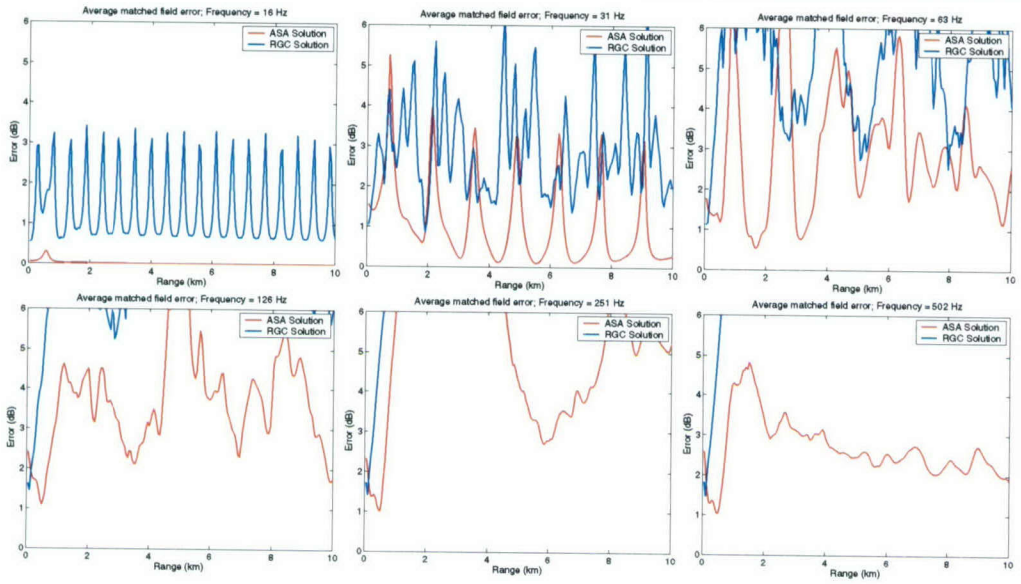

Figure 48: GAIT V&V Test Case 6 – Depth averaged matched field error showing the GAIT GS solution as the red line. The blue line denotes the RGC inversion algorithm also evaluated by the GAIT V&V committee. The top left is 16 Hz, middle top is 31 Hz, top right is 63 Hz, bottom left is 126 Hz, middle bottom is 251 Hz and bottom right is 502 Hz. (Graphics courtesy of Martin Siderius – SAIC)

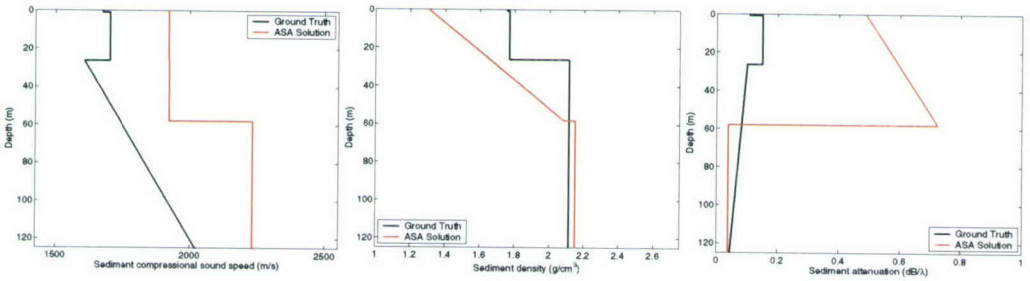

Figure 49: GAIT V&V Test Case 10A – Geoacoustic properties (sound speed, density and attenuation from left to right) for ground-truth (black line) and GAIT GS inversion using PE 5.1 (red line). (Graphics courtesy of Martin Siderius – SAIC)

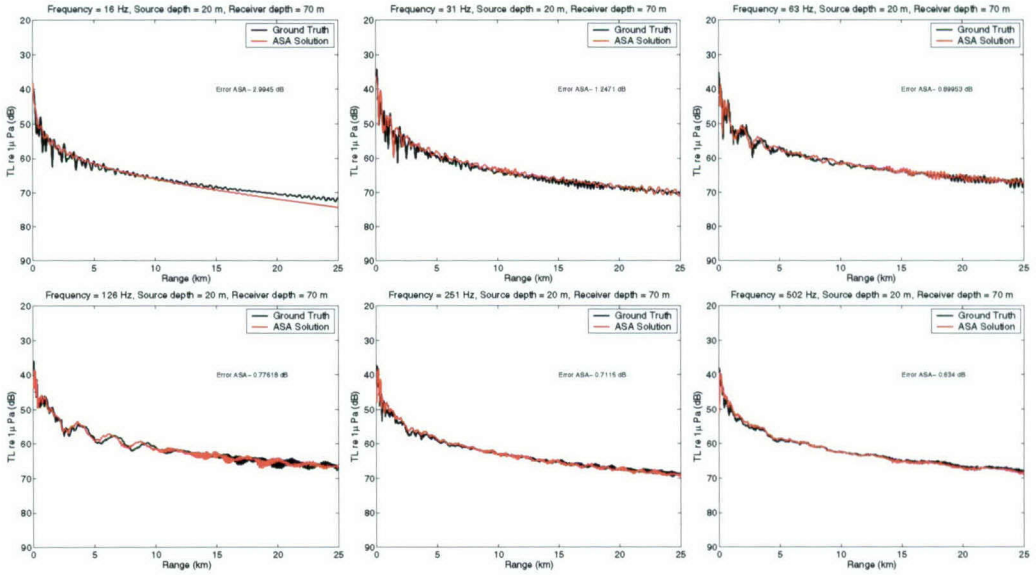

Figure 50: GAIT V&V Test Case 10A – One third octave band averages at center frequencies (from top left to bottom) 16, 31, 63, 126, 251 and 502 Hz. The black curves were generated using the ground-truth geoacoustic properties and the red curves were generated from the GAIT GS inverted geoacoustic parameters. (Graphics courtesy of Martin Siderius – SAIC)

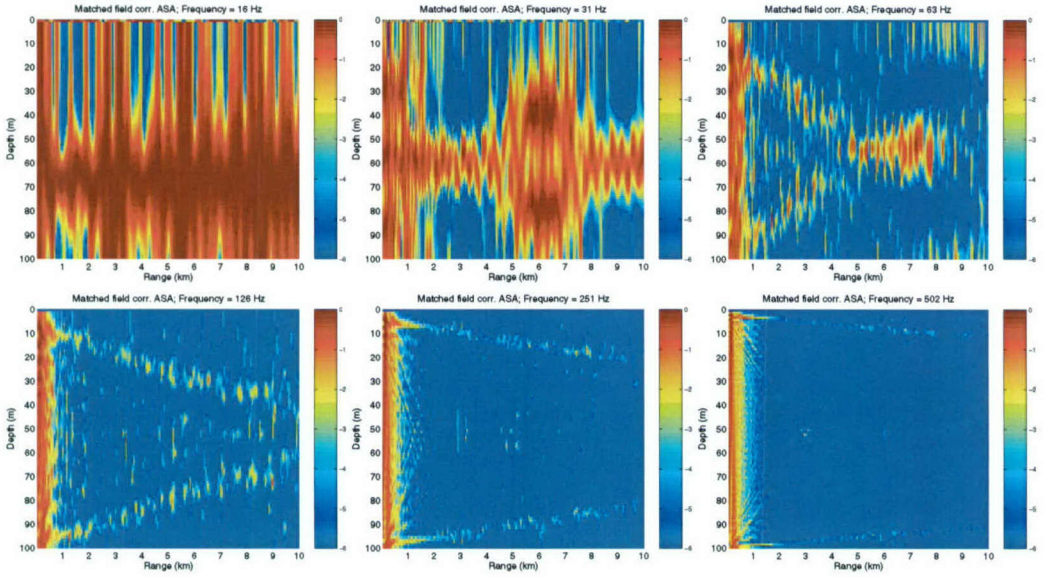

Figure 51: GAIT V&V Test Case 10A – Targets are generated at each range/depth cell on a 60 m vertical array using the ground-truth seabed properties. These are correlated with the same range-depth cell calculated using the geoacoustic properties from the GAIT GS inversion. Perfect agreement is red (0 dB) and blue indicates poorer agreement. The top left is 16 Hz, middle top is 31 Hz, top right is 63 Hz, bottom left is 126 Hz, middle bottom is 251 Hz and bottom right is 502 Hz. (Graphics courtesy of Martin Siderius – SAIC)

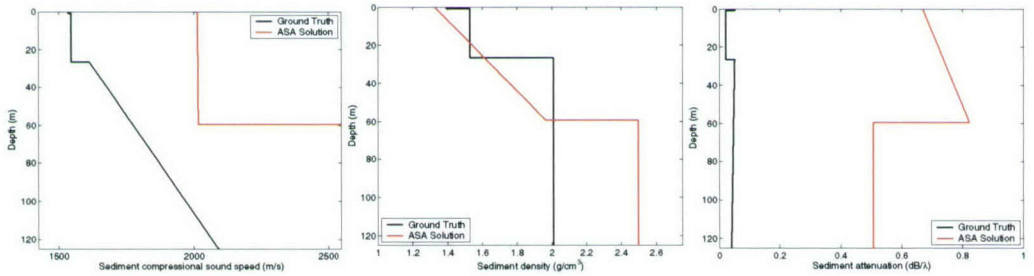

Figure 52: GAIT V&V Test Case 10B – Geoacoustic properties (sound speed, density and attenuation from left to right) for ground-truth (black line) and GAIT GS inversion using PE 5.1 (red line). (Graphics courtesy of Martin Siderius – SAIC)

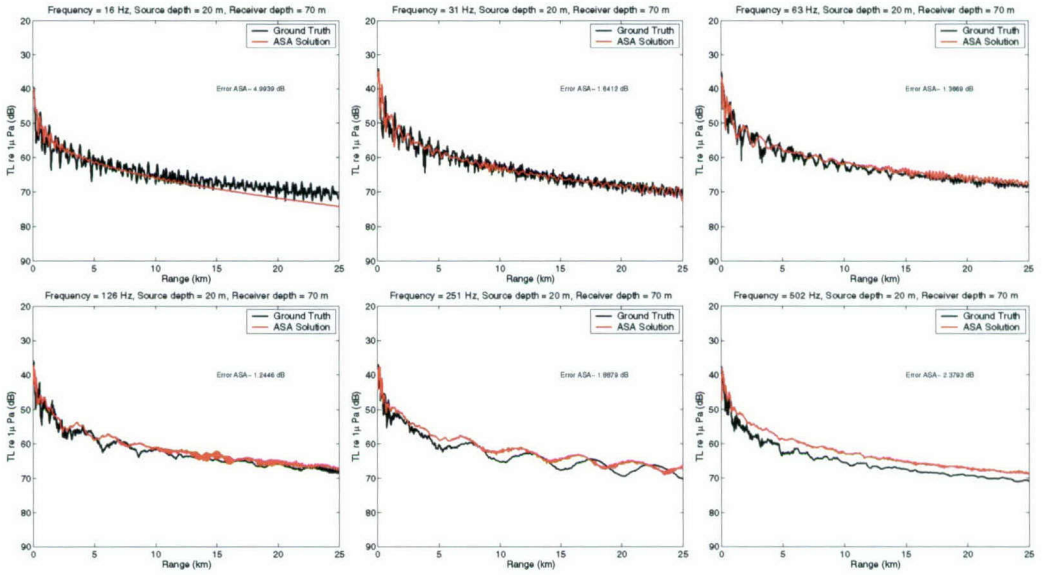

Figure 53: GAIT V&V Test Case 10B – One third octave band averages at center frequencies (from top left to bottom) 16, 31, 63, 126, 251 and 502 Hz. The black curves were generated using the ground-truth geoacoustic properties and the red curves were generated from the GAIT GS inverted geoacoustic parameters. (Graphics courtesy of Martin Siderius – SAIC)

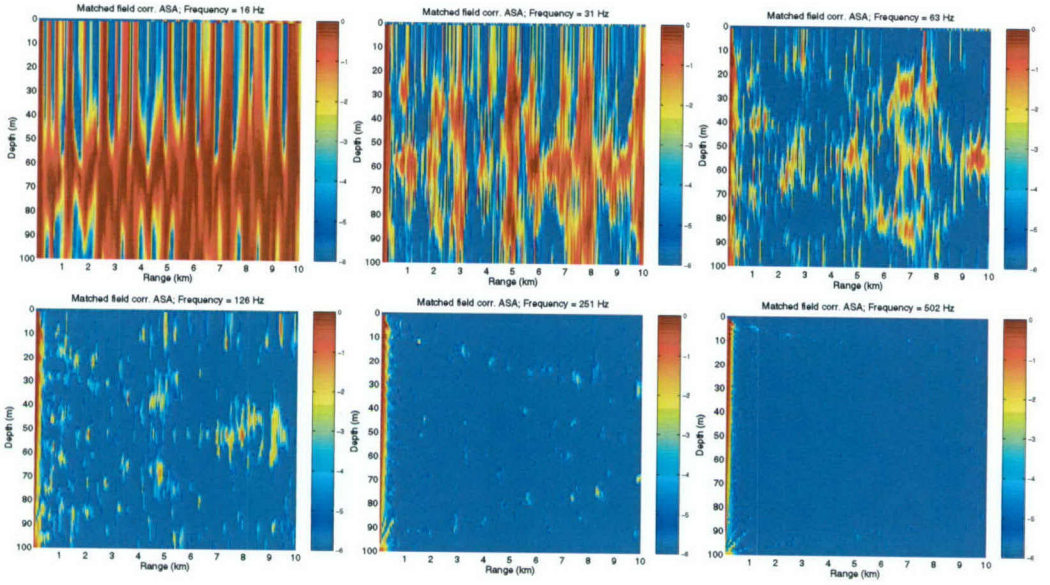

Figure 54: GAIT V&V Test Case 10B – Targets are generated at each range/depth cell on a 60 m vertical array using the ground-truth seabed properties. These are correlated with the same range-depth cell calculated using the geoacoustic properties from the GAIT GS inversion. Perfect agreement is red (0 dB) and blue indicates poorer agreement. The top left is 16 Hz, middle top is 31 Hz, top right is 63 Hz, bottom left is 126 Hz, middle bottom is 251 Hz and bottom right is 502 Hz. (Graphics courtesy of Martin Siderius – SAIC)

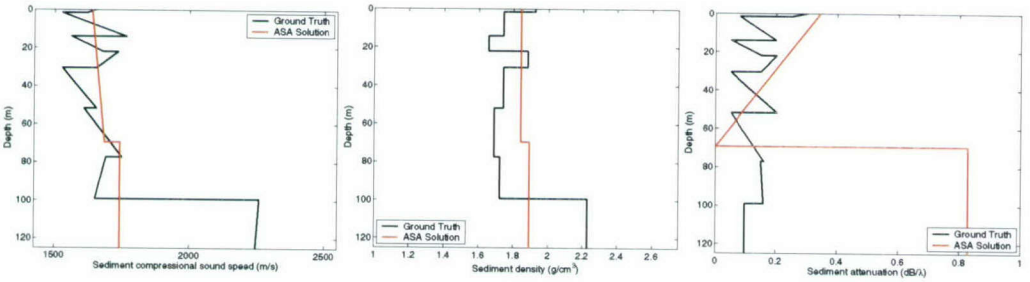

Figure 55: GAIT V&V Test Case 10C – Geoacoustic properties (sound speed, density and attenuation from left to right) for ground-truth (black line) and GAIT GS inversion using PE 5.1 (red line). (Graphics courtesy of Martin Siderius – SAIC)

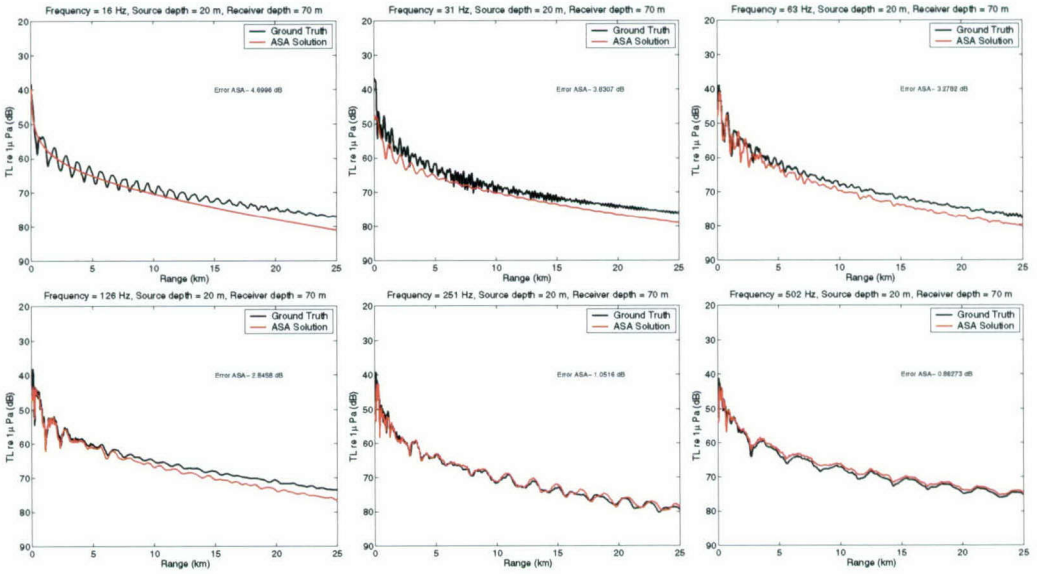

Figure 56: GAIT V&V Test Case 10C – One third octave band averages at center frequencies (from top left to bottom) 16, 31, 63, 126, 251 and 502 Hz. The black curves were generated using the ground-truth geoacoustic properties and the red curves were generated from the GAIT GS inverted geoacoustic parameters. (Graphics courtesy of Martin Siderius – SAIC)

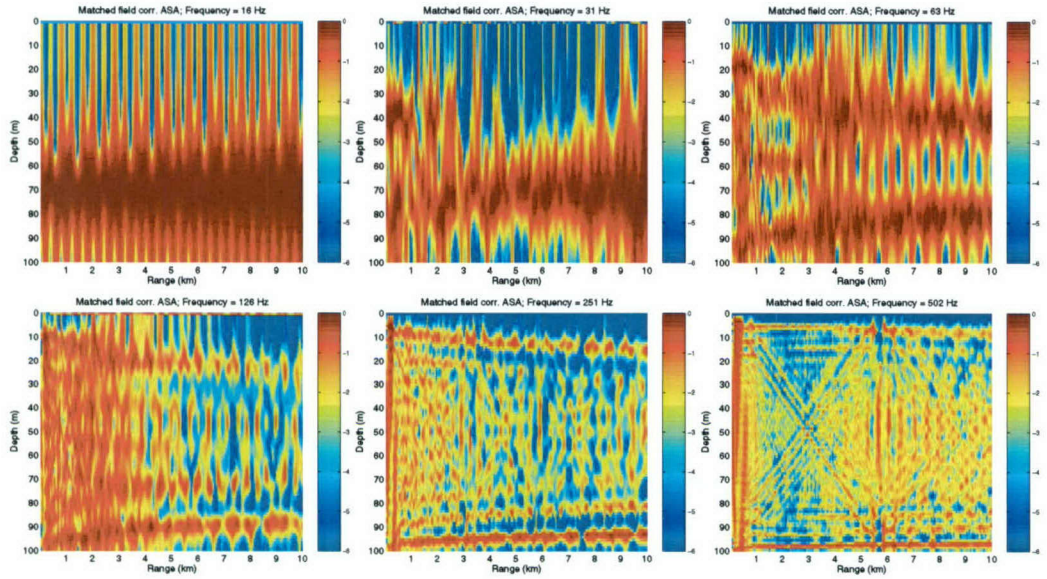

Figure 57: GAIT V&V Test Case 10C – Targets are generated at each range/depth cell on a 60 m vertical array using the ground-truth seabed properties. These are correlated with the same range-depth cell calculated using the geoacoustic properties from the GAIT GS inversion. Perfect agreement is red (0 dB) and blue indicates poorer agreement. The top left is 16 Hz, middle top is 31 Hz, top right is 63 Hz, bottom left is 126 Hz, middle bottom is 251 Hz and bottom right is 502 Hz. (Graphics courtesy of Martin Siderius – SAIC)

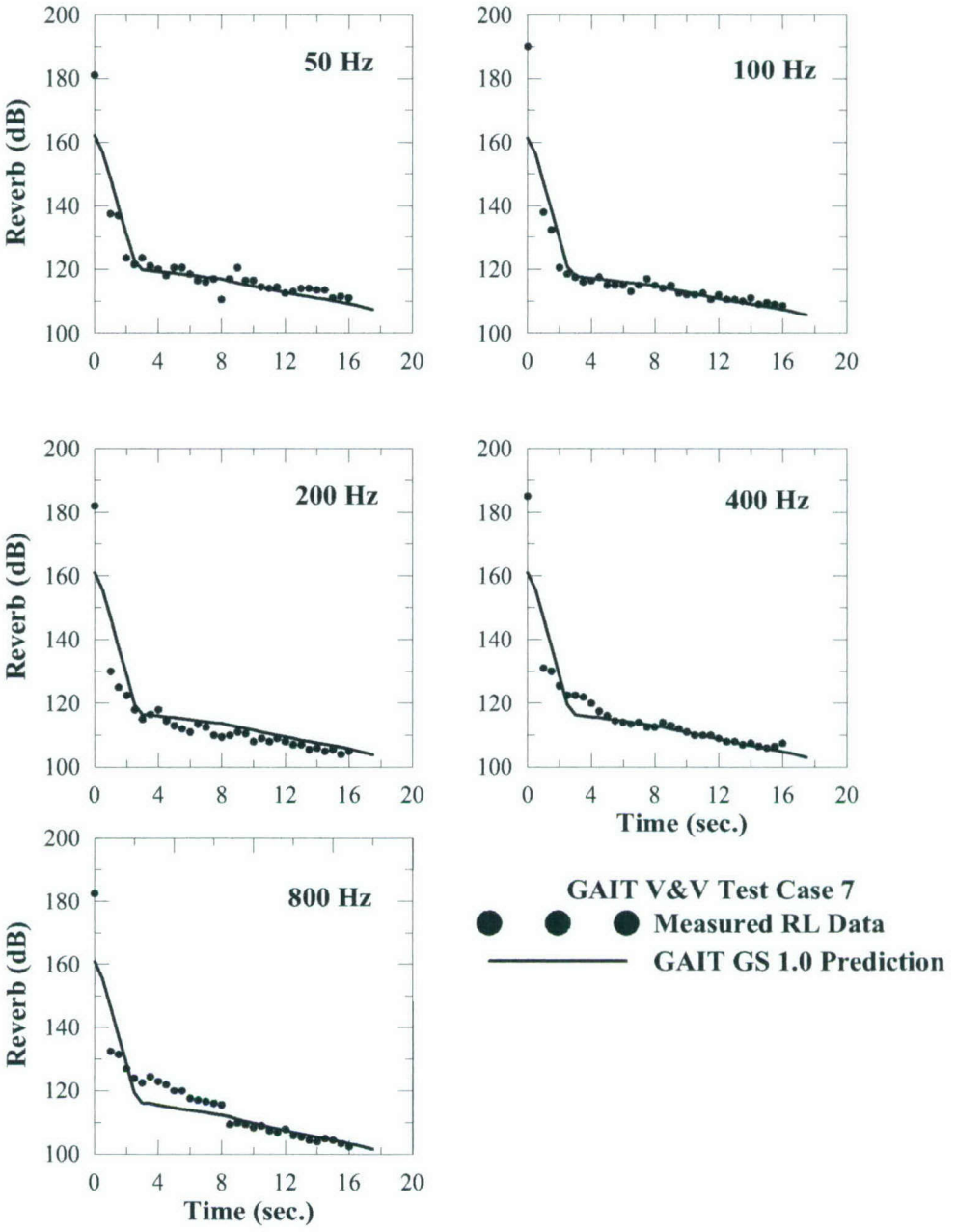

Figure 58: GAIT V&V Test Case 7 –Band averaged reverberation data (black circles) at center frequencies (from top left to bottom) of 50, 100, 200, 400 and 800 Hz. The black curves were generated using the GAIT GS (using ASPM 5.1) inverted geoacoustic parameters.

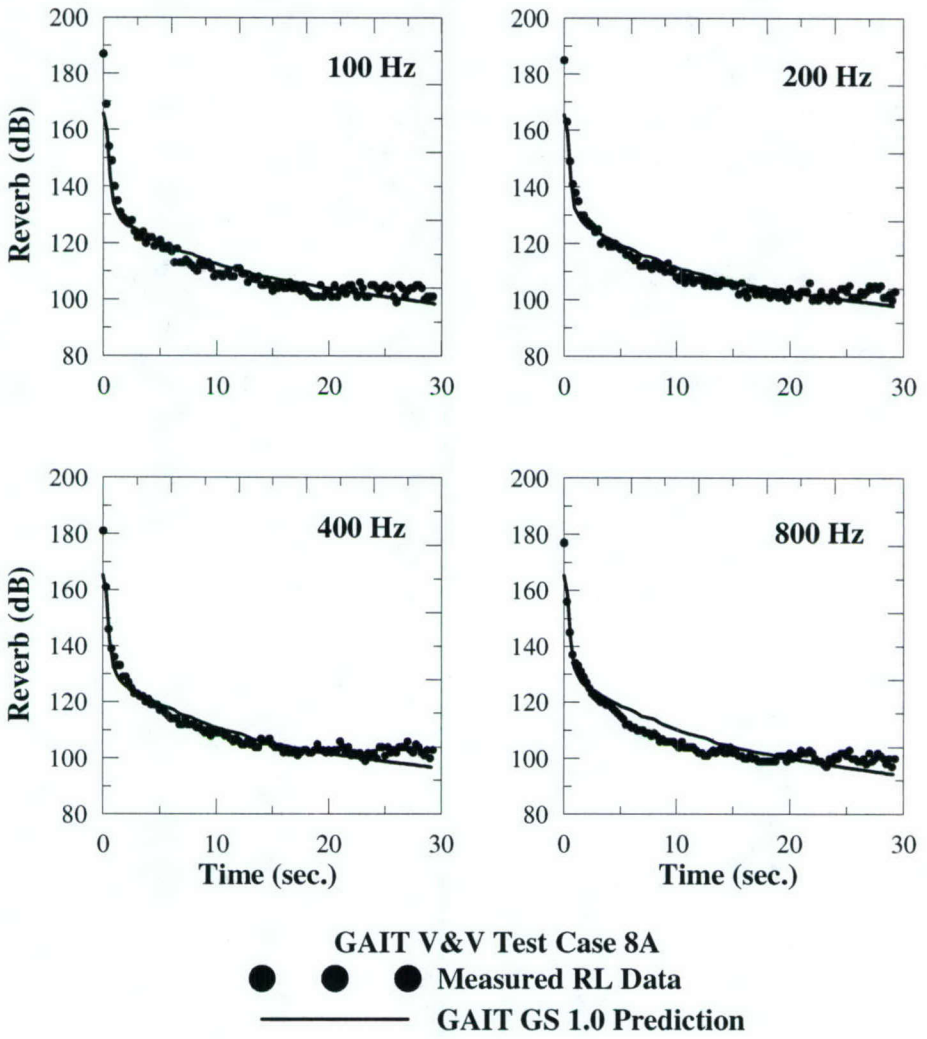

Figure 59: GAIT V&V Test Case 8A –Band averaged reverberation data (black circles) at center frequencies (from top left to bottom) of 100, 200, 400 and 800 Hz. The black curves were generated using the GAIT GS (using ASPM 5.1) inverted geoacoustic parameters.

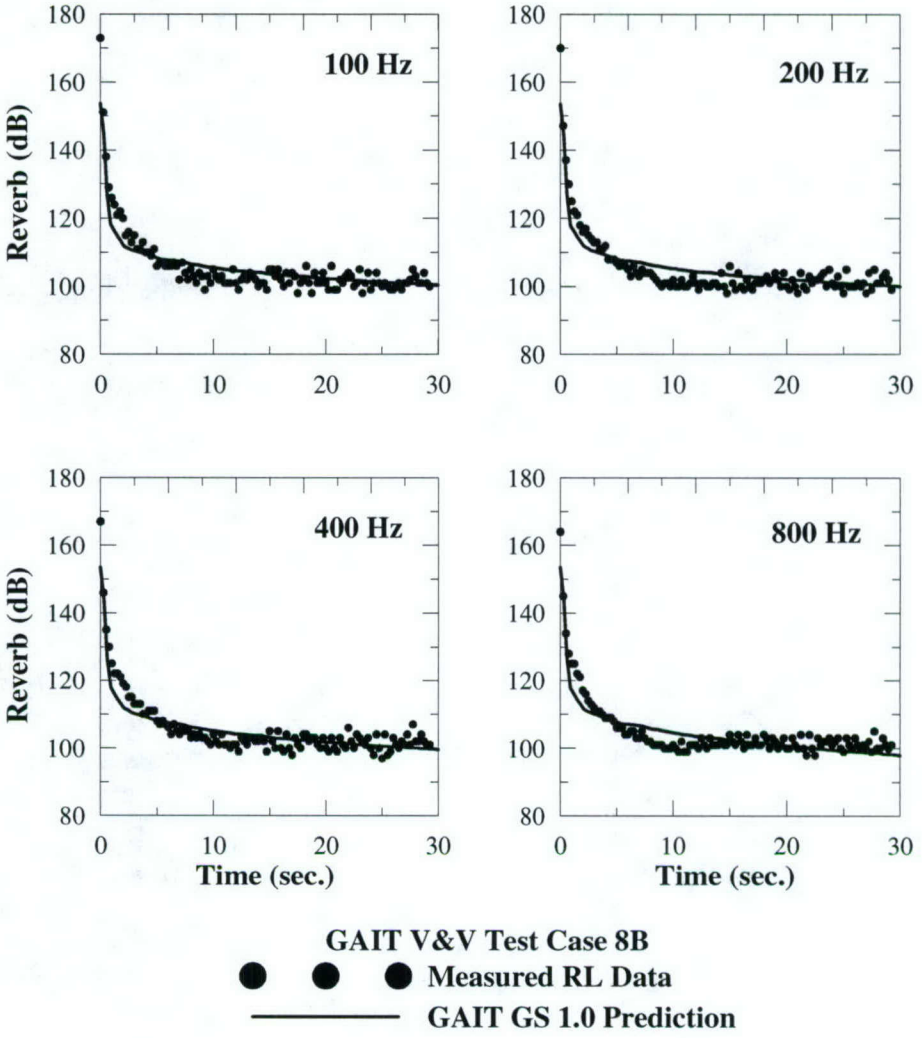

Figure 60: GAIT V&V Test Case 8B –Band averaged reverberation data (black circles) at center frequencies (from top left to bottom) of 100, 200, 400 and 800 Hz. The black curves were generated using the GAIT GS (using ASPM 5.1) inverted geoacoustic parameters.

Report Preparation

This report was written in Microsoft Word 2003 and is provided in hardcopy format and on a CDR disk in both Word and Adobe Acrobat (PDF) format. This report was prepared and submitted by the following individuals:

Peter Neumann
Planning Systems Inc.
741 Galen Drive
State College, PA 16803-1121
(814) 861-2612 (Phone)
pneumann@plansys.com

Gregory Muncill
Planning Systems Inc.
12030 Sunrise Valley Drive
Suite 400, Reston Plaza 1
Reston, VA 20191-3453
(703) 788-7703 (Phone)
(703) 390-5084 (Fax)
gmuncill@plansys.com